Institut für Technische Chemie
der Technischen Universität München
Lehrstuhl II

Butane skeletal isomerization on sulfated zirconia at low temperature

Xuebing Li

Vollständiger Abdruck der von der Fakultät für Chemie der Technischen Universität München
zur Erlangung des akademischen Grades eines

Doktors der Naturwissenschaften

genehmigten Dissertation.

Vorsitzender: Univ. –Prof. Dr. Notker Rösch

Prüfer der Dissertation:

        1.   Univ. –Prof. Dr. Johannes A. Lercher

        2.   Priv.-Doz. Dr. Reiner Anwander

Die Dissertation wurde am 08.06.2004 bei der Technischen Universität München eingereicht
und durch die Fakultät für Chemie am 13.07.2004 angenommen.

Abstract:

Butane skeletal isomerization reaction on sulfated zirconia at low temperature was studied to investigate the general features of the active structure and the reaction mechanism. Labile sulfate species, which can be removed by water washing and restored by gaseous SO_3 sulfation, were discovered to be the key components in active sulfated zirconia for butane skeletal isomerization. The initial step of n-butane isomerization on sulfated zirconia was concluded to be the *in situ* generation of butene by oxidative dehydrogenation of n-butane. Isomerization takes place as monomolecular skeletal isomerization of the n-butyl carbenium ion to the iso-butyl carbenium ion. The chain reaction is propagated by a hydride transfer from n-butane to the iso-butyl carbenium ion.

Untersuchungen zur Charakterisierung genereller Merkmale der aktiven Zentren und des Reaktionsmechanismus der Skeletisomerisierung von Butan bei niedrigen Temperaturen wurden an sulfatisiertem Zirkondioxid durchgeführt. Labile Sulfatspezies, die durch Wasser entfernt und durch eine Sulfatisierungsbehandlung mit SO_3 wiederhergestellt werden können, haben sich als Schlüsselkomponenten für die Butanisomerisierungsreaktion an sulfatisiertem Zirkondioxid herausgestellt. Als Initialschritt der Butanisomerisierung auf sulfatisiertem Zirkondioxid wurde die *in-situ* Generierung von Buten durch oxidative Dehthrierung von n-Butan identifiziert. Die Isomerisierung geschieht als Skelettisomerisierung des n-Butylcarbenium Ions zu einem iso-Butylcarbenium Ion. Die Kettenreaktion wird durch Hydridtransfer von n-Butan auf das iso-Butylcarbenium Ion fortgesetzt.

To my father,

to Limei,

to Xian

Acknowledgements

I would like to thank my professor, Prof. Dr. Johannes A. Lercher for giving me the opportunity to finish my PhD work in his laboratory. His scientific insights and supports in my work and life are especially valuable for the implement of this work. Thanks are also given to Dr. R. Olindo, Dr. K. Nagaoka and Dr. L. J. Simon not only for their patience in correcting my papers and thesis, but also for fruitful discussions throughout my PhD study.

Thanks are given to Professor J. Sauer, Professor H. Papp and Dr. F. Jentoft for fruitful discussion in project meetings; Dr. A. Jentys, Dr. T. Müller and Dr. J Find for scientific suggestions; Dr. C. Breitkopf, Dr. S. Wrabetz, M. Standke, Dr. K. Meinel and Dr. A. Hofmann for their cooperation and discussion; Dr. S. Zheng for his helping in scientific work and life from I came to Germany to his leaving to China. R. Su for her valuable helps with German documents; Dr. M. Smidt for his excellent computer techniques; A. Hartung for helping me go through German documents; other members from TCII group, Andreas F., C. Sievers, Phlips, Maria, Adam, Alex G., Ayumu, Fred, Stefen G., Jochen, Florencia, Anil, Linda, Van Nhu, Krishna, Stefen F., Gabriela, Iker, Toshi, Oriol, Jan K., Jan-Olaf, Hendrik and Jeno for all sorts of help inside the lab; the Deutsche Forschung Gemeinschaft (DFG) for financial support.

I would like to thank Frau Schüler and Frau Hermann for their help.
Technical supports from Xaver, Andreas M, Martin N are highly appreciated.

The encouragements from my family and friends are especially helpful to my PhD study. I would like to thank my wife, Limei, for her love, supports and understanding throughout the years. Sorry to Xian, my son, I did not have enough much time to spend with you.

Xuebing
June 2004

Table of contents

Chapter 1

Introduction

1.1. General introduction

iso-Butene, product of dehydrogenation of iso-butane, is very important intermediate in the production of poly-isobutylene, tert-butyl alcohol, methyl tert-butyl ether, *etc.*. Butane is available from natural gas sources, which usually contain only very limited amounts of iso-butane. Therefore, the isomerization of n-butane to iso-butane is of substantial importance in the petrochemical industry.

Butane isomerization is a very old process, having been used in refineries since the Second World War. Nowdays, the most prevalent method of producing iso-butane from n-butane is the UOP Butamer process, using platinum chloride catalyst. In the Butamer process, n-butane combined with hydrogen and a chlorinated organic compound flows through one or two fixed bed reactors in series, containing platinum chloride on alumina catalyst. The hydrogen is used to suppress the polymerization of olefin intermediates, while the chlorine source is used to maintain catalyst activity.

The main disadvantages of the commercial processes for n-butane isomerization are the corrosiveness and the high cost of catalyst disposal. Thus, improvement in acidic catalysts and processes for n-butane isomerization are urgently sought after. The catalysts of the new generation should be active at low temperature in order to shift the thermodynamic equilibrium of n-butane skeletal isomerization towards the desired branched product. The most quoted candidate catalysts for n-butane isomerization at low temperature are sulfated zirconia and promoted sulfated zirconia, which have been studied for more than two decades. These catalysts are thought to be the promising catalysts for industrial processes due to their high activity, ease of safe handling and lack of corrosiveness.

Despite the significant number of papers dealing with sulfated zirconia catalysts, the exact nature of the active sites is not clearly established. Furthermore, the mechanistic details of n-butane skeletal isomerization are not completely known.

1.2. Fundamental knowledge of saturated hydrocarbon chemistry

Hydrocarbons are compounds of carbon and hydrogen, which play an important role in chemistry. Hydrocarbons, in which all atoms are bonded to each other by single sigma bond, are named alkanes or paraffins and the general formula being C_nH_{2n+2}. Alkanes can be straight chain or branched. Cycloalkanes are cyclic saturated hydrocarbons containing carbon ring(s). Carbon can also form multiple bonds with other carbon atoms, which results in unsaturated hydrocarbons, *i.e.* olefins, acetylenes, dienes or polyenes.

The modern life of human is affected by a large energy demand. Our major energy sources are fossil fuels, *i.e.* oil, gas and coal, as well as atomic energy and hydro-energy. Fossil fuels are basically hydrocarbons with different H:C ratio, as illustrated in Table 1.1 [1].

Table 1.1 H:C ratio in natural hydrocarbon sources

Methane	4.0
Natural gas	3.8
Petroleum crude	1.8
Tar sands bitumen	1.5
Shale oil (raw)	1.5
Bituminous coal	0.8

Methane is the main component (generally > 80 %) of natural gas. Gas liquids ("wet" gases) contain significant amounts of C_2-C_6 alkanes. Petroleum or crude oil is a complex mixture of many hydrocarbons, predominantly straight-chain alkanes with small amounts of branched alkanes, cycloalkanes and aromatics. The quality of petroleum varies according to the specific gravity and viscosity. In general, light oils, characterized by low specific gravity and viscosity, are richer in straight-chain hydrocarbons and more valuable than the heavy oil. Extra heavy oils, the bitumens, having a high viscosity, contain high concentration of resins and asphaltenes. Coals are fossil with low hydrogen content.

Distillation of crude oil yields several fractions which find different applications. However, the quality of the fractions obtained directly by distillation seldom meet the required specifications for various applications. Refining and upgrading of the naphtha fraction, attempted to obtain higher octane number, are necessary to meet the requirements of internal-combustion engines in today's automobiles. The main hydrocarbon refining and conversion processes are cracking, dehydrogenation, and isomerization. Table 1.2 gives the octane number of saturated and branched hydrocarbons [2]. The branched alkanes have a considerably higher octane number than their linear counterparts. Therefore, isomerization of hydrocarbons will substantially improve the combustion properties of gasoline.

Table 1.2 Octane number of straight-chain and branched paraffinic hydrocarbons

Paraffinic hydrocarbons	Octane number
n-Butane	94
iso-Butane	100
n-Pentane	63
2-methylbutane	90
2,2-Dimethylpropane	116
n-Hexane	32
2-Methylpentane	66
3-Methylpentane	75
2,2-Dimethylbutane	94.6
2,3-Dimethylbutane	95
n-Heptane	0
2-Methylhexane	45
3-Methylhexane	65
3-Ethylpentane	68
2,2-Dimethylpentane	80
2,3-Dimethylpentane	82
2,4-Dimethylpentane	80
3,3-Dimethylpentane	98
2,2,3-Trimethylbutane	116
n-Octane	-19
2-Metylheptane	23.8
3-Metylheptane	35
4-Metylheptane	39
2,2,3-Trimetylpentane	105
2,2,4-Trimetylpentane	100
2,3,3-Trimetylpentane	99
2,3,4-Trimetylpentane	97

iso-Butane, the product of n-butane isomerization, reacts under mild acidic conditions with olefins to give highly branched hydrocarbons in the gasoline range. Moreover, its dehydrogenation product, iso-butene, is a very important intermediate in the production of poly-isobutylene, tert-butyl alcohol, methyl tert-butyl ether, and other products. However, straight chain saturated hydrocarbons or paraffins, as their name indicates (*parum affinis*: slight reactivity), have very little reactivity, which has to be overcome for their further conversion.

In 1933, Nenitzescu and Dragan [3] reported that n-hexane can be converted to its isomers when refluxed with aluminum chloride, which was thought to be the first reportage of catalyzed isomerization of saturated hydrocarbons. Later on, in 1946, Bloch, Pines, and Schmerling [4] observed that aluminium chloride in the presence of HCl could isomerize n-butane to iso-butane.

At present, the isomerization of gasoline or naphtha, a fraction of distillation of crude oil, converts the straight chain hydrocarbons to its branched isomers, significantly raising its octane number. The most common naphtha isomerization processes used in the industry are the UOP's Penex process, the Union Carbide's Total Isomerization Process (TIP), the Union Carbide Hysomer process and the BP Isomerization process, where naphtha is combined with hydrogen and flows through one or two fixed bed reactors in series. The presence of hydrogen prevents coking and deactivation of the catalyst. In the TIP and Hysomer processes, using platinum supported on zeolite as catalyst, at the reaction temperature higher than 200 °C, while the Penex process and the BP process, using platinum chloride supported on alumina as catalyst, operate at temperatures below 200 °C. Figure 1.1 depicts a generic process flow diagram of Penex or BP processes for isomerization of naphtha [5].
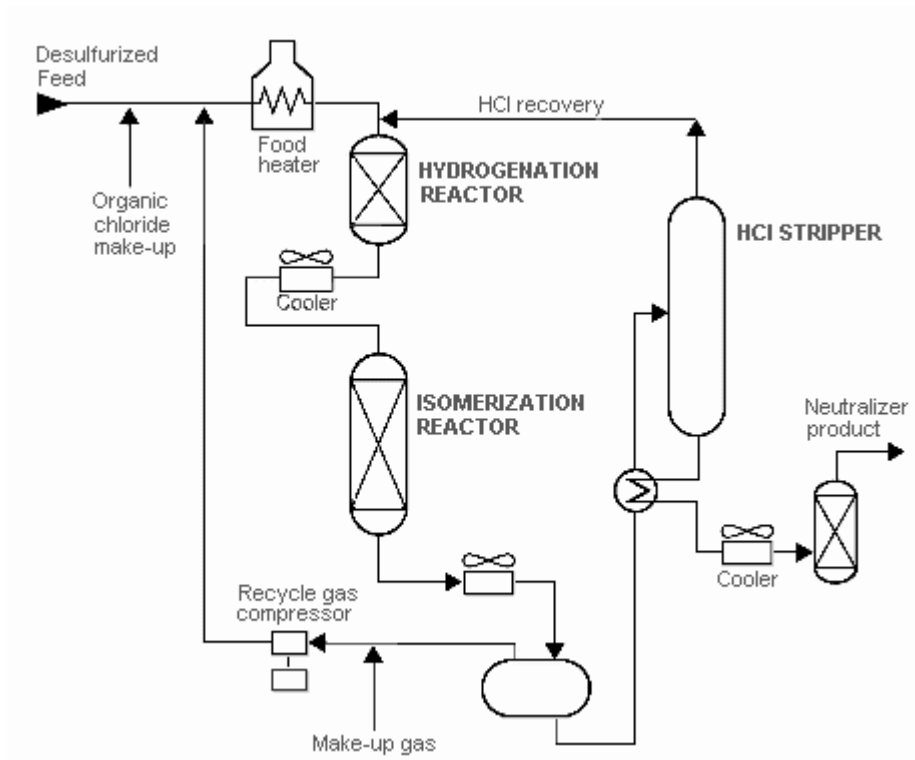
Figure 1.1 Scheme of naphtha isomerization

For the isomerization of n-butane to iso-butane, the most prevalent method is the UOP Butamer process [5]. In this process, n-butane is combined with hydrogen and with a chlorinated organic compound. The hydrogen is used to suppress the polymerization of olefin intermediates, while the chlorine source is used to maintain the catalyst activity. The feed flows through one or two fixed bed reactors in series, containing platinum chloride on alumina as catalyst. Figure 1.2 describes the UOP Butamer process flow diagram for n-butane isomerization.
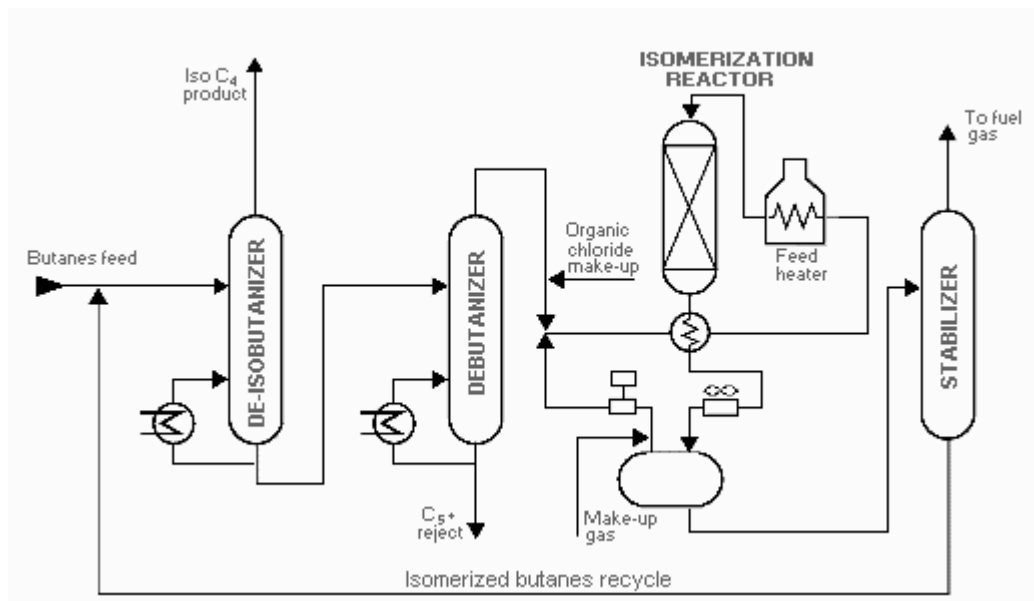
Figure 1.2 Scheme of butane isomerization (UOP Butamer process)

The equilibrium between n-butane and iso-butane is temperature dependent. As shown in Table 1.3 [6], at 180 °C the equilibrium composition contains about 45 % of iso-butane and 55 % of n-butane, but at –6°C, 85 % of iso-butane can be obtained. Therefore, in order to obtain a maximum ratio iso-butane/n-butane, it would be advantageous to carry out the isomerization at low temperature. Since the early 1960s, superacid are known to react with saturated hydrocarbons, even at temperature much lower below 0 °C, which also initialed extensive studies devoted to hydrocarbons conversion [7].

Table 1.3 Equilibrium composition of n-butane and iso-butane

	Temperature (°C)				
	-6	38	66	93	180
iso-Butane	85	75	65	57	45
n-Butane	15	25	35	43	55

Since the early reports of Nenitzescu on alkane isomerization on wet aluminum chloride in 1933 [3], all mechanistic studies have led to a general agreement on the carbenium-type nature of the reaction intermediates in acid catalyzed hydrocarbon conversion. At first, the hypothesis about the formation of carbenium ions in solution was put forward by Meerwein who observed that the rate of camphenhydrochloride rearrangement into isobornylchloride increases with the dielectric constants of the solvent [8]. Later on, the carbenium ion mechanisms were also suggested for a number of other organic reactions [9]. However, we should bear in mind that the existence of carbenium ions in solution was drawn from the composition and stereochemistry of the resulting final products or by indirect arguments based on the kinetics of the corresponding reactions. Therefore, the direct observation of carbocations in solutions of super acids by NMR and other spectral techniques by Olah and co-workers [10] was a very important step for hydrocarbon chemistry. The ^{13}C chemical shifts of the positively charged carbon atoms in aliphatic carbenium ions are at least 350 ppm higher than that of the corresponding neutral hydrocarbon.

The stability of carbenium ion is very different. In general, tertiary carbenium ions are the most stable, while the primary ones are the least stable. Therefore, the carbenium ion formation is easier at tertiary carbon atoms. The stability of carbenium ion also can explain why only the tertiary carbenium ion, *i.e.* t-butyl cation, was formed when n-butane or iso-butane reacted with $HSO_3F:SbF_5$, the magic acid [11].

However, the adsorbed carbocations on zeolite or other solid acids are not similar to those present in liquid superacids. In fact due to the basicity of surface oxygen, the carbenium ions form more or less covalent surface alkoxides. The ^{13}C MAS NMR study of active intermediates resulting from the interaction of ^{13}C enriched propene [12], tert-butanol [13, 14] and isobutanol [15, 16] with acid hydroxyl groups in hydrogen forms of zeolites indicates that the ^{13}C chemical shifts are only 70-80 ppm, instead of 300-350 ppm for carbenium ions in superacid.

The corresponding elementary steps of hydrocarbon conversion on solid acids involve a partial dissociation or stretching of the C-O bond of the alkoxides, resulting in high energetically excited ion pairs, which resembles the free or weakly solvated carbenium ions in superacid solution. The activation energy of partial dissociation of the C-O bond of alkoxides is around 100 kJ/mol, which should be added to the activation energy of conversion of carbocations on zeolites [17].

1.3. History of sulfated zirconia and other anions modified metal oxides

Due to the more severe environmental legislation, non-polluting and efficient catalytic technologies as alternatives for the present processes using highly corrosive catalysts, attract immense research efforts. The solid acids, for instance, acid-treated clays, zeolites, zeotypes, ion-exchange resins and metal oxides, should replace the highly corrosive, hazardous and polluting liquid acids, which are widely used in chemical industry. Due to its high activity, sulfated zirconia was believed to be the most promising catalyst among the solid acids for several important acid-catalysed industrial reactions.

1.3.1. Discovery of unique catalytic property of sulfated zirconia

The first report of sulfated zirconia as catalyst for paraffin conversion traces back to the patent of Holm and Bailey in 1962 [18]. These authors reported that a sulfate-treated zirconia-gel modified by platinum is active for n-pentane isomerization and the activity as well as the selectivity being similar to those of commercial catalysts.

It is strange that the unique catalytic property of sulfated zirconia for paraffin isomerization has not attracted much attention for more than one decade after its discovery. In the late 1970's, Arata *et al.* [19, 20] observed that the sulfate treated metal oxides, ZrO_2 or Fe_2O_3, are able to isomerise n-butane at low temperature (room temperature), like very strong acids or superacids (SbF_5-HF and SbF_5-FSO_3H) can do. Based on the titration method of Hammett indicators these catalysts were claimed to be superacid. Other sulfated metal oxides, *i.e.* sulfated TiO_2, SiO_2 and SnO_2 [21], have also been found to be active in n-butane isomerozation. In addition, commercial γ-Al_2O_3 can also be used for preparation of active catalysts for alkane conversion [22, 23].

Thereafter, sulfated zirconia became the subject of many investigations devoted to the understanding of the nature of active sites, mechanism of alkane isomerization or even to the influence of multi-factors.

1.3.2. Promoted sulfated zirconia

The modification of sulfated zirconia with various transition metals such as Pt [24], Fe and Mn [25], has been found to improve the catalytic activity and the stability against the rapid deactivation of sulfated zirconia.

The promotion of sulfated zirconia with Pt has been first adopted in the patent of Holm and Bailey [18] for isomerization of n-pentane. The incorporation of Pt on the catalyst surface

and the presence of hydrogen in the reaction mixture have been found to increase the catalytic activity of sulfated zirconia and to improve the catalyst lifetime.

The promoting effect of Fe and Mn, which also attracts intensive investigation, was first discovered by Hsu *et al.* [25]. These authors reported that sulfated zirconia doped with 1.5 % Fe and 0.5 % Mn is two or three order magnitude more active for n-butane isomerization at low temperature than unpromoted sulfated zirconia. They postulated that this enhancement is due to the generation of additional strong acid sites. On the contrary, Adeeva *et al.* [26] proposed that this promoting effect is caused by the formation of more alkene intermediate species. Ni [27] was also used as an activity promoter for sulfated zirconia. However, Gao *et al.* [28] reported that Ni has a detrimental effect on the catalytic performance of sulfated zirconia.

In addition to the promoting effect of transition metals, other elements were found to have a positive effect on the catalytic activity and stability of sulfated zirconia. Gao *et al.* [29] first reported that the incorporation of small amounts of Al into sulfated zirconia enhances the catalytic activity and stability, when the isomerization reaction of n-butane is performed at 250 °C in the presence of hydrogen. Pinna *et al.* [30] further confirmed the promoting effect of Al. Moreover, Ga [31], which is in the same group of Al, also exhibits a promoting effect on the catalytic activity of sulfated zirconia.

1.3.3. Modification of zirconia with other anions (WO_4^{2-}, PO_4^{3-})

Modification of zirconia with other anions, like WO_4^{2-} [32] or PO_4^{3-} [33] can also generate strong acid sites on zirconia surface. Especially, WO_4^{2-} modified zirconia (tungstated zirconia), was thought to be the alternative catalyst for sulfated zirconia because, in spite of its lower activity, the surface tungsten species are more stable than the sulfate groups. Like sulfated zirconia, also tungstated zirconia was reported to be superacid on the basis of titration with Hammett indicators [32]. The addition of a metal component (< 1 wt.% Pt) into tungstated zirconia system and the presence of H_2 in the reaction mixture can effectively overcome the low selectivity to isomers in alkane isomerization with excellent stability [34]. Contrary to the sulfated zirconia, Fe and Mn have no promoting effect on the catalytic behavior of tungstated zirconia [35].

PO_4^{3-} promoted zirconia, which is the subject of only few recent studies, is another active catalyst for hydrocarbons conversion [33].

1.4. Preparation methods of sulfated zirconia

The catalytic performance of sulfated zirconia is significantly dependent on the preparation methods and on the activation procedures before reaction. A variety of synthesis methods has been developed in the last two decades. These methods differ mainly from the zirconia precursor, sulfation agent, calcination procedure and also activation conditions.

1.4.1. Conventional method

Sulfated zirconias used in the patent of Holm and Bailey [18] and in the report of Arata *et al.* [19] were prepared following the two steps procedure illustrated in Figure 1.3. This preparation method was also widely used in the later researches and therefore is denoted here as "conventional method". In the first step the zirconium hydroxide is precipitated by adding aqueous ammonia to a solution of a zirconium salt, such as $ZrOCl_2$ or $ZrO(NO_3)_2$. The second step consists in the sulfation of zirconium hydroxide with H_2SO_4 or $(NH_4)_2SO_4$ solution. The resulting sulfated zirconium hydroxide must be finally calcined in air at 550-650 °C to generate strong acidity.
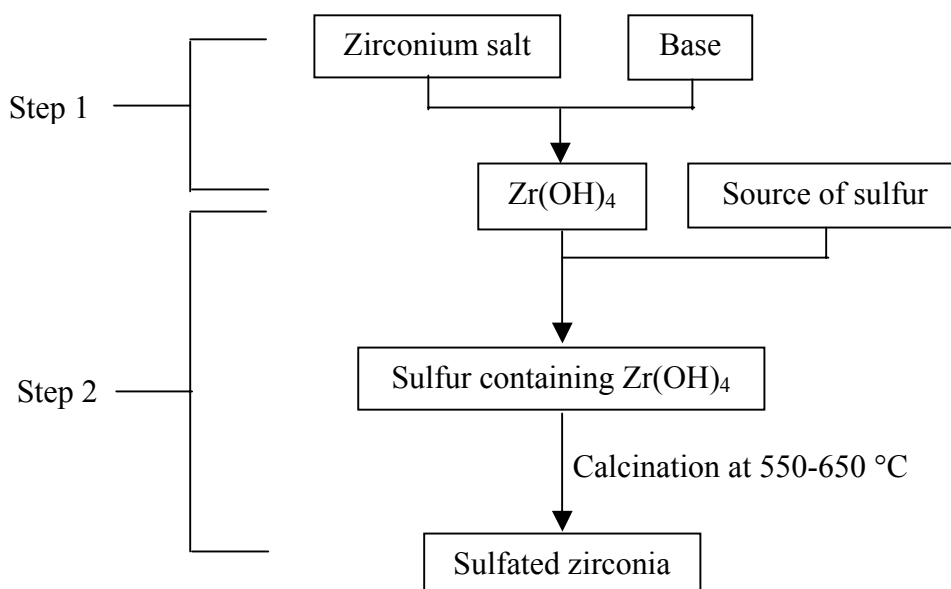

Figure 1.3 Scheme of the conventional method for the preparation of sulfated zirconia

Generally, $ZrOCl_2$ or $ZrO(NO_3)_2$ are used for zirconium hydroxide preparation. Zirconium hydroxide can also be prepared by sol-gel method [36]. The concentration of H_2SO_4 solution is $1N$ and the ratio between liquid and solid in sulfation process may vary from 2 to 10 ml/g.

1.4.2. Non-conventional methods

Although the two steps method described above is widely used, other methods (non-conventional methods) have been also developed, mainly for better understanding the influence of preparation procedure. Among the non-conventional methods, one step method and sulfation of crystalline zirconia method are the techniques most used in recent studies.

Ward and Ko [37] prepared sulfated zirconia following a single step method based on sol-gel synthesis. Zirconium n-propoxide was first mixed with n-propanol, nitric acid and sulfuric acid. This solution was then mixed with another solution containing n-propanol and water, and the mixture was vigorously stirred for gelation. A zirconia-sulfate aerogel was obtained after supercritical drying with CO_2. By calcination at 773 K, sulfates were expelled onto the surface and transformed into the active species.

Another one step method for sulfated zirconia preparation is the thermal decomposition of zirconiumsulfate: $Zr(SO_4)_2 \rightarrow ZrO_2 + 2SO_3$ [38]. The released SO_3 may be retained on the zirconia surface. However, this method is not so attractive because it is difficult to control the sulfate content.

In recent years, direct sulfation of crystalline zirconia by H_2SO_4 or $(NH_4)_2SO_4$ solution has been used for the better understanding the origin of the activity of sulfated zirconia catalysts. In 1995, Comelli *et al.* [39] reported that the sulfation of crystalline zirconia leads to an inactive catalyst for n-butane isomerization, which is in consistent with the results of the earlier researches. However, Ward and Ko [40] reported that, after sulfation, crystalline zirconia aerogel was active for n-butane isomerization. They concluded that the content of surface hydroxyl groups was the determining factor for generating acidity. Vera *et al.* [41] also confirmed the importance of the surface OH groups for the formation of active sites by sulfation. Sulfation of crystalline zirconia with sulfuric acid at 300 °C could overcome the inertness of the crystalline zirconia surface and induce catalytic activity for n-butane isomerization.

However, Morterra *et al.* [42] demonstrated that sulfation of zirconia stabilized in the cubic or tetragonal phases by incorporation of Y_2O_3 resulted in catalytic active sulfated zirconia; on the contrary, sulfation on crystalline monoclinic zirconia was not effective for active sties generation. Therefore, they concluded that the *metastable* tetragonal phase and the cubic phase are the active phases. CaO-stabilized cubic zirconia can also be used for preparation of active sulfated zirconia [43].

Sulfation on metal oxides by gaseous sulfur sources was also confirmed to be effective method. Iron oxide treated by H_2S and SO_2 followed by oxidation at 400-450 °C was found to

be active for the isomerization of cyclopropane [44]. It has also been reported that zirconia modified by H_2S and SO_2 followed by oxidation was an active catalyst for 1-butene double bond isomerization at 20 °C [45]. Gaseous SO_3 can also be used for preparation of active sulfated metal oxides of strong acidity; Where SO_3 was used as sulfur source without additional oxidation step [46, 47].

1.4.3. Influence of preparation parameters on the properties of sulfated zirconia

Various parameters during sulfated zirconia preparation have been studied thoroughly, *i.e.* zirconia precursor, sulfur source, calcination procedure and also the activation treatment before reaction.

At the beginning, it was reported that only the amorphous zirconia hydroxide prepared by hydrolysis of a zirconium salt can be used for the synthesis of active sulfated zirconia [19], the sulfation of crystalline zirconia being not effective for generating the strong acidity required in n-butane isomerization. However, Riemer *et al.* [48] reported an exception to this rule. They prepared sulfated zirconia by sulfuric acid impregnation of a zirconia sample obtained by calcination of a commercial zirconium hydroxide, followed by further calcination at 600 °C. This material exhibited the same surface sulfate structure and proton chemical shift as those of the sample prepared from zirconium hydroxide. As expected, the sample was also active for n-butane isomerization.

Zirconia can exist in three different crystalline isomorphs: monoclinic (M), stable at temperature below 1373 K; tetragonal (T), stable between 1373 to 2173 K; and cubic (C), stable above 2173 K. Nevertheless, the T and C forms can be generated at low temperature as metastable structures. The addition of anions, such as sulfate, as well as of some metal oxides, *i.e.* Y_2O_3 and CaO, can stabilize the metastable phases.

Sulfated zirconia prepared by conventional method is mainly metastable tetragonal phase, which leads to the postulation that the metastable phases are the active phases for sulfated zirconia. This has also been confirmed by the studying of sulfation on different zirconia crystalline phases. After sulfation and calcination treatment, Y_2O_3-stabilized tetragonal or cubic zirconia was active for n-butane isomerization reaction, while, the sulfation of crystalline monoclinic zirconia resulted in an almost inactive sample [42]. However, Stichert *et al.* reported that monoclinic sulfated zirconia could also be active in n-butane isomerization [49, 50]. However, comparing to the tetragonal one, the monoclinic sulfated zirconia had only one-fourth of the catalytic activity, which indicats that tetragonal phase favorites n-butane isomerization.

Besides the bulk phase, the surface properties of zirconia have also been considered one of the determining factors for the generation of active sites. Vera *et al.* [41] and Ward and Ko [40] demonstrated that the intensity of the IR bands corresponding to hydroxyl groups of crystalline zirconia is the crucial parameter for the active catalysts. Later on, Vera *et al.* [51] proposed that the defects of zirconia (oxygen vacancies), are related to the catalytic activity for n-butane isomerization through charge abstraction and stabilization of the ionized intermediates.

A variety of sulfur sources can be used for the preparation of sulfated zirconia. In general, H_2SO_4 or $(NH_4)_2SO_4$ are used as sulfation agents and the sulfation is carried out by impregnation. However, Sohn and Kim [45] have also sulfated catalysts with CS_2, SO_2 and H_2S. After oxidation at high temperature, these materials were active for n-butene isomerization, which indicates that the oxidation state 6+ of sulfur is important for the generation of strong acid sites.

The occupation area of sulfate ion based on the dynamic diameter is 0.31 nm^2, which indicates that the concentration of sulfate groups for monolayer coverage is 3.2 sulfur atoms nm^{-2} [52]. Since the conventional method for sulfated zirconia preparation resulted in a BET area around 100-150 m^2/g, the monolayer occupation of sulfate ion should be around 5.2-7.9 wt % (S wt % = 1.78-2.6 %). It has been proposed that the poly-sulfate, in addition to the sulfate, was also present on the zirconia surface, even for sulfate concentrations lower than the monolayer [53]. Fărcașiu *et al.* [54] reported that the catalytic activity for isomerization of methylcyclopentane (MCP) was a function of the sulfur content of sulfated zirconia.

The calcination is a crucial step for the generation of strong acidity of sulfated zirconia. It has also been suggested that the sulfated zirconia precursor should be calcined at 550-650 °C in air for several hours to obtain an active catalyst for alkane conversion. Calcination at higher temperature leads to an inactive catalyst with mere Brønsted acid sites and lower sulfate content. One of the functions of calcination step is to transform the inactive amorphous zirconium hydroxide into active tetragonal zirconia by dehydration and severing the sulfate group to bind with the zirconia surface to form the active sites [55]. However Morterra *et al.* emphasised that another important function of the calcination is to selectively partially remove sulfate groups thus creating strong Lewis acids (coordinatively unsaturated Zr(IV)) [56, 57].

## 1.5. Nature of active sites of sulfated zirconia

The general features of the active sites of sulfated zirconia have been explored frequently. However, no consensus has been reached. In fact the nature and the strength of acid sites as well as the structure of sulfate groups remain object of debate.

1.5.1. Superacid or strong acid

In 1979, Hino *et al.* first stated that sulfated zirconia is a superacid on the basis of measurements with Hammett indicators [19]. They concluded that the H_0 value of sulfated zirconia is lower than -14.52, and therefore, in the range of superacids. Furthermore, the TPD measurement of ammonia adsorption also confirmed this conclusion [52]. However, the most straightforward evidence for the superacidity of sulfated zirconia was its highly catalytic activity in alkanes conversion at low temperature, which also has been used as reaction test for the strength of acid sites.

It has been suggested that the sulfate groups on active sulfated zirconia present the bridging bidentated structure represented in Scheme 1. According to this model, the strength of Lewis acid sites Zr^{4+} is increased by the inductive effect of the sulfate groups in the complex. The model also demonstrated that it is possible to convert Lewis acid sites into Brønsted acid sites by water adsorption.

Using Raman and ^1H MAS NMR spectroscopy, Riemer *et al.* [48] proposed the structure model shown in Scheme 2 and they rationalized the origin of the Brønsted acidity to the bridging hydroxyl groups. The ^1H MAS NMR spectrum of sulfated zirconia showed a band at $\delta = 5.85$ ppm, which was 2 ppm downshift compared to that of pure zirconia and higher than that of the zeolite HZSM-5 (4.3). Since the ^1H chemical shift is related to the acid strength of surface OH group if there is no hydrogen bond formation, they pointed out that the highly acidic property (superacidity) of sulfated zirconia is due to the high electronegativity of Zr^{4+}.
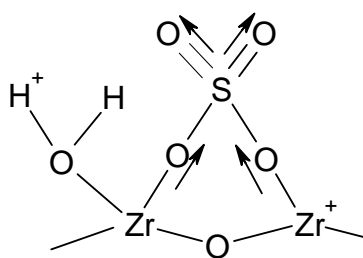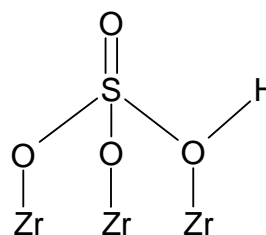
Scheme 1   **Scheme 2**

However, more and more characterization results revealed that the acidity of sulfated zirconia was similar to that of sulfuric acid, and therefore sulfated zirconia is not a superacid. Study of the interaction of 4-nitrotoluene and 4-nitrofluorobenzene with sulfated zirconia using UV spectroscopy instead of the visual observation of color changes in Hammett titrations, demonstrated that the acid strength of sulfated zirconia is similar to that of 100 % sulfuric acid [58].

Through IR spectroscopy measurements, using benzene and CO as probe molecules, Kustov [59] observed that both Brønsted and Lewis acidity of zirconia are enhanced by sulfation. In addition, adsorption of H_2 and CH_4 indicated that the modification with sulfate induces a weakening of the polarizing ability of Lewis acid-base pair. However, the shift of OH group after adsorption of benzene was smaller than that of zeolite HZSM-5. Thus, the Brønsted acid strength of sulfated zirconia is weaker than that of H-X zeolite. A model (Scheme 3) was proposed where the enhanced electron accepting properties of the three-coordinate zirconium was attributed to the inductive electronwithdrawing effect of the sulfate group or to its direct interaction of Zr with an oxygen atom of the sulfate group.

Another structure for sulfate group present on active samples was proposed by F. Babou *et al.* [60] based on the quantum and IR studies (Scheme 4). Sulfated zirconia was considered as sulfuric acid grafted at the surface of zirconia in a state very sensitive to dehydration. At high dehydration condition, $(SO_3)_{ads}$ species exhibit strong Lewis acid property; while at intermediate dehydration condition, H_3O^+ and HSO_4^- species induce a very strong Brønsted acidity which is very close to that of sulfuric acid.
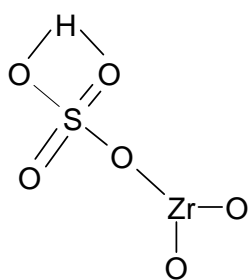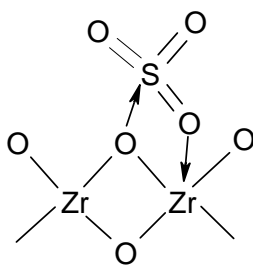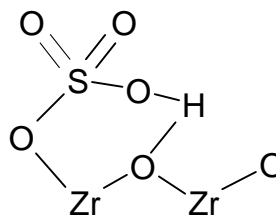
Scheme 3   **Scheme 4**   **Scheme 5**

Based on IR and NMR measurements, Adeeva *et al.* [26] concluded that the Brønsted acidity of sulfated zirconia is weaker than that of HZSM-5 and H-Y zeolites and the Lewis acidity of sulfated zirconia is lower than that of the trigonal coordinated Al^{3+} of γ-Al_2O_3. These authors attributed the relatively large chemical shift of the proton NMR line of sulfated

zirconia to the hydrogen bonds rather than to superacidity. Therefore, they proposed that the structure of the OH groups of sulfated zirconia is similar to that of the LF protons of zeolite H-Y (Scheme 5).

1.5.2. Brønsted or Lewis active acid sites

Yamaguchi proposed that Lewis acid sites of sulfated zirconia were responsible for the activation of alkane at low temperature, which was confirmed by the IR spectroscopy of Pyridine [61]. When sulfated zirconia was evacuated at 500 °C, only Lewis acid sites were observed. The authors suggested that the structure of catalytically active species or of the species responsible for giving highly acidic properties, involves an organic sulfate structure with a metal cation, which acts as a Lewis acid, as shown in Scheme 6. The importance of the coordinative unsaturated sites was also illustrated, which suggested that the active sites are developed at the edge or corner of the metal oxide surface.

Scheme 6

The strong Lewis acid sites were also confirmed by IR spectroscopy of CO at 300 K. In addition, the conversion of Lewis to Brønsted acid induced by rehydration of activated sulfated zirconia was demonstrated using IR spectroscopy of pyridine [39, 60]. The detrimental effect of hydration and CO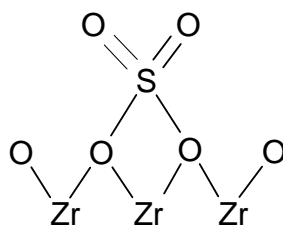 suggested that the Lewis acid sites, generated from the coordinatively unsaturated Zr^{4+}, are crucial for the reaction of alkanes on sulfated zirconia at low temperature [39, 62].

At present, a consensus has been achieved that active sulfated zirconia, when evacuated at 300-450 °C, possesses not only Lewis acidity but also Brønsted acidity. Arata *et al.* [21] pointed out the importance of the Brønsted acid, since the superacidity of sulfated zirconia was measured using Hammett indicator, which is only valid for the evaluation of Brønsted acid strength. Ward and Ko [40] proposed that the strong Brønsted acidity of sulfated zirconia generated from the surface OH groups and proton donating ability was strengthened by the electron inductive effect of the S=O band, as shown in Scheme 7. On the other hand, Kustov

et al. [59] and Adeeva *et al.* [26] attributed the Brønsted acidity to the bi-sulfate species instead of OH groups directly bonded to Zr atoms.

Contrary to the detrimental effect of hydration [39], Song *et al.* [63] and Dumesic *et al.* [64] reported the promoting effect of minor amounts of water on the catalytic activity. The catalytic activity of an *ex-situ* calcined catalyst, which was rehydrated by the atmospheric moisture before activated at 250 °C, was much higher than that of an *in-situ* calcined sample, which was extra dry. It was also shown that the sample activated at higher temperature, 773 K, exhibited an activity much lower than that activated at lower temperature (588 K). Adding of 75 μmol water/g onto the catalytic surface of the sample activated at 773 K promoted the activity by an order of magnitude, while larger dosing poisoned the catalyst.

Recently, direct conversion of alkane into carbonyl-containing organic compounds in the presence of sulfated zirconia has been reported by Stepanov *et al.* [65, 66], which provided a new insight to the negative effect of CO on the alkane isomerization reaction. The suppression of the isomerization reaction could not be resulted from the blocking of Lewis acid sites, but from changing the reaction route from isomerization to carbonylation.
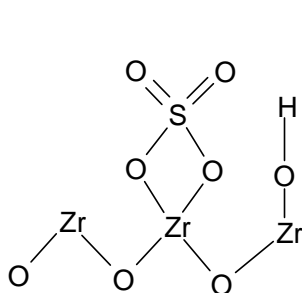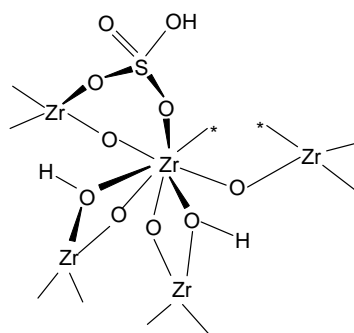
Scheme 7   **Scheme 8**

In addition, several authors have attributed the catalytic activity to a synergistic effect between both types of acid sites. The active structure proposed by Clearfield *et al.* [67] (Scheme 8) described one step formation of Brønsted and Lewis acid sites. The bisulfate group acts as highly acidic Brønsted acid sites due to the electron withdrawing effect of the neighboring Lewis acid sites. It is inferred that the combination of the bisulfate with adjacent Lewis acid sites is responsible for the strong acidity. Morterra *et al.* [68] also postulated the synergistic effect of Brønsted and Lewis acid sites for the generation of strong acidity of sulfated zirconia based on IR and Microcalorimetric measurements.

1.5.3. Surface sulfate state

Since the strong acidity of sulfated zirconia is generated from the introduction of the surface sulfate species, the sulfate state is also an interesting subject for the study of active sulfated zirconia.

Based on IR measurements, Yamaguchi [61] proposed that the sulfate species after hydration is similar to the inorganic chelating bidentate species. Removal of water resulted in the formation of an organic-like sulfate with a stronger covalent character of the S=O double bond, as shown in Scheme 6. The model proposed by Arata *et al.* [19] also involves a bidentate sulfate (Scheme 1) but instead of chelating a single Zr atom, the sulfate bridges across two Zr atoms.

Model 1   **Model 2**   **Model 3**
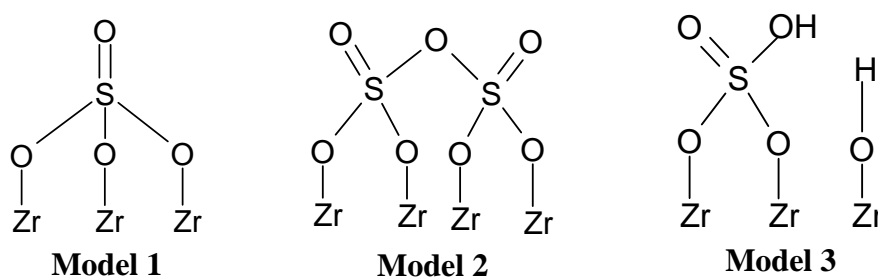
Scheme 9

However, based on IR experiments isotopic exchange with ^{18}O, Lavalley *et al.* [69] proposed a structure model (Scheme 9, Model 1) of sulfated zirconia with tridentate sulfate species containing only one S=O. On sulfated zirconia with higher sulfate content, poly-sulfate species are formed, as shown in Scheme 9, Model 2. However, in the presence of moisture, the structure represented in Model 1 is converted to a bridged bidentate form (shown in Model 3), which accounts for the increase in Brønsted acidity. Riemer *et al.* [48] agreed that tridentate sulfate are the main species on zirconia surface (Scheme 2). However, they suggested a HSO_4^- group is present at the surface, (O-H stretching band at 3650 cm^{-1}). White *et al.* [70] proposed penta-coordinated sulfur structure in the active sulfated zirconia (Scheme 10).
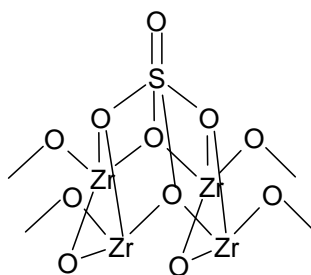
Scheme 10

Mono-dentate bisulfate species (HSO_4^-) are present in the models proposed independently by Kustov *et al.* [59] (Scheme 3) and Adeeva *et al.* [26] (Scheme 5) and the OH group of the bisulfate specie is hydrogen-bonded to one surface oxygen atom of zirconia. However, bi-dentate bisulfate-like specie were attributed to the formation of Brønsted acid sites in the active structure models of Clearfield *et al.* [67], Morterra *et al.* [71], and Lavalley *et al.* [69]. The model proposed by Riemer *et al.* [48] (Scheme 2) involves a tri-dentate bisulfate-like species. However, F. Babou *et al.* [60] suggested that sulfated zirconia is sulfuric acid grafted on the zirconia surface (Scheme 4).

1.6. Proposed mechanisms for alkane skeletal isomerization on sulfated zirconia at low temperature

The most intriguing catalytic property of sulfated zirconia is its ability to isomerize alkanes, especially n-butane, at extremely low temperature, which is generally considered associated to superacidity. Even if the carbenium ion or alkoxy species are generally considered as the active intermediates, the initial step and the skeletal isomerization mechanism is still a subject of discussion.

1.6.1. Initial step

Four different mechanisms have been proposed for describing the initialization of the skeletal isomerization of alkane in the presence of sulfated zirconia, which were summarized by Sommer *et al.* [72], as shown in Figure 1.4.

1. protolysis of C-H or C-C bond:
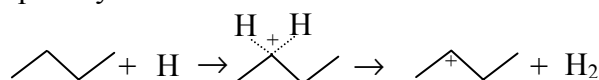
2. Hydride abstraction by a Lewis acid site:
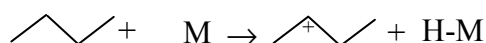
3. traces of olefin in the feed:

4. oxidation of the C-H bond:
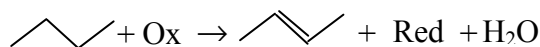
Figure 1.4 Proposed mechanisms of the initial step of n-butane isomerization on sulfated zirconia

In 1984, Haag and Dessau [73] suggested the ability of solids to protolyse non-activated C-H and C-C bonds on the basis of methane and hydrogen formation in the initial stages of 2-methylpentane cracking at 500 °C on H-ZSM5 zeolite. These results are in agreement with the concept of σ-basicity of C-H or C-C bond as proposed by Olah in 1972 [10]. Recently, Gates [74, 75, 76, 77] reported the catalytic activity of Fe and Mn promoted sulfated zirconia for the conversion of propane, ethane and methane. They suggested that sulfated zirconia based catalysts are able to activate the alkanes by formation of carbonium ion. However, this mechanism was criticized due to the lack of the evidence of superacidity of sulfated zirconia, which is necessary to protolyse C-H and C-C bonds.

The formation of carbenium ions by hydride abstraction from alkane in the presence of Lewis acid sites was also proposed in the induction period of alkane isomerization reaction on sulfated zirconia [78]. However, as suggested by Sommer, the formation of a weak metal-hydride bond from 100 kcal/mol strong C-H bond is not thermodynamically favorable under acidic conditions [72].

Protonation of traces of olefin impurities in the feed by Brønsted acid has also been proposed for the generation of the active species, carbenium ion. Tabora *et al.* [79] observed that sulfated zirconia exhibits an extremely low catalytic activity for n-butane skeletal isomerization at initial period before losing all activity when the butene impurities were completely removed from the reactant mixture.

On the other hand, even n-butane was carefully purified using an olefin trap, sulfated zirconia still showed an obvious activity for n-butane skeletal isomerization, which suggests that butene species could be formed *in situ* on the catalytic surface. Fărcaşiu *et al.* [80, 81] ascribed the initial activity to carbocation precursors formed through one electron oxidation of hydrocarbon by the sulfate groups; thus, sulfated zirconia possesses not only strong acid properties, but also oxidative property. For the isomerization reaction of n-butane, the promoting effect of transition metals was also believed to be the enhancement of the oxidative property of sulfated zirconia [26, 82]. Carbenium ion, which was assumed to be the active species for the alkane activation on acid catalysts, could be formed *via* protonation of butene by Brønsted acid sites. Therefore, the amount of the butene, in the feed as impurities or formed *in situ* could be the determining parameter for the reaction.

1.6.2. Skeletal isomerization step

In respect to the skeletal isomerization of carbenium ion on solid acid, inter-molecular and intra-molecular route are the main mechanisms proposed [72, 83, 84, 85,]. Since the higher

energetic demanding of intra-molecular skeletal isomerization of butyl-carbenium ion by formation of a primary one, the inter-molecular mechanism was speculated to be the favorite route, in which the reaction proceeds by the alkylation of butene with butyl carbenium ion and followed by cracking of C_8 intermediate. The kinetic results of butane isomerization were in agreement with the inter-molecular mechanism from the previous literature [86]. The high iso-butane selectivity (90-92 %) during n-butane reaction was explained by the different stability and reactivity of the C_8 isomers, while the low reaction rate of iso-butane was ascribed to the space hindrance of two iso-butyl groups. The kinetics of n-butane reaction in the presence of hydrogen at high pressure was also studied [87] and the reaction order of n-butane was higher than 1. Therefore, the inter-molecular mechanism was concluded to be predominant pathway in the reaction.

However, the intra-molecular mechanism was also proposed to be prevailing during alkane isomerization. The labeled carbon distribution in the products of mono ^{13}C labeled n-butane isomerization on sulfated zirconia in the presence of hydrogen revealed the intra-molecular route [88]. On the other hand, the cracking products of branched octants on sulfated zirconia at 373 K were found far different from those of n-butane reaction, which suggests that C_8 species should not be the main intermediates for iso-butane formation [89].

1.7 Scope and structure of this thesis

Sulfated zirconia as the alternative catalyst for short alkane isomerization process has been studied for over two decades owing to its unique catalytic activity at low temperature, especially for n-butane. The mechanisms of alkane activation on sulfated zirconia as well as the active structure of such a catalyst, however, are still the subjects under discussion. Therefore, this work aims at elucidating the mechanism of n-butane skeletal isomerization at 373 K and the crucial components of the active structure of sulfated zirconia.

The importance of the labile sulfates in active sulfated zirconia for n-butane isomerization is described in *Chapter 2*. The initial step and propagation step of n-butane skeletal isomerization on sulfated zirconia at 373 K was studied in *Chapter 3* and *4*. In *Chapter 5* is reported a novel method for preparation of active sulfated zirconia, gaseous SO_3 sulfation on crystalline zirconia, which circumvented the high temperature calcination step. Finally, the results of this thesis are summarized in *Chapter 6*.

References

[1]   G.A. Olah, Hydrocarbon Chemistry, John Wiley &Sons, Inc., 1995, p. 5.

[2]   F. Asinger, Paraffins, Pergamon Press, New York, 1968, P. 695.

[3]   C.D. Nenitzescu, A. Dragan, Chem. Ber. 66 (1933) 1892.

[4]   H.S. Bloch, H. Pines, L. Schmerling, J.Am.Chem.Soc. 69 (1946) 153.

[5]   UOP website.

[6]   F. Asinger, Paraffins, Pergamon Press, New York, 1968, P. 696-697.

[7]   G.A. Olah, G.K.S. Prakash, J. Sommer, Superacids, Wiley-Interscience, New York, 1985.

[8]   H. Meerwein, K. van Emster, Chem. Ber. 55 (1922) 2500.

[9]   R.C. Whitmore, J. Am. Chem. Soc. 54 (1932) 3274.

[10]   G.A. Olah, Angew. Chem. 12 (1973) 173.

[11]   G.A. Olah, J. Lukas, J. Am. Chem. Soc. 89 (1967) 2227.

[12]   J.F. Haw, B.R. Richardson, I.S. Oshiro, N.D. Lazo, J.A. Speed, J. Am. Chem. Soc. 111 (1989) 2052.

[13]   M.T. Aranson, R.J. Gorte, W.E. Farneth, D.J. White, J. Am. Chem. Soc. 111 (1989) 840.

[14]   A.G. Stepanov, K.I. Zamaraev, J.M. Thomas, Catal. Lett. 13 (1992) 407.

[15]   A.G. Stepanov, V.N. Romannikov, K.I. Zamaraev, Catal. Lett. 13 (1992) 395.

[16]   A.G. Stepanov, K.I. Zamaraev, Catal. Lett. 19 (1992) 153.

[17]   V.B. Kazansky, Catal. Today 51 (1999) 419.

[18]   V.C.F. Holm, G.C. Bailey, US Patent 3032599 (1962).

[19]   M. Hino, S. Kobayashi, K. Arata, J. Am. Chem. Soc. 101 (1979) 6439.

[20]   M. Hino, K. Arata, J. Chem. Soc. Chem. Commun. (1979) 477.

[21]   K. Arata, Adv. Catal. 37 (1990)165.

[22]   T. Yang, T. Chang, C. Yeh, J. Mol. Catal. A 115 (1997) 339.

[23]   C. Yeh, T. Yang, T. Chang, J. Mol. Catal. A 123 (1997) 163.

[24]   M. Hino, K. Arata, J. Chem. Soc. Chem. Commun. (1995) 789.

[25]   C.Y. Hsu, C.R. Heimbuch, C.T. Armes, B.C. Gates, J. Chem. Soc. Chem. Commun. (1992) 1645.

[26]   V. Adeeva, J.W. de Haan, J. Janchen, G.D. Lei, V. Schunemann, L.J.M. van de Ven, W.M.H. Sachtler, R.A. van Santen, J. Catal. 151 (1995) 364.

[27]   G.D. Karles, J.G. Ekerdt, Prepr. Am. Chem. Soc. Div. Pet. Chem. 37 (1992) 239.

[28]   Z. Gao, Y. Tang, J. Cheng, Huaxue Wuli Xuebao 6 (1993) 480 see CA 121:133367p.

[29]   Z. Gao, Y. Xia, W. Hua, C. Miao, Top. Catal. 6 (1998) 101.

[30]   P. Canton, R. Olindo, F. Pinna, G. Strukul, P. Riello, M. Meneghetti, G. Cerrato, C. Morterra, A. Benedetti, Chem. Mater. 13 (2001) 1634.

[31]   J.A. Moreno, G. Poncelet, J. Catal. 203 (2001) 453.

[32]   M. Hino, K. Arata, J. Chem. Soc. Chem. Commun. (1987) 1259.

[33]   J.C. Yori, C.L. Pieck, J.M. Parera, Catal. Lett. 52 (1998) 227.

[34]   S. Kuba, B.C. Gates, P. Vijayanand, R.K. Grasselli, H. Knözinger, Chem. Commun. (2001) 507.

[35]   M. Scheithauer, R. E. Jentoft, B. C. Gates, H. Knözinger, J. Catal. 191 (2000) 271.

[36]   D.A. Ward, E.I. Ko, Ind. Eng. Chem. Res. 34 (1995) 421.

[37]   D.A. Ward, E.I. Ko, J. Cat. 150 (1994) 18.

[38]   E. Escalona Platero, M. Penarroya Mentruit, Catal. Lett. **3**0 (1995) 31.

[39]   R.A. Comelli, C.R. Vera, J.M. Parera, J. Catal. 151 (1995) 96.

[40]   D.A. Ward, E.I. Ko, J. Cat. 157 (1994) 321.

[41]   C.R. Vera, J.M. Parera, J. Catal. 165 (1997) 254.

[42]   C. Morterra, G. Cerrato, F. Pinna, M. Signoretto, J. Catal. 157 (1995) 109.

[43]   A.F. Bedilo, A.S. Ivanova, N.A. Pakhomov, A.M. Volodin, J. Mol. Catal. A: Chemical 158 (2000) 409.

[44]   T. Yamaguchi, T. Jin, K. Tanabe, J. Phys. Chem. 90 (1986) 3148.

[45]   J.R. Sohn, H.W. Kim, J. Mol. Catal. 52 (1989) 361.

[46]   J.F. Haw, J. Zhang, K. Shimizu, T. N. Venkatraman, D.P. Luigi, W. Song, D.H. Barich, J.B. Nicholas, J. Am. Chem. Soc. 122 (2000) 12561.

[47]   J. Zhang, J.B. Nicholas, J.F. Haw, Angew. Chem. Int. Ed. 39 (2000) 3302.

[48]   T. Riemer, D. Spielbauer, M. Hunger, G.A.H. Mekhemer, H. Knözinger, J. Chem. Soc. Chem. Comm. (1994) 1181.

[49]   W. Stichert, F. Schüth, J. Catal. 174 (1998) 242.

[50]   W. Stichert, F. Schüth, S. Kuba, H. Knözinger, J. Catal. 198 (2001) 277.

[51]   C.R. Vera, C.L. Pieck, K. Shimizu, J.M. Parera, Appl. Catal. A 230 (2002) 137.

[52]   N. Katada, J. Endo, K. Notsu, N. Yasunobu, N. Naito, M. Niwa, J. Phys. Chem. B 104 (2000) 10321.

[53]   E. Escalona Platero, M. Peñaroya Mentruit, C. Otero Arean, A. Zecchina, J. Catal. 162

(1996) 268.

[54]   D. Fărcaşiu, J.Q. Li, S. Cameron, Appl. Catal. A 154 (1997) 173.

[55]   T. Yamaguchi, K. Tanabe, Mater. Chem. Phys. 16 (1986) 67.

[56]   C. Morterra, G. Cerrato, M. Signoretto, Catal. Lett. 41 (1996) 101.

[57]   C. Morterra, G.Cerrato, G. Meligrana, M. Signoretto, F. Pinna G. Strukul, Catal. Lett. 73 (2001) 113.

[58]   B. Umansky, W.K. Hall, J. Catal. 124 (1990) 97.

[59]   L.M. Kustov, V.B. Kazansky, F. Figueras, D. Tichit, J. Catal. 150 (1994) 143.

[60]   F. Babou, G. Coudurier, J.C. Vedrine, J. Catal. 152 (1995) 341.

[61]   T. Yamaguchi, Appl. Catal. 61 (1990) 1.

[62]   Morterra, C., Cerrato, G., Di Ciero, S., Signoretto, M., Minesso, A., Pinna, F., and Strukul, G., Catal. Lett. 49 (1997) 25.

[63]   S.X. Song, R.A. Kydd J. Chem. Soc. Faraday Trans. 94 (1998) 1333.

[64]   M.R. Gonzalez, J.M. Kobe, K.B. Fogash, J.A. Dumesic, J. Catal. 160 (1996) 290.

[65]   A.G. Stepanov, M.V. Luzgin, A.V. Krasnoslobodtsev, V.P. Shmachkova, N.S. Kotsarenko, Angew. Chem. Int. Ed. 39 (2000) 3658.

[66]   M.V. Luzgin, A.G. Stepanov, V.P. Shmachkova, N.S. Kotsarenko, J. Catal. 203 (2001) 273.

[67]   A. Clearfield, G.P.D. Serrete, A.H. Khazi-Syed, Catal. Today 20 (1994) 295.

[68]   C. Morterra, G. Cerrato, V. Bolis, S. Di Ciero, M. Signoretto, J. Chem. Soc., Faraday Trans. 93 (1997) 1179.

[69]   M. Bensitel, O. Saur, J.C. Lavalley, B.A. Morrow, Mater. Chem. Phys. 19 (1988) 147.

[70]   R.L. White, E.C. Sikabwe, M.A. Coelho, D.E. Resasco, J. Catal. 157 (1995) 755.

[71]   C. Morterra, G. Cerrato, C. Emanuel, V. Bolis, J. Catal. 142 (1993) 349.

[72]   J. Sommer, R. Jost, M. Hachoumy, Catal. Today 38 (1997) 309.

[73]   W.O. Haag, R.M. Dessau, in: Proc. 8th Int. Congress on Catalysis, Berlin Vol. 2, Dechema, Frankfurt am Main, 1984, p. 305.

[74]   T.K. Cheung, B.C. Gates, J. Chem. Soc., Chem. Commun. (1996) 1937.

[75]   T.K. Cheung, B.C. Gates, J. Catal. 168 (1997)522.

[76]   T.K Cheung, F.C. Lange, B.C. Gates, J. Catal. 159 (1996) 99.

[77]   S. Rezgui, A. Liang, T.K. Cheung, B.C. Gates, Catal. Lett. 53 (1998) 1.

[78]   M. Marczewski, J. Chem. Soc., Faraday Trans., 82 (1986) 1687.

[79]   J.E. Tabora, R.J. Davis, J. Am. Chem. Soc. 118 (1996) 12240.

[80] R. Srinivasan, R.A. Keogh, A. Ghenciu, D. Fărcaşiu, B.H. Davis, J. Catal. 158 (1996) 502.

[81] D. Fărcaşiu, A. Ghenciu, J.Q. Li, J. Catal. 158 (1996) 116.

[82] K.T. Wan, C.B. Khouw, M. E. David, J. Catal. 158 (1996) 311.

[83] H. Matsuhashi, H. Shibata, H. Nakamura, K. Arata, Appl. Catal. A 187 (1999) 99.

[84] V. Adeeva, G.D. Lei, W.M.H. Sachtler, Catal. Lett. 33 (1995) 135.

[85] F. Garin, L. Seyfried, P. Girard, G. Maire, A. Abdulsamad, J. Sommer, J. Catal. 151 (1995) 26.

[86] K.B. Fogash, R.B. Larson, M.R. Gonzalez, J.M. Kobe, J.A. Dumesic, J. Catal. 163 (1996) 138.

[87] H. Liu, V. Adeeva, G.D. Lei, W.M.H. Sachtler, J. Mol. Catal. A 100 (1995) 35.

[88] F. Garin, L. Seyfried, P. Girard, G. Maire, A. Abdulsamad, J. Sommer, J. Catal. 151 (1995) 26.

[89] A. Sassi, J. Sommer, Appl. Catal. A General 188 (1999) 155.

Chapter 2

Labile sulfates as key components in active sulfated zirconia for n-butane isomerization at low temperature

Abstract

A wide variety of sulfate species exists on sulfated zirconia and many of these species have been connected to the catalytic performance. Some of these groups show strong interactions with polar molecules indicating that they may play a role for the catalytic properties. In order to differentiate between these groups and to explore the role of labile soluble sulfate for n-butane skeletal isomerization, active sulfated zirconia was washed with water. Water washing removed around 40 % of the sulfate species and led to a catalyst inactive for the alkane isomerization. This indicates that the labile sulfate plays a key role for the catalysis. The water soluble fraction of the sulfate exists as highly covalent sulfate species characterized by an S=O vibration between 1390 and 1410 cm^{-1} on the activated sulfated zirconia. Brønsted acid sites related to the sulfate groups are shown to be indispensable for activating n-butane, while Lewis acid sites do not directly participate in the alkane conversion catalysis.

2.1. Introduction

Sulfated zirconia and other sulfated metal oxides have been studied for over two decades owing to their high catalytic activity for activation of short alkanes at low temperature [1]. However, a general consensus on their surface chemical properties has not been reached. There are pronounced debates on the strength and type of acid sites, the state of the sulfate and the influence of the zirconia support [1, 2]. Because the strong acidity of sulfated zirconia is related to the introduction of sulfate species on the zirconia surface, the state of the sulfate has been frequently explored.

Using IR spectroscopy to investigate sulfated zirconia, Yamaguchi [3] proposed that the sulfate species after hydration is similar to inorganic chelating bidentate species. Removal of water resulted in the formation of a sulfate resembling more organic sulfates with a stronger covalent character of the S=O double band. The model proposed by Arata *et al.* [4] also involves a bidentate sulfate.

However, Lavalley *et al.* [5] proposed a structure model of sulfated zirconia with tridentate surface sulfate species containing just one S=O bond based on their IR results of ^{18}O exchange using $H_2^{18}O$ vapor at 450°C. The results of Riemer *et al.* [6] also supports the presence of tridentate surface sulfate species. However, these authors suggested a HSO_4^- group being present at the surface, because an O-H stretching band at 3650 cm^{-1} was observed in the presence of sulfates, which was absent on the sulfate-free material. White *et al.* [7], in contrast, proposed a penta-coordinated sulfur in the active structure of sulfated zirconia.

Mono-dentate bisulfate species (HSO_4^-) are proposed in models independently by Kustov *et al.* [8] and Adeeva *et al.* [9]. The bisulfate OH group is hydrogen-bonded to one surface oxygen atom of zirconia. Bi-dentate bisulfate-like species were also affiliated with the formation of Brønsted acid sites in the active structure models of Clearfield *et al.* [10], Morterra *et al.* [11] and Lavalley *et al.* [5]. The model proposed by Riemer *et al.* [6] involves a tri-dentate bisulfate-like species. In contrast, Babou *et al.* [12] suggested sulfated zirconia to be sulfuric acid grafted at the zirconia surface. A compilation of these species is presented in Table 2.1 as an overview for a starting point of discussion.

IR spectroscopy [13] and calculations based on density functional theory [14] demonstrated that several kinds of sulfur species could be present on sulfated zirconia. It is, however, also suggested that the caution should be taken when linking such spectroscopic studies with catalytic activity, since the information derived could originate from "spectator" sulfate groups [15].

Table 2.1 Sulfated zirconia surface models proposed in the previous literatures.

Authors	Surface model	Authors	Surface model
Yamaguchi [3]		Kustov *et al.* [8]	
Arata *et al.* [4]		Adeeva *et al.* [9]	
Lavalley *et al.* [5]		Clearfield *et al.* [10]	
Riemer *et al.* [6]		Morterra *et al.* [11]	
White *et al.* [7]		Babou *et al.* [12]	

The problem is complicated by the fact that sulfated zirconia is a very sensitive material and many variants may exist, despite the fact that industrial catalysts have been developed [16, 17]. Thus, we have decided to revisit the problem of the nature of the catalytically active surface and the elementary steps of alkane activation of these materials in a larger team of several groups addressing the problem rigorously in a multitude of approaches ranging from surface science *via* model catalysts to explore industrial catalysts.

In this study, we present here for the first time direct evidence that in a commercial sample of active sulfated zirconia only a part of the sulfate groups, which can be removed by water washing, are the key elements for active species able to convert light alkanes at low temperatures. In order to preliminary characterize and understand the nature and function of the labile sulfate, activated samples and those in contact with adsorbed probe molecules were

investigated with IR spectroscopy and a variety of physicochemical techniques and tested for the isomerization of n-butane.

2.2. Experimental

2.2.1. Catalyst preparation

Sulfate-doped zirconium hydroxide was obtained from Magnesium Electron, Inc. (XZO 1077/01). The received material was heated up to 873 K with an increment of 10 K/min in static air and kept at 873 K for 3 h. This material is denoted as SZ in the following.

To wash this calcined material 20 g of SZ was suspended in 400 ml bi-distilled water for 20 min and then filtered. The washing procedure was repeated 3 times. Then, the filter cake was dried at room temperature. The resulting powder is denoted as SZ-WW.

2.2.2. Catalyst characterization

The BET surface area and pore size of sulfated zirconias were determined using a PMI automated BET-sorptometer at 77.3 K using nitrogen as sorbate gas.

The sulfate content (SO_4^{2-} mmol/g) of the catalysts was determined using ion chromatography (IC) as described in ref. [18]. For this, 0.02 g of sulfated zirconia was suspended in a 0.01 N solution of NaOH for 20 min. Then, the solution was filtered through a 0.45 μm filter. The sulfur content in the liquid was determined by the ion chromatography (Metrohm, 690 ion chromatograph equipped an IC anion column).

The XRD patterns of the sulfated zirconias were measured with a *Philips X'Pert-1* XRD powder diffraction-meter using Cu Kα radiation.

IR spectra of catalyst samples were collected using a Bruker IFS 88 (or alternatively a Perkin–Elmer 2000) spectrometer at 4 cm^{-1} resolution. Self-supporting wafers with a density of 5–10 mg/cm^2 were prepared by pressing the sample. The wafers were placed into in a stainless steel cell with CaF_2 windows, heated up gradually with 10 K/min to 673 K in a flow of helium (10 ml/min), and held at that temperature for 2 hours. A spectrum was recorded after the temperature was stabilized at 373 K. For adsorption of pyridine and CO_2 the experiments were conducted in a high vacuum cell with a base pressure of 10^{-6} mbar. The sample wafer was heated up gradually with a rate of 10 K/min to 673 K and held at that temperature for 2 hours. The samples were exposed subsequently to 0.1 mbar pyridine at 373 K and to 2 mbar CO_2 at ambient temperature. Subsequent evacuation and thermal treatments are described in the results section.

2.2.3. n-Butane isomerization

Isomerization of n-butane reactions was carried out in a quartz micro tube reactor (8mm inner diameter) under atmospheric pressure. Sulfated zirconia pellets (0.2 g, 355-710 μm) were loaded into the reactor and activated *in situ* at 673 K for 2 h in He flow (10 ml/min). Then, the catalyst was cooled to the 373 K and the reactant mixture (5 % n-butane in He, total flow of 20 ml/min) was passed through the catalyst bed. The n-butane (99.5 %, Messer) reactant was passed through an olefin trap containing activated H-Y zeolite (20g) before it was mixed with He in order to remove olefin impurities and traces of water. Traces of butenes were not detected in the reactant mixture after purification. The reaction products were analyzed on-line using an HP 5890 gas chromatography (GC) equipped with a capillary column (PLOT Al_2O_3, 50m × 0.32 mm × 0.52mm) connected to a flame ionization detector (FID).

2.3. Results and interpretation

2.3.1. Chemical and physicochemical properties

The sulfate content (SO_4^{2-} mmol/g), the (BET) specific surface area and the average pore size are compiled in Table 2.2. The calcined sulfated zirconia (SZ) and the water washed sample (SZ-WW) have high specific surface areas of 109 m^2/g and 130 m^2/g, respectively. It is important to note that the surface bound sulfate of calcined commercial sulfated zirconia is partially water soluble. This is clearly seen in the fact that the sulfate content of the water washed sample (SZ-WW) was 0.25 mmol/g, while the parent sample (SZ) had 0.44 mmol/g. This difference indicates that approximately 40 % of the total sulfate can be removed by washing with water as described.

Table 2.2 Physical properties of sulfated zirconia samples

Sample	BET area (m^2/g)	Sulfate content SO_4^{2-} (mmol/g)	Pore size (nm)
SZ	109	0.44	3.6
SZ-WW	130	0.25	3.6

The XRD pattern of SZ (see Figure 2.1) is characteristic of pure tetragonal zirconia. Washing with water reduced the fraction of the tetragonal phase and induced the appearance of a monoclinic phase in SZ-WW.
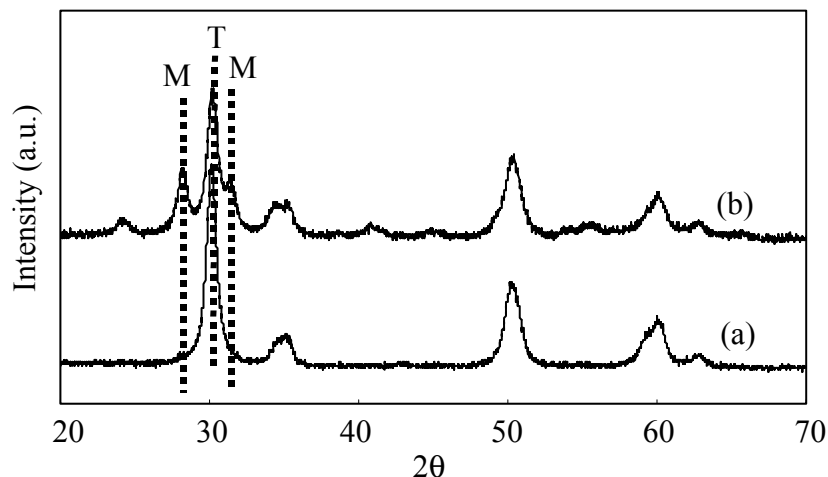
Figure 2.1 XRD profiles of sulfated zirconias (a) SZ and (b) SZ-WW

2.3.2. IR spectroscopy

Surface hydroxyl and sulfate groups of the activated samples

The IR spectra of sulfated zirconia (SZ) and water washed sulfated zirconia (SZ-WW) samples activated in He up to 673 K are shown in Figure 2.2, which were normalized by the thickness of the wafer. In the region of hydroxyl vibrations (Figure 2.2 (A)), the SZ sample showed a weak band at 3578 cm^{-1}, a strong asymmetric band at 3634 cm^{-1} with a shoulder at 3660 cm^{-1} and very weak bands at 3740 and 3710 cm^{-1}. Washing with water (SZ-WW, see Fig. 2.2 (A) (b)) led to the disappearance of the bands at 3578 and 3634 cm^{-1} and to an increase in the intensity of the OH band at 3660 cm^{-1}. In addition, a group of small bands at 3775, 3760 and 3747 cm^{-1} was also observed.

For activated zirconia, two bands attributed to the OH groups have been reported [19, 20]. The higher frequency band ($\sim$3760 cm^{-1}) is attributed to terminal OH groups, which are mono-coordinated to the ZrO$_2$ surface. The lower frequency band ($\sim$3680 cm^{-1}) is attributed to the bridging OH groups, which are bi- or tri- coordinated to the zirconia surface. The broad band at 3500 to 3600 cm^{-1} is attributed to strongly hydrogen bonded OH groups [19].

The increase in the terminal and bridged OH groups by water washing indicates that the removal of water soluble sulfate groups induces more sites for generating zirconia surface OH groups. The lower wavenumber of the bridged OH group in the presence of water soluble sulfate (compared to the wavenumber of OH groups in the water washed sample) is attributed to the surface inductive effect of the sulfate group *via* electron withdrawal and bond polarization [21]. The multiplicity of components in the 3500-3800 cm^{-1} region is attributed to

31

surface heterogeneity. In the presence of water soluble sulfates, a weak, broad band at 3578 cm^{-1} characteristic of hydrogen bonded OH groups was observed after activation.

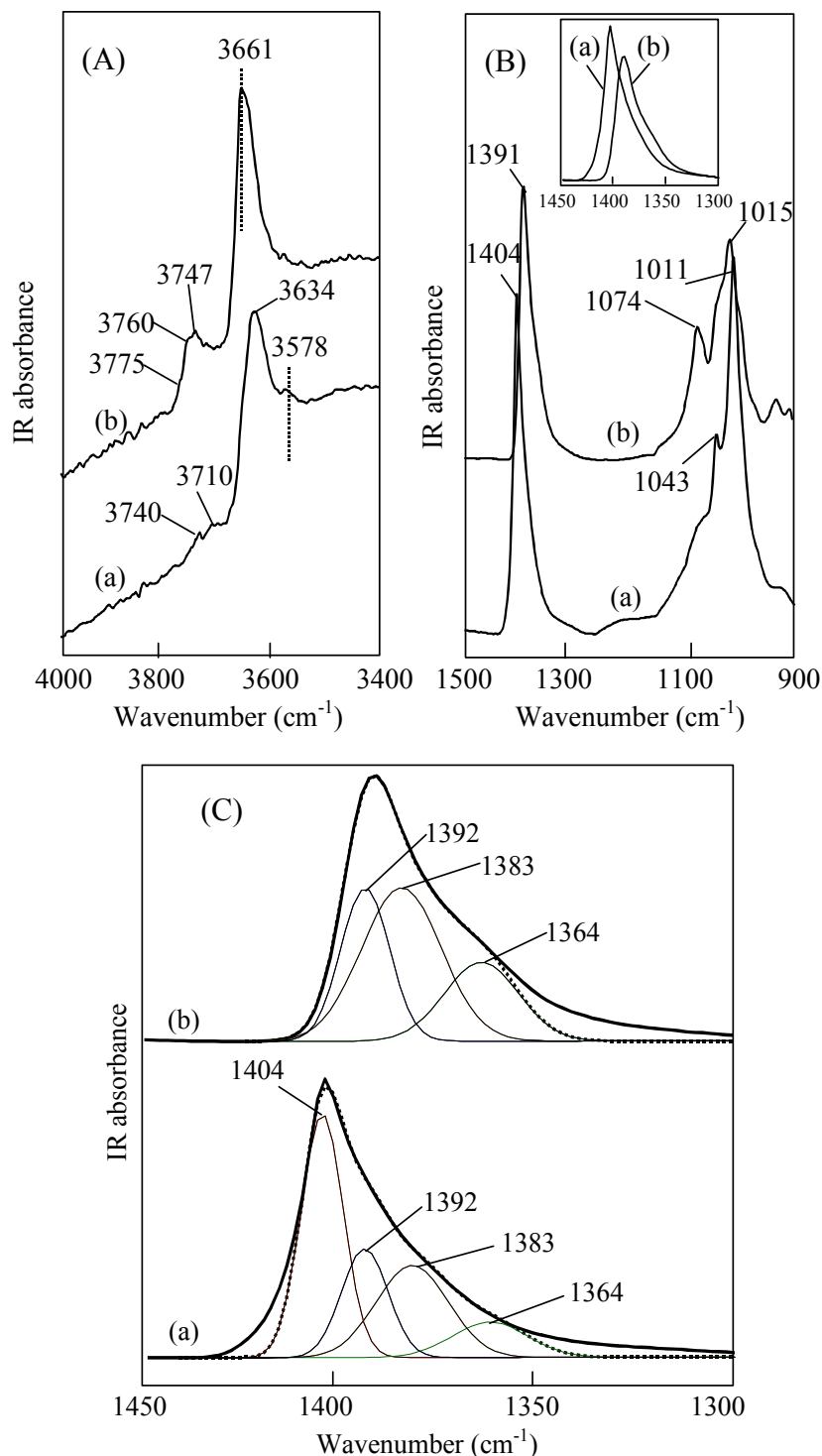**Figure 2.2** IR spectra of sulfated zirconia samples at 373 K after *in situ* activation in He at 673 K for 2 h (a) SZ and (b) SZ-WW

The IR spectra of sulfate groups of these two samples after activation are shown in Figure 2.2 (B). Both spectra exhibit two groups of bands at 1300-1450 cm^{-1} and 900-1150 cm^{-1}, which is in good agreement with the IR spectra of sulfated zirconia reported previously [22,

23]. The group of bands between 1300 and 1450 cm^{-1} is attributed to S=O stretching vibrations of sulfate groups. The bands at 900-1150 cm^{-1} are assigned to the vibrations of S-O bonds of sulfate species connected to the zirconia surface.

The S=O stretching band of SZ was located at a rather high frequency, with a pronounced maximum at 1404 cm^{-1} and a broad portion to the low frequency side. The spectrum of SZ-WW showed the maximum of this band at 1391 cm^{-1} and the intensity was lower than with SZ. The insert in Figure 2.2 (B) shows the S=O stretching bands of these two samples. The IR bands of S=O vibration of SZ and SZ-WW were fitted using a minimum number of bands and constant wavenumbers and half widths (see Figure 2.2 (C)).

The deconvolution results reveal that water washing reduces the portion of sulfate group at the higher frequency (1410 -1390 cm^{-1}) in the region of S=O stretching vibration of sulfate groups. Higher wavenumbers of the S=O stretching vibration indicate a higher S=O bond order [24, 25]. Therefore, we conclude that water washing reduces the fraction of the most covalent sulfate. In addition to the changes of the S=O vibration band, the intensity of the S-O stretching vibration bands also decreased and shifted to higher wavenumbers after water washing (see Figure 2.2 (B)). SZ showed the S-O band at 1011 cm^{-1} with a minor contribution at 1043 cm^{-1}, while in the IR spectrum of activated SZ-WW the bands appeared at 1015 cm^{-1} and 1074 cm^{-1} respectively. Thus, the separation of the S=O and S-O vibrations is larger in the water soluble fraction than in the sulfate groups after washing.

IR spectra of adsorbed pyridine

IR spectra of adsorbed pyridine on SZ and SZ-WW at 373 K followed by evacuation at the same temperature are shown in Figure 2.3. Bands at 1544 and 1445 cm^{-1} indicate that after activation in vacuum at 673 K, Lewis and Brønsted acid sites are present on SZ. On SZ-WW only the band at 1445 cm^{-1}, characteristic for Lewis acid sites, was detected. The concentrations of the acid sites of these two samples are compiled in Table 3 using molar absorption coefficients of the bands of adsorbed pyridine equal to those determined for zeolites [26]. The concentrations of acid sites of these two samples demonstrate that water washing removes the Brønsted acidity of sulfated zirconia and increases the Lewis acid sites from 0.106 to 0.163 mmol/g. It is interesting to note that for the two samples reported here, the total concentration of Lewis and Brønsted acid sits was nearly constant, (0.16 mmol/g). This suggests that Brønsted and Lewis acid sites on the sulfated zirconia samples investigated are related.

As shown in Figure 2.3, a marked shift of the band of S=O vibration after pyridine

adsorption indicates a strong impact of the adsorbed pyridine molecule on the sulfate. A similar effect has been reported previously [27, 28]. Note that the pyridine-sulfate interaction shifts all components of the S=O bands to lower wavenumbers, *i.e.*, to 1343 cm⁻¹ for SZ and to 1333 cm⁻¹ for SZ-WW, which indicates that all sulfate groups are located at the metal oxide surface and are influenced by or interact with pyridine. The band of the S-O vibration shifted approximately 30 cm⁻¹ to higher wavenumbers after pyridine adsorption. It indicates that the spectral separation between S=O and S-O decreased further by the interaction with the base. It can be speculated that the ionic character of the group increased in that process.

Table 2.3 Concentration of Brønsted and Lewis acid sites relative to pyridine adsorption/evacuation on sulfated zirconia samples.

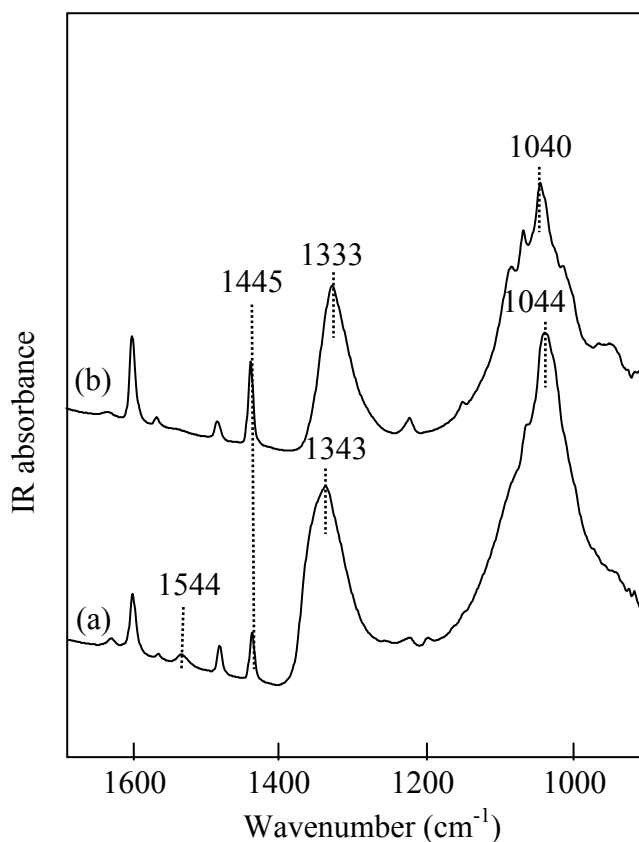| Sample	Brønsted acid (mmol/g)	Lewis acid (mmol/g)
SZ	0.050	0.106
SZ-WW	0	0.163

Figure 2.3 IR spectra of pyridine (0.1 mbar) adsorption followed by evacuation at 373 K on sulfated zirconia samples activated in vacuum at 673 K for 2 h (a) SZ and (b) SZ-WW

IR spectra of adsorbed CO$_2$

CO$_2$ is a suitable probe to characterize the surface basicity of metal oxide systems [29, 30]. The carbonate species formed after adsorption give rise to bands between 2000 and 1000 cm^{-1}. However, CO$_2$ is also a weak base, which can reversibly form weakly (and linearly) coordinated species with Lewis acid sites. Thus, CO$_2$ adsorption at room temperature can be used to probe base sites and the strongest fraction of Lewis acid sites.
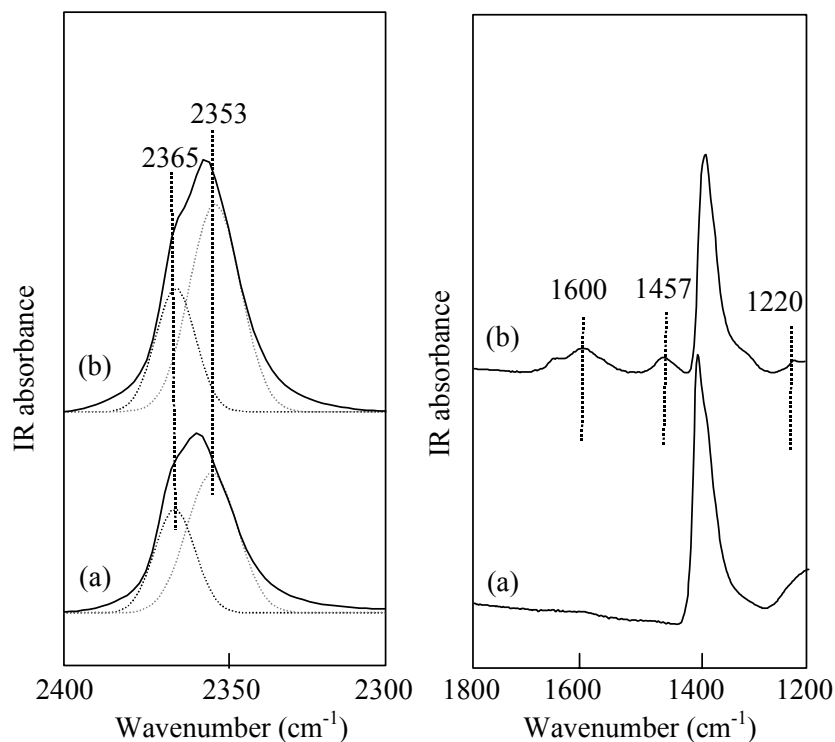
Figure 2.4 IR spectra of 2 mbar CO$_2$ adsorption at room temperature on sulfated zirconia samples activated at 673 K in vacuum for 2 h (a) SZ; (b) SZ-WW.

Figure 2.4 shows the IR spectra of SZ and WW-SZ (activated in vacuum for 2 h at 673 K) after equilibration with 2 mbar CO$_2$ at room temperature. With both samples bands at 2353 cm^{-1} and 2365 cm^{-1} attributed to linearly coordinated CO$_2$ were observed. As the upward shift of the asymmetric stretching band of adsorbed CO$_2$ is related to the strength of the bonding by the Lewis acid site [30], we conclude that the Lewis acid strength is not changed in the presence or absence of labile sulfate groups. The intensity of the band of adsorbed CO$_2$ on SZ-WW is significantly higher than that on SZ indicating a significantly higher concentration of Lewis acid sites on SZ-WW.

With SZ, bands between 1800 and 1200 cm^{-1} characteristic for carbonates were not observed. With SZ-WW, two pronounced bands at 1600 cm^{-1} and 1457 cm^{-1} with another

35

minor band at 1220 cm^{-1} characteristic of bicarbonate were observed. This implies that removing the water soluble sulfate by washing strongly increased the concentration of basic sites on the surface of the resulting material.

2.3.3. Catalytic activity for n-butane skeletal isomerization

Figure 2.5 shows the catalytic activity versus time on stream for n-butane skeletal isomerization at 373 K on SZ and SZ-WW. It should be emphasized that great care has been taken to remove all traces of butenes from n-butane, as such impurities (causing much higher activity) lead to uncontrollable behavior and mask differences between the catalysts. The butenes impurity in n-butane in this study was below 1 ppm (undetectable by the GC analysis used).

Under the reaction conditions employed an induction period of approximately 4 h was observed. It has been suggested that carbenium ion type intermediates, formed by protonation of butene, accumulate on the catalytic surface during this period [31]. After the induction period, SZ shows a maximum catalytic activity of 0.015 μmol/g·s with an iso-butane selectivity of 96 %. The variation of reaction conditions reported in the literature (reaction temperature, butane concentration, atmosphere, *etc.*) makes unfortunately nearly impossible to directly compare the reaction rates.

The problem of the direct comparison is well illustrated by the data of Sayari *et al.* [31] and Tabola *et al.* [32] performing the reaction at 363 and 373 K. Tabola *et al.* reports the maximum activity to be approximately 40 μmol/g·s, which is orders of magnitude higher than our results. The higher activity is attributed to the presence of 4000 ppm butene in n-butane. It is interesting to note in this context that these authors also demonstrated that removal of olefin impurities with 2 g of activated SZ induced an extremely low activity for a short period before the materials became totally inactive.

The removal of the water soluble sulfate fraction on calcined sulfated zirconia resulted in a sample (SZ-WW) which was inactive for n-butane skeletal isomerization at 373 K.
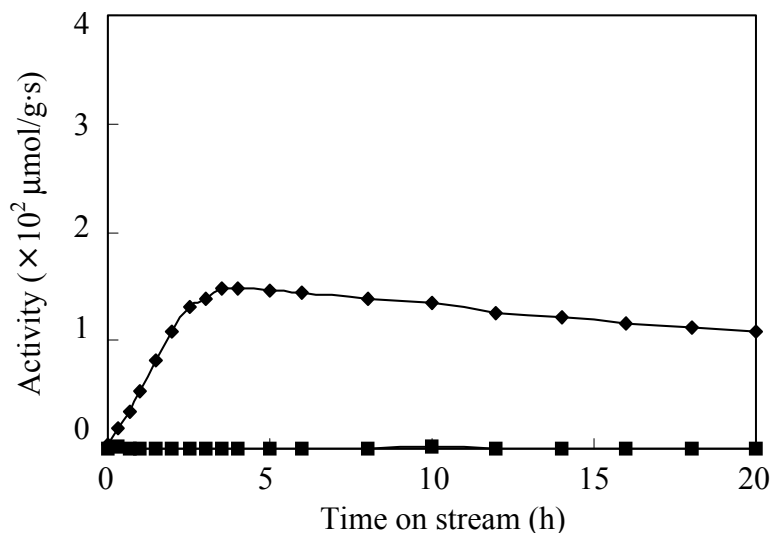
Figure 2.5 n-Butane skeletal isomerization reaction (5 % n-butane in He,
20 ml/min) rate versus time on stream on activated sulfated
zirconias at 373 K (■) SZ-WW and (◆) SZ.

2.4. Discussion

All sulfate species of sulfated zirconia are highly covalently bound to the surface compared to the inorganic sulfate salts, which can be clearly inferred from the differences in the IR spectra of ionic SO_4^{2-} (band between 1050-1250 cm^{-1}) and surface bound sulfate (bands centered at 1200 cm^{-1}) [21]. Together with the partial hydroxylation, the higher covalence of the sulfate groups has been affiliated with the high acid strength of sulfated zirconia.

The S=O bands of sulfates were observed at 1404 cm^{-1} for SZ and at 1391 cm^{-1} for SZ-WW suggesting that the labile sulfate species in SZ is more covalent than the water insoluble sulfate of the SZ-WW sample. The IR spectra also showed that the highly covalent (labile) sulfate has a large spectral separation of the vibration of S=O and S-O bands, which indicates that the bonding electrons in the sulfate groups are relatively well-localized, compared to the symmetric inorganic sulfate (one broad band between 1200 and 1100 cm^{-1}). The downward shift of the sulfate S=O band and the upward shift of the S-O band upon interaction with pyridine are attributed to an increase in the ionic properties of sulfate generated by the interaction with a base molecule.

The removal of the labile fraction of the sulfate induces the formation of bicarbonates, when the sample is exposed to CO_2. This indicates that the base strength of at least a fraction of the surface is as high as that of pure ZrO_2, as the carbonate formed on SZ-WW is identical with the carbonates on pure ZrO_2. From this we conclude that the removal of a fraction of the

sulfate has led to parts of the surface being bare of sulfate groups.

A consensus has been reached that active sulfated zirconia, when evacuated at 300-450 °C possessed not only Lewis but also Brønsted acid sites. The nature and formation of the Brønsted acid sites on sulfated zirconia is, however, still debated. Ward and Ko [33] proposed that the strong Brønsted acidity of sulfated zirconia is generated from the surface OH group and that the proton donating ability was enhanced by the electron inductive effect of S=O group. On the other hand, Kustov *et al.* [8] and Adeeva *et al.* [9] attributed the formation of Brønsted acid to the surface bi-sulfate species. Consensus has been reached, however, that the surface coordinated unsaturated zirconium sites (CUS Zr^{4+}) are responsible for the formation of the Lewis acid sites.

It is striking that the washing procedure led to an increase in the concentration of Lewis acid sites. Adsorbed pyridine and CO_2 indicate that the strength of the Lewis acid sites is similar for SZ and SZ-WW. With both probe molecules the wavenumbers of the characteristic bands of the adsorbed species were identical with both samples explored. This is important as it resolves an old conflict with respect to the role of Lewis acid sites for catalysis.

In previous reports [34, 35], the catalytic activity of sulfated zirconia has also been attributed to the presence of Lewis acid sites, whose strength is enhanced by the electron withdrawing of sulfate groups. Here, we prepared two samples with exactly the same Lewis acid strength, SZ and SZ-WW. However, SZ-WW is inactive despite a higher concentration of Lewis acids sites of equal strength. Therefore, we conclude that Lewis acid sites are not directly involved in the isomerization of alkanes by sulfated zirconia at low temperature.

The increase in the concentration of Lewis acid sites by water washing, on the other hand, indicates that at least some of the labile sulfate groups are located on top of Lewis acid sites, presumably at the defective sites of zirconia surface. By interaction with the sulfate groups, these sites are saturated and Lewis acidity is lost. Thus, the presence of the labile sulfate groups on the surface diminishes not only the basic sites, but also a portion of Lewis acid sites. The fact that the sum of Brønsted and Lewis acid sites remains constant for the two samples suggests that the Brønsted acid sites are affiliated with sulfate groups covering Lewis acid sites. It also demonstrates unequivocally that Brønsted acid sites are indispensable for the skeletal isomerization of n-butane.

2.5. Conclusion

At least two types of sulfate groups exist on the surface of active sulfated zirconia. One of those types of sulfate groups can be removed by washing with water at ambient temperature. Approximately 40 % of the sulfur in the sulfated zirconia can be removed in this way. A fraction of the sulfate removed *via* this way is located on top of a Lewis acid site (coordinatively unsaturated Zr^{4+}), which has a more covalent S=O bond than all species remaining on the surface after washing. It can be clearly identified by a narrow S=O band at 1404 cm^{-1}. The hydroxyl groups affiliated with these labile sites and the sites of the catalytically active Brønsted acid sites are characterized by a broad IR band characteristic of hydrogen bonded OH groups. The exact nature of this site is not subject of the present contribution. It is shown, however, that the OH groups of ZrO_2 are not involved in the catalysis and in the generation of strong Brønsted acid sites able to protonate pyridine.

The catalytic isomerization of n-butane requires the labile sulfate. In the absence of the labile sulfate the material is completely inactive for n-butane isomerization at 373 K. Because the washing procedure increases the concentration of Lewis acid sites without decreasing their strength, we can unequivocally conclude that Lewis acid sites of sulfated zirconia are insufficient to catalyze n-butane isomerization. We conclude in consequence that Brønsted acid sites affiliated with the labile sulfate groups are indispensable for this reaction.

References

[1]   X. Song, A. Sayari, Catal. Rev. Sci. Eng. 38 (1996) 329.

[2]   G. Yadav, J.J. Nair, Micropor. Mesopor. Mater. 33 (1999) 1.

[3]   T. Yamaguchi, Appl. Catal. 61 (1990) 1.

[4]   K. Arata, M. Hino, Appl. Catal. 59 (1990) 197.

[5]   M. Bensitel, O. Saur, J.C. Lavalley, B.A. Morrow, Mater. Chem. Phys. 19 (1988) 147.

[6]   T. Riemer, D. Spielbauer, M. Hunger, G.A.H. Mekhemer, H. Knözinger, J. Chem. Soc.

Chem. Comm. (1994) 1181.

[7]   R.L. White, E.C. Sikabwe, M.A. Coelho, D.E. Resasco, J. Catal. 157 (1995) 755.

[8]   L.M. Kustov, V.B. Kazansky, F. Figueras, D. Tichit, J. Catal. 150 (1994) 143.

[9]   V. Adeeva, J.W. de Haan, J. Janchen, G.D. Lei, V. Schunemann, L.J.M. van de Ven, W.M.H. Sachtler, R.A. van Santen, J. Catal. 151 (1995) 364.

[10]   A. Clearfield, G.P.D. Serrete, A.H. Khazi-Syed, Catal. Today 20 (1994) 295.

[11]   C. Morterra, G. Cerrato, F. Pinna, M. Signoretto, J. Phys. Chem. 98 (1994) 12373.

[12]   F. Babou, G. Coudurier, J.C. Vedrine, J. Catal. 152 (1995) 341.

[13]   C. Morterra, G. Cerrato, C. Emanuel, V. Bolis, J. Catal. 142 (1993) 349.

[14]   F. Haase, J. Sauer, J. Am. Chem. Soc. 120 (1998) 13503.

[15]   M. Benaïssa, J.G. Santiesteban, G. Díaz, C.D. Chang, M. José-Yacamán, J. Catal. 161 (1996) 694.

[16]   M.J. Clveland, C.D. Gosling, J. Utley, J. Elstein, NPRA 1999 Annual Meeting.

[17]   T. Kimura, Catal. Today 81 (2003) 57.

[18]   P. Canton, R. Olindo, F. Pinna, G. Strukul, P. Riello, M. Meneghetti, G. Cerrato, C. Morterra, A. Benedetti, Chem. Mater. 13 (2001) 1634.

[19]   W. Hertl, Langmuir, 5 (1989) 96.

[20]   A.A. Tsyganenko, V.N. Filimonov, J. Mol. Struct. 19 (1973) 579.

[21]   C. Morterra, G. Cerrato, G. Meligrana, M. Signoretto, F. Pinna G. Strukul, Catal. Lett. 73 (2001) 113.

[22]   C. Morterra, G. Cerrato, C. Emanuel, V. Bolis, J. Catal. 142 (1993) 349.

[23]   C. Morterra, G. Cerrato, F. Pinna, M. Signoretto, J. Catal. 157 (1995) 109.

[24]   T. Yamaguchi, T. Jin, K. Tanabe, J. Phys. Chem. 90 (1986) 3148.

[25]   M. Waqif, J. Bachelier, O. Saur, J.C. Lavalley, J. Mol. Catal. 72 (1992) 127.

[26]   C.A. Emeis, J. Catal. 141 (1993) 347.

[27]   D. Spielbauer, G. A. H. Mekhemer, M. I. Zaki and H. Knözinger, Catal. Lett. 40 (1996) 71.

[28]   E. Escalona Platero, M. Peñaroya Mentruit, C. Otero Arean, A. Zecchina, J. Catal. 162 1996) 268.

[29]   J.C. Lavalley, Catal. Today 27 (1996) 377.

[30]   V. Bolis, G. Magnacca, G. Cerrato, C. Morterra, Thermochim. Acta 379 (2001) 147.

[31]   A. Sayari, Y. Yang, X. Song, J. Catal. 167 (1997) 346.

[32]   J. E. Tabora, R. J. Davis, J. Am. Chem. Soc. 118 (1996) 12240.

[33]   D. A. Ward and E. I. Ko, J. Catal. 157 (1995) 321.

[34]   C. Morterra, G. Cerrato, F. Pinna, M. Signoretto, G. Strukul, J. Catal., 149 (1994) 181.

[35]   R.A. Keogh, R. Srinivasan, B.H. Davis, J. Catal., 151 (1995) 292.

<div align="right">

Chapter 3

</div>

Activation of n-butane isomerization on sulfated zirconia: oxidation of n-butane by surface groups

Abstract

Catalytic activation and conversion of light alkanes by sulfated zirconia (SZ), such as n-butane isomerization, is unequivocally shown to be initiated by a stoichiometric step producing small concentrations of olefins. The initiation step has been identified to be an oxidation reaction (C_4H_{10} + $SO_4^{2-}(SO_3)$ $\rightarrow$ C_4H_8 + H_2O + $SO_3^{2-}(SO_2)$) producing stoichiometric amounts of butenes, water and SO_2. A combination of thermal desorption methods and *in situ* spectroscopy has been used to determine all three reaction products. Supporting the important role of butene for catalytic activity, it is also shown additionally that supplying or removing butene in the overall reaction directly correlates with the catalytic activity, *i.e.*, butene impurities and the presence of oxygen increase, while the presence of hydrogen decreases the maximum activity observed. The thermodynamics of the reduction of different SZ surface structures by n-butane has been examined by density-functional (DFT) calculations with periodic boundary conditions. The calculations show that sulfate rich surface structures of SZ are the most likely to oxidize butane.
.

3.1. Introduction

Solid acids are environmentally benign catalysts for low temperature activation and transformation of alkanes. Among these, sulfated zirconia attracted marked interest during the past two decades [1] since Arata *et al.* [2, 3] rediscovered and reported the catalytic activity of sulfated metal oxides for n-butane activation. Despite these efforts and the development of industrial catalysts, consensus on the mechanism of alkane conversion has not been achieved, which is well documented in several reviews [1, 4, 5, 6].

The majority of reports propose that carbenium ion intermediates are the active species during catalysis at steady state. However, neither the nature of these carbenium ions nor the mechanism of their formation is well understood. Several hypotheses have been proposed. Gates *et al.* [7, 8, 9, 10] suggested that the catalytic activity of modified sulfated zirconia for the conversion of propane, ethane and methane is caused by the protolytic activation of short alkanes such as shown occurring with superacids in the liquid phase (see Equation 1 for n-butane as example).

$$\bigwedge\!\!\diagdown\!\!\diagup + \ H^+ \rightarrow \ \overset{H \underset{+}{} H}{\bigwedge\!\!\diagdown\!\!\diagup} \rightarrow \ \bigwedge\!\!\!\diagup\!\!\diagdown\!\!\diagup + \ H_2 \qquad\qquad (1)$$
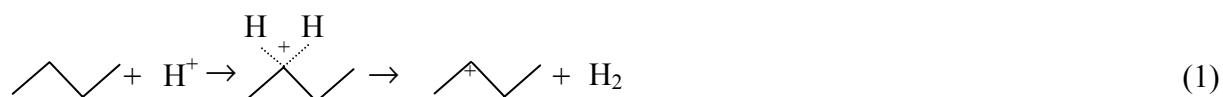
Later, however, it has been shown that SZ possesses high acid strength, but its strength does not exceed that of sulfuric acid, HZSM-5 or H-mordenite [11, 12]. Thus, considering the temperatures at which n-butane isomerization takes place, the reaction pathway seems unlikely.

At the same time, Tabora *et al.* [13] observed that sulfated zirconia exhibited extremely low catalytic activity for n-butane isomerization after removing all butene impurities from the feed. Thus, it was proposed that the butene impurities present in the reactant initiate n-butane reaction on SZ, *via* formation of carbenium ion intermediates.

$$\bigwedge\!\!\diagdown\!\!\diagup + \ H^+ \rightarrow \bigwedge\!\!\!\underset{+}{\diagup}\!\!\diagdown\!\!\diagup \qquad\qquad (2)$$

However, as sulfated zirconia still shows catalytic activity for n-butane isomerization after removal of butene impurities, it is suggested that butene species are formed *in situ*. Fǎrcaşiu *et al.* [14, 15] ascribed the initial activity to carbocation precursors formed through one electron oxidation of the alkane by sulfate groups. The promoting effect of transition metals doping sulfated zirconia was also attributed to the enhancement of the oxidative properties [16, 17]. What has been unclear and unproven in this group of proposed

mechanisms was the nature of the redox cycle involved. Evidence for the reduction and oxidation products has not been given and in consequence the mechanism was at best discussed as one of the possibilities for a reaction pathway.

The formation of butene by the oxidative species of sulfated zirconia or promoted sulfated zirconia could follow the Equation 3.

$$\text{/\textbackslash\textbackslash/} + \text{Ox.} \rightarrow \text{/\textbackslash\textbackslash/} + \text{Red.} + H_2O \qquad (3a)$$

$$\text{/\textbackslash\textbackslash/} + \text{Ox.} \rightarrow \text{/\textbackslash\textbackslash/} + \text{Red.} * H_2O \qquad (3b)$$

With Ox. = SO_3 and Red. = SO_2 this is an exothermic process with a reaction enthalpy of -28 kJ/mol [18]. DFT calculations reported below show that on the surface of SZ, Equation 3b, the corresponding reaction might be even more exothermic with the reaction energies up to -67 kJ/mol.

In this work, unequivocal direct evidence for all three potential reaction products of the initial alkane oxidation are given using thermal desorption/reaction of n-butane, *in situ* IR spectroscopy during reaction, and quantification of the SO_2 formed on the catalyst. It is emphasized that n-butane used in this study was carefully purified from traces of olefin before contacting it with sulfated zirconia. In order to demonstrate the subtle influences of the reaction conditions, the catalytic results are also compared with the conversion of unpurified n-butane and the conversion of the purified n-butane in the presence of hydrogen and oxygen. DFT calculations with periodic boundary conditions are carried out to explore the thermodynamics of the reduction and the accompanying water adsorption of different SZ surface structures by n-butane.

3.2. Experimental

3.2.1. Catalyst preparation

Sulfate-doped zirconium hydroxide was obtained from Magnesium Electron, Inc. (XZO 1077/01). The as-received sample was heated up to 873 K with a ramp rate of 10 K/min for 3 h in static air to form sulfated zirconia with 0.44 mmol/g sulfate and total surface area of 109 m^2/g.

3.2.2. Catalyst characterization

The ***temperature programmed desorption and reaction (TPD)*** of n-butane from SZ was measured in vacuum. The SZ sample was activated in vacuum (p = 10^{-3} mbar) at 673 K for 2 h and cooled to 323 K for n-butane adsorption. 2 mbar of n-butane (purified with an olefin trap containing activated commercial zeolite H-Y) was allowed to equilibrate with the sample for 5 min. After reducing the pressure to 10^{-3} mbar, TPD was carried out up to 873 K with a heating increment of 10 K/min. The desorbing species were detected by a mass spectrometer (QME 200, Pfeiffer vacuum).

For ***determining the amount of SO$_2$ produced*** during activation, n-butane reaction and temperature programmed desorption after the reaction, 100 ml of 0.005 N NaOH solution in a washing flask was used to collect SO_2 and SO_3 in the educts. The gases were trapped as sulfate and sulfite. Only the sulfate concentrations were determined by ion chromatography (Metrohm, 690 ion chromatograph equipped an IC anion column). Sulfite was oxidized in a second experiment with H_2O_2 (200 μl 30 %) and the solution was reanalyzed. The concentration of sulfite was determined from the difference between the two experiments.

In situ IR spectroscopy was used to monitor adsorbed species during n-butane isomerization using a Bruker IFS 88 spectrometer at 4 cm^{-1} resolution. Self-supporting wafer (5–10 mg/cm^2) were prepared by compacting the sample. The wafers were placed into in a stainless steel cell with CaF$_2$ windows, heated up with 10 K/min to 673 K in He flow (10 ml/min), and activated at that temperature for 2 hours. The wafer was then cooled to 373 K and the reactant mixture (5 % n-butane in He, total flow of 20 ml/min) was flown into the cell and a spectrum was collected every minute. n-Butane was purified with an olefin trap containing activated HY zeolite to remove the butene impurities.

3.2.3. n-Butane isomerization

n-Butane isomerization was carried out in a quartz micro tube reactor (8mm inner diameter) under atmospheric pressure. 0.2 g of sulfated zirconia pellets (355 - 710μm) were loaded into the reactor and activated *in situ* at 673 K for 2 h in He flow (10 ml/min). The catalyst was cooled to 373 K and the reactant mixture (5 % n-butane in He, total flow of 20 ml/min) was flown through the catalyst bed. n-Butane (99.5 %) was passed through an olefin trap containing activated H-Y zeolite before it was mixed with He. The butene concentration in the resulting gas was below the detection limit (1 ppm). Reaction products were analyzed on-line using an HP 5890 gas chromatography (GC) equipped with a capillary column (Plot Al$_2$O$_3$, 50m × 0.32 mm × 0.52mm) connected to a flame ionization detector (FID).

The skeletal isomerization of unpurified n-butane, containing 26 ppm 2-butene (molar basis), on sulfated zirconia at 373 K was also performed to investigate the influence of butene impurities in the feed.

n-Butane isomerization at 373 K were also carried out in the presence of different concentrations of hydrogen or oxygen for studying the influence enhancing or reducing the concentration of olefins on the catalytic activity.

3.2.4. Computational methods

The density-functional calculations used the gradient corrected Perdew-Wang functional PW91 [19, 20, 21, 22, 23]. Core electrons were described with the projector augmented wave scheme [24, 25]. The valence electrons were described by a plane wave basis set with an energy cutoff of 400 eV. Periodic boundary conditions were applied to an 1x2 surface cell of the t-ZrO_2(101), which includes four Zr atoms which miss one coordination compared to the bulk. A slab of five layers was used with three bottom layers fixed to the bulk positions. The cell sizes were a=6.425 Å, b=7.284 Å and c=30.000 Å. Further details are given in reference [26]. All calculations are made with the VASP code [27, 28, 29].

3.3. Results

3.3.1. Determination of the reaction products of the initiation reaction

The initiation reaction as formulated in Equations 3 is a stoichiometric reaction and should produce a measurable but small concentration of SO_2, H_2O and butene. The stoichiometry of the overall catalytic reaction requires, however, that the majority of catalytic cycles occur in a way that does not remove the hydrogen *via* oxidation, *i.e.*, that an efficient mechanism of hydrogen transfer exists. The experiments below establish this initiation as proven elementary step.

Evidence for butene formation by TPD of n-butane

As under steady state conditions butenes are not detected in the reaction products, temperature programmed reaction is used to give direct evidence of alkenes formed by suppressing subsequent reactions of the reactive alkenes. Figure 3.1 shows the evolution of butane and butene from SZ after n-butane adsorption at 323 K during TPD. Butene (m/e = 56) desorbed at low temperatures with a maximum rate at 380 K and a broad shoulder between 500 and 700 K. Note that much lower rates and quantities of desorbing butane were observed,

as most of it was already removed by the short evacuation period prior to TPD. Masses higher than that of the butane molecular peak were not observed. The fragment pattern observed in the mass spectra fits perfectly to the fragmentation pattern of butenes allowing us to exclude also the presence of other alkanes or alkenes. Thus, TPD of n-butane clearly shows that butene is formed from butane adsorbed on SZ at low temperatures. Molecular hydrogen gas was not observed during these experiments allowing us to exclude a route *via* the direct dehydrogenation.

However, also neither water nor SO_2 was detected in parallel to the desorbing butene. However, in contrast to H_2 which is only very weakly adsorbed on the sulfate modified oxides, water and SO_2 would be so strongly adsorbed that desorption would be shifted to higher temperatures and at these temperatures the formation is partly masked by the partial decomposition and dehydration of sulfated zirconia. The mass spectrometric analysis makes also difficult to differentiate between desorbing SO_2 and SO_3.
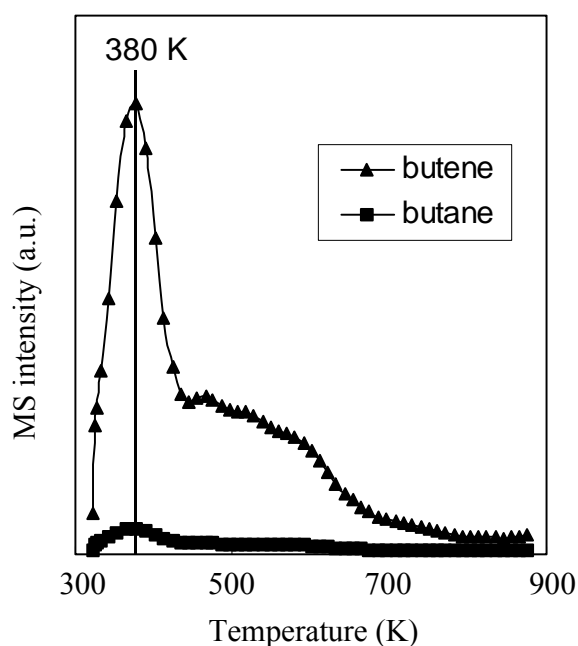

Figure 3.1 Peak desorption intensity of butene (m/e=56) and butane (m/e=58) during a vacuum TPD (heating rate of 10 K/min) after adsorption of 2 mbar of n-butane on activated sulfated zirconia at 323 K.

Determination of SO_2 formed

Thus, in order to qualitatively and quantitatively determine desorbing SO_x, the gases after the tubular reactor were passed through a NaOH washing solution. For this purpose, a larger catalyst bed (2 g of sulfated zirconia) was used. Desorbed SO_3 leads directly to sulfates, while

sulfites have to be oxidized by H_2O_2. Pretreatment of the solution with H_2O_2 was therefore used to differentiate between the formation of SO_2 and SO_3.

The sulfate ion peaks in the ion chromatography spectra are shown in Figure 3.2. During activation up to 673 K, a small amount sulfate species decomposed and desorbed as SO_3 from the catalyst (see Figure 3.2 (b)). This amount corresponded to 3 % of the total sulfate content of the SZ studied. During the reaction at 373 K sulfur compounds did not evolve from the reactor (see Figure 3.2 (c)). Thus, we concluded that SO_2 was either not formed during reaction or if it was, it was retained on the catalyst surface as sulfite group.
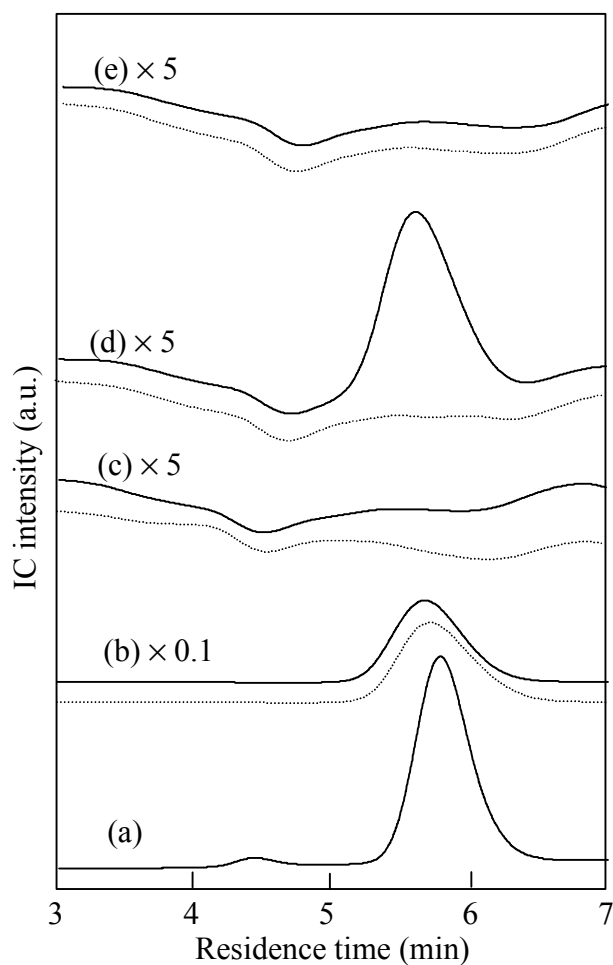

Figure 3.2 Sulfate ion peaks in IC spectra, dotted line: without adding H_2O_2; solid line: adding H_2O_2 200 μl (a) 5 mg/l of sulfate as standard, (b) after activation of sulfated zirconia at 673 K in He, (c) after the reaction at 373 K for 10 h (d) after increasing temperature from 373 K to 673 K following to the reaction and (e) after increasing temperature from 373 K to 673 K following to He treatment at 373 K.

In order differentiate between the two possibilities the reactor was purged with He for 30 min and then the temperature was increased with 10 K/min to 673 K in He flow. In contrast to

the activation of SZ, the solution of the trapped gases showed only a significant amount of sulfate ions after oxidation with H_2O_2 (Figure 3.2 (d)). Thus, we conclude that SO_2 and not SO_3 evolved from the reactor. Approximately 0.2 % of the total sulfate species in SZ were reduced by reaction with n-butane for 10 hours. The control experiment of increasing the temperature from 373 K to 673 K after exposing the activated catalyst to flowing He at 373 K did not lead to the evolution of SO_x (Figure 3.2 (e)).

Determination of water formed by *in situ* IR spectroscopy

The *in situ* IR spectra of SZ during n-butane reaction at 373 K are shown in Figure 3.3 (A) and (B). After activation at 673 K for 2 h the SZ sample showed a strong IR band at 3636 cm^{-1} with a shoulder at 3660 cm^{-1} and a weak band at 3580 cm^{-1} in the region of OH groups. The bands at 3636 and 3580 cm^{-1} are attributed to OH groups associated with the sulfate groups, while the shoulder at 3660 cm^{-1} is associated with ZrOH groups. In contact with butane a weak broad band between 3500 and 3600 cm^{-1} appeared, which is attributed to molecules hydrogen bonding to OH groups. Additionally, the IR band at 3580 cm^{-1} increased in intensity.
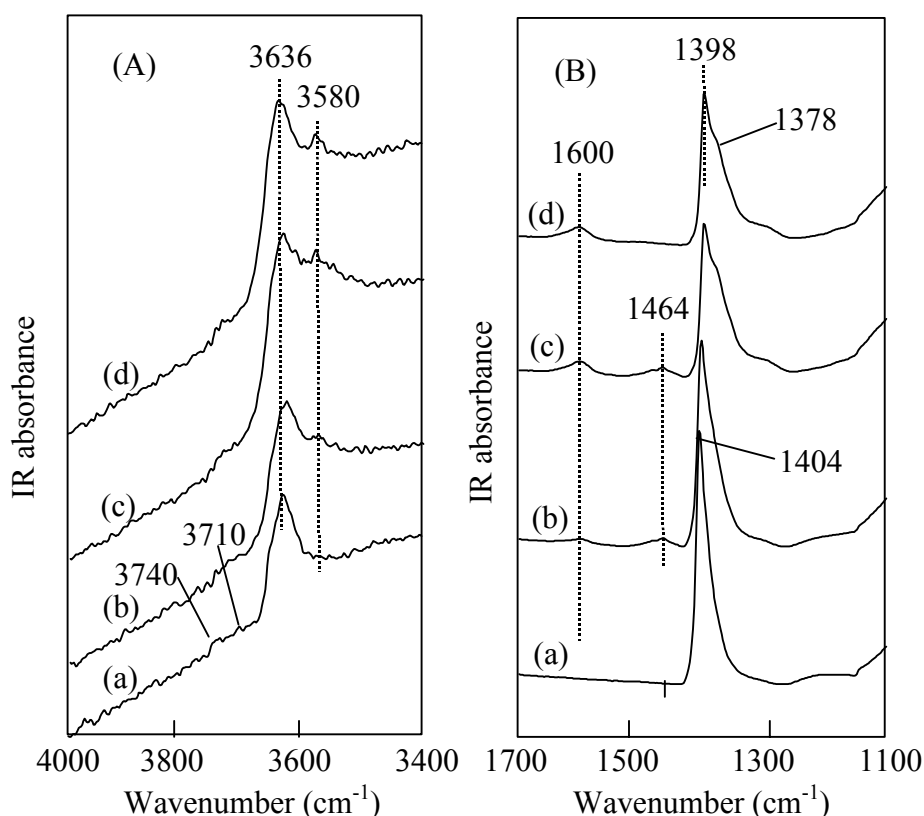

Figure 3.3 IR spectra of *in situ* n-butane reaction on sulfated zirconia at 373 K (5 % n-butane in He, 20 ml/min). (a) after activation (b) reaction for 60 min (c) reaction for 200 min (d) He purge for 10 min follows to the reaction.

Activated SZ showed a pronounced group of bands at 1300-1450 cm^{-1} with a maximum at 1404 cm^{-1}, which is assigned to the stretching vibrations of S=O bond (see Figure 3.3 (B)) in various sulfate groups. During n-butane isomerization, the band broadened and shifted to lower wavenumbers, *i.e.*, to 1398 cm^{-1} with a shoulder at 1378 cm^{-1} after reaction for 200 minutes. The band at 1464 cm^{-1} observed after bringing SZ in contact with butane is assigned to the CH$_2$ deformation vibration of butane. It disappeared after He purge for 10 min.

The formation of water during reaction is verified by the increasing intensity of the water deformation band at 1600 cm^{-1} with the time on stream. As shown in Figure 3.4, the evolution of the catalytic activity in the induction period occurred in parallel to concentration of water formation. The gradually formation of water on SZ indicates the oxidation of n-butane at 373 K is the determining step for the compiling of active species, which corresponds to the period of increasing activity in n-butane isomerization.
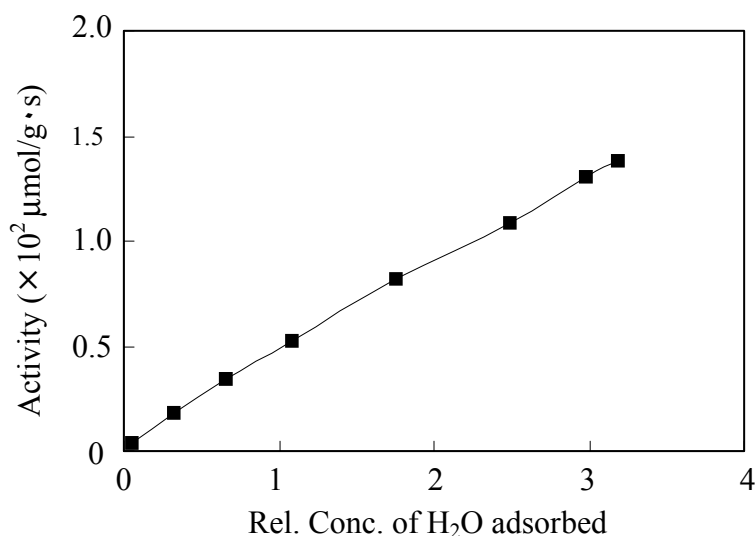

Figure 3.4 Correlation between catalytic activity of sulfated zirconia for n-butane isomerization at 373 K during induction period and the concentration of water formed during *in situ* IR reaction.

3.3.2. Promoting effect of butene impurities on the catalytic activity

Figure 3.5 shows the n-butane isomerization activity versus time on stream (TOS) on SZ at 373 K with purified and unpurified n-butane. The butene impurities significantly enhanced the catalytic activity. Both reactions showed a period of increasing activity, during which the active species, *i.e.,* carbenium-type intermediates, and water (see above) accumulate on the surface. Reaching the maximum activity was followed by gradual deactivation. The induction period for the reaction of purified n-butane was around 4 h, which was much longer than that of reactant without purification (1.5 h) under identical reaction conditions. The iso-butane

selectivity of both reactions was higher than 95% and the byproducts of the reaction were primarily propane, iso-pentane and n-pentane (the ratio of iso- to n-pentane was 4-5).
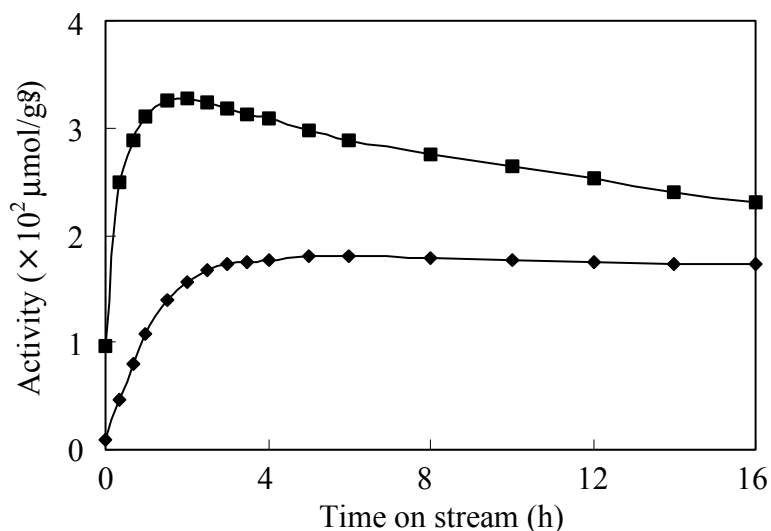

Figure 3.5 Catalytic activity of sulfated zirconia at 373 K for the isomerization reaction of n-butane (20 ml/min of 5 % n-butane in He) (♦) purified with olefin trap (■) unpurified and containing 26 ppm 2-butene.

3.3.3. Influence of H_2 and O_2 on the catalytic activity

Adding H_2 and O_2 to the carrier gas allows to important questions to be answered, *i.e.*, the role of hydrogen lies in reducing traces of olefins and/or intercepting possible hydride transfer reactions, and the role of oxygen is mainly to increase the local concentration of olefins. The reaction rates versus time on stream in the presence of hydrogen with different concentration are shown in Figure 3.6. The presence of hydrogen significantly lowered the catalytic activity, even when only 0.5 % H_2 was present in the feed. The catalytic activity was indirectly related to the concentration of H_2 (negative reaction order) in agreement with previous reports that hydrogen has a strongly negative effect on the rate of alkane isomerization [30].

Figure 3.7 shows the influence of the presence of oxygen in the reactant on the catalytic activity. With increasing oxygen partial pressure the initial increase in activity was higher and shorter, followed by rapid deactivation with TOS. For instance, the catalysts operated in the presence of 5 % oxygen was completely deactivated after 16 h TOS, while the one in the absence of oxygen or in the presence of hydrogen still had a very stable activity.
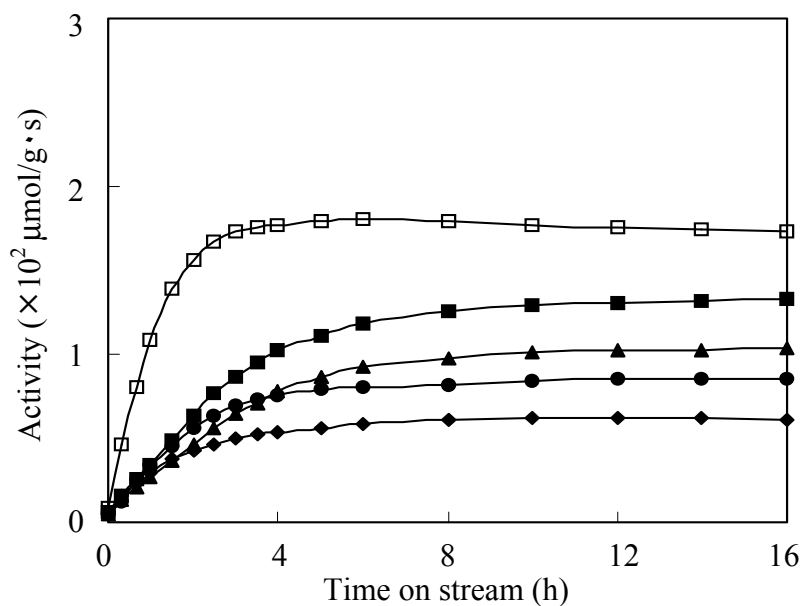
Figure 3.6 Catalytic activity of sulfated zirconia for the isomerization reaction of n-butane (20 ml/min of 5 % n-butane in He) at 373 K in the presence of hydrogen. The concentration of hydrogen in the feed: (□) 0 %, (■) 0.5 %, (▲) 1.5 %, (●) 2.5 %, (◆) 5 %.
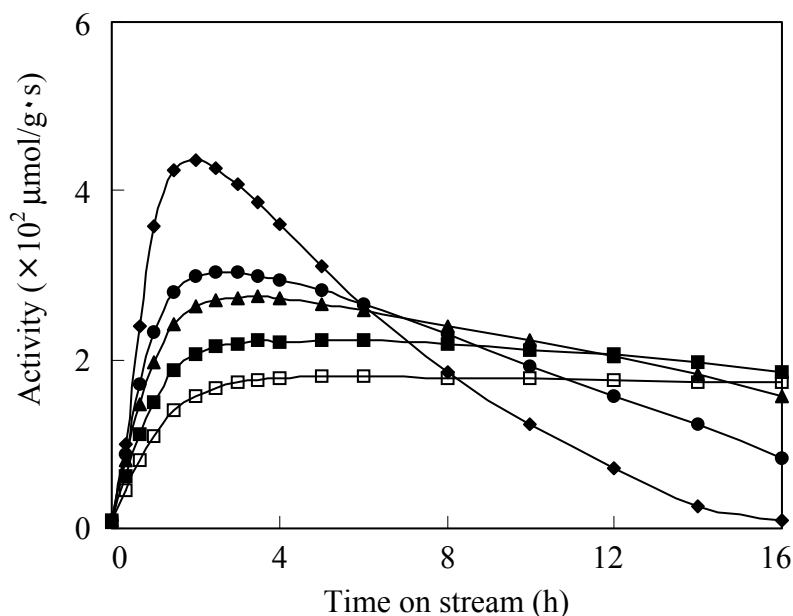

Figure 3.7 Catalytic activity of sulfated zirconia for the isomerization reaction of n-butane (20 ml/min of 5 % n-butane in He) at 373 K in the presence of oxygen. The concentration of oxygen in the feed: (□) 0 %, (■) 0.5 %, (▲) 1.5 %, (●) 2.5 %, (◆) 5 %.

3.3.4. Calculated reduction energies

In a previous DFT study we have calculated the structures and stabilities of different surface species for increasing loading of H_2SO_4 or SO_3 and H_2O adsorbed from the gas phase on t-ZrO_2(101) [26]. For a given composition different "isomeric" surface structures are examined and their stabilities compared. For example, H_2O can dissociate on the surface into H^+ and OH^- and form a bridging and a terminal hydroxyl group. The surface composition is written in brackets, *e.g.* [SO_3,OH^-,H^+,H_2O] denotes a surface phase with one SO_3 and two H_2O molecules adsorbed on a 1x2 t-ZrO_2(101) surface cell. One water molecule is dissociatively adsorbed. The surface phase [SO_4^{2-},OH^-,$3H^+$] has the same total composition, one SO_3 and two H_2O molecules on the surface, but $SO_3 \cdot H_2O$ is present as H_2SO_4 which is dissociatively adsorbed as SO_4^{2-},$2H^+$ and the second H_2O molecules is also dissociatively adsorbed.

The relative stability of surface structure with different composition depends on the concentration of sulfur containing species in the gas phase with which the surface is assumed to be in equilibrium. If we assume that H_2SO_4 and H_2O are present in the gas phase, the pyrosulfate phase [$S_2O_7^{2-}$,$2H^+$,H_2O] (Figure 3.8) is the prevailing structure for wide temperature and partial pressure ranges. If we assume equilibrium with SO_3 and H_2O in the gas phase the proton free [SO_3] structure dominates over wide temperature and partial pressure ranges. The vibrational spectra discussed in section 3.3.1 (Figure 3.3 (B)) indicate the presence of pyrosulfate species in the SZ sample used in this study. In a previous work we show that only loadings of two sulfates per 1x2 t-ZrO_2(101) surface cell exhibit vibrations above 1400 cm^{-1} and only pyrosulfate species vibrate in the region of 1420 – 1400 cm^{-1}. Coadsorption of water to the prevailing [$S_2O_7^{2-}$,$2H^+$,H_2O] species (ν(S=O) = 1421 cm^{-1}) [26], yielding [$S_2O_7^{2-}$,$2H^+$,$2H_2O$] (ν (S=O) = 1409 cm^{-1}), results in a red shift of the S=O mode of 12 cm^{-1}.

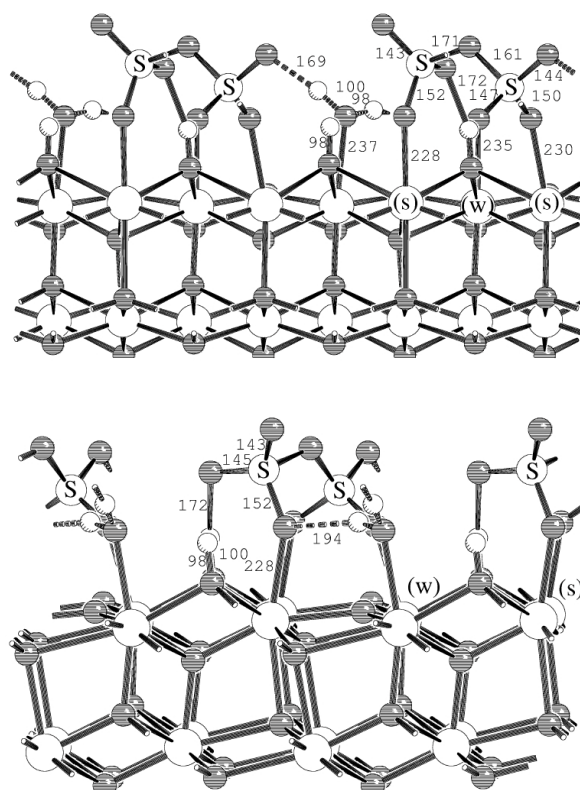**Figure 3.8** The structure of $[S_2O_7^{2-},2H^+,H_2O]$.

To characterize the oxidizing power of SZ, we calculate the reduction energy, ΔE_{red}, *i.e.* the energy of the following reaction:
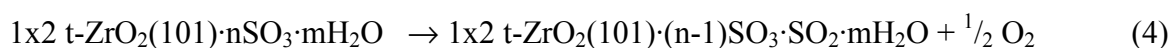
$$1x2 \text{ t-ZrO}_2(101)\cdot n\text{SO}_3\cdot m\text{H}_2\text{O} \rightarrow 1x2 \text{ t-ZrO}_2(101)\cdot(n-1)\text{SO}_3\cdot\text{SO}_2\cdot m\text{H}_2\text{O} + {}^1\!/_2 \text{ O}_2 \qquad (4)$$

Table 3.1 shows the results for the dominating $[SO_3]$ and $[S_2O_7^{2-},2H^+,H_2O]$ phases and for phases which a different number of H_2O molecules on the surface. The sulfated surfaces are much more easily reduced than the clean ZrO_2 surface. The reduction energies for the sulfated phases are roughly in the range between the gas phase reduction energies of H_2SO_4 (176 kJ/mol) and SO_3 (94 kJ/mol). They depend on the sulfur concentration of the surface. Surface structures with one SO_3 on the 1x2 surface cell have larger reduction energies, between 200 and 173 kJ/mol depending on the number of H_2O molecules on the surface. Surface structures with two SO_3 molecules on the 1x2 surface cell have lower reduction energies, between 165 and 106 kJ/mol. The prevailing $[SO_3]$ and $[S_2O_7^{2-},2H^+,H_2O]$ structures have reduction energies of +173 and +156 kJ/mol, respectively. The lowest reduction energy is found for the $[S_2O_7^{2-},2H^+]$ surface structure, +106 kJ/mol.

Table 3.1 also shows the heats of reduction at 298 and 398 K differ from the energies by not more than 10 kJ/mol. For the gas phase species comparison can be made with

experimental reaction heats. This indicates an error of about 20 kJ/mol of the calculated values.

Table 3.1 The reduction energy, ΔE_{red}, for the loss of ½ O_2 of different SZ structures in kJ/mol.

	ΔE_{red}	ΔH_{red}^{298K}	ΔH_{red}^{398K}
pure 1x2 t-ZrO_2(101)	554.5		
$[SO_3]^a$	173.2	174.1	166.2
$[SO_3,OH^-,H^+]$	177.6		
$[SO_4^{2-},2H^+]$	179.2		
$[SO_3,OH^-,H^+,H_2O]^a$	199.9	199.4	191.6
$[SO_4^{2-},2H^+,OH^-,H^+]$	189.9		
$[SO_4^{2-},2H^+,3H_2O]^a$	184.8	184.5	176.0
$[2SO_3]^a$	161.8	163.0	155.1
$[S_2O_7^{2-},2H^+]$	106.3	109.5	101.6
$[S_2O_7^{2-},2H^+,H_2O]^a$	155.5	156.5	148.4
$[SO_4^{2-},HSO_4^-,3H^+]^a$	164.6	166.4	158.6
$[S_2O_7^{2-},2H^+,2H_2O]$	124.3		
H_2SO_4 (gas)	176.3	154.0^b	153.8
SO_3 (gas)	94.3	80.8^c	80.9

[a] These structures are most stable for specific pressure and temperature regions.
[b] observed value 196.5 kJ/mol [18].
[c] observed value 98.9 kJ/mol [18].

3.4. Discussion

The presented data show for the first time that in the initiation step butene is formed together with water and SO_2 or sulfite following the reaction mechanism noted in Equation 3. This demonstrates the strong oxidizing ability of labile sulfate groups identified to be indispensable for catalysis in an earlier contribution [31]. The alkene formed reacts immediately with Brønsted acid sites of sulfated zirconia forming an alkoxy group or carbenium ion, which is the key intermediate. The accumulation of the alkoxy groups/carbenium ions seems to be the most important change in the surface chemistry during the activation (induction) period observed in so many studies and also in the present work. Water and SO_2 also formed in this step remain on the surface in a non-dissociated state.

The favorable reaction energies for the oxidative dehydrogenation of butane according to Equation 3 explain the initial butene formation. On the surface of SZ one of the SO_3 species is reduced to SO_2 and the H_2O molecule formed remains on the surface:

$$C_4H_{10} + 1x2\ t\text{-}ZrO_2(101)\cdot nSO_3\cdot mH_2O \rightarrow C_4H_8 + 1x2\ t\text{-}ZrO_2(101)\cdot(n-1)SO_3\cdot SO_2\cdot(m+1)H_2O \quad (5)$$
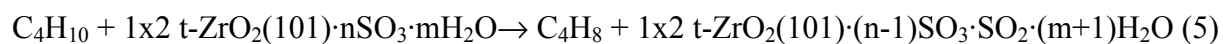
Table 3.2 shows the calculated energies for this reaction. For surface structures with a single sulfur atom per (1x2) surface unit cell the reaction energies are positive (6 to 47 kJ/mol depending on the water content), while structures with two sulfur atoms per cell have negative reaction energies (-10 to –67 kJ/mol). The reaction of one of the dominating pyrosulfate surface structures, $[S_2O_7^{2-},2H^+,H_2O]$, with butane yields the $[SO_4^{2-},SO_2,2H^+,2H_2O]$ structure shown in Figure 3.9 (reaction energy -10 kJ/mol). In this reaction, the pyrosulfate splits into a tri-dentate sulfate species and SO_2 which is not directly coordinated to the surface, but only to two water molecules via two hydrogen bonds (Figure 3.9). The energy expense for the removal of SO_2 is $E_{diss,SO2}$ = 34 kJ/mol. The less stable pyrosulfite structure would look like Figure 3.8, with one oxygen atom removed. Reaction 5 does not consider adsorption of butane/butene on the SZ surface. We expect that the adsorption energies of both species are similar or that butene binds more strongly than butane because of specific interactions with the double bond.

In the gas phase, Equation 4, the calculated reaction energy is –14 kJ/mol, *i.e.* the oxidative dehydrogenation of butane by SO_3 in the gas phase is also thermodynamically favored. The calculated reaction enthalpy at 298 K is –11 kJ/mol and the corresponding experimental value is -28 kJ/mol. The difference of 17 kJ/mol is in the expected error range of DFT calculations

Table 3.2 The calculated total reaction energy, ΔE_{total}, of different SZ structures with n-butane in kJ/mol (following Equation 5).

SZ	SZ_{red},OH_2	ΔE_{total}
$[SO_3]$ [a]	$[SO_2,OH^-,H^+]$	37.1
$[SO_3,OH^-,H^+]$	$[SO_2,OH^-,H^+,H_2O]$	47.0
$[SO_4^{2-},2H^+]$	$[SO_3^{2-},2H^+,OH^-,H^+]$	5.6
$[2SO_3]$ [a]	$[SO_4^{2-}, SO_2,2H^+]$	-36.1
$[S_2O_7^{2-},2H^+]$	$[S_2O_6^{2-},2H^+,H_2O]$	-66.8
$[S_2O_7^{2-},2H^+,H_2O]$ [a]	$[SO_4^{2-}, SO_2,2H^+,2H_2O]$	-10.1
$[SO_4^{2-},HSO_4^-,3H^+]$ [a]	$[S_2O_6^{2-},2H^+,2H_2O]$	-26.7
H_2SO_4 (gas)	$SO_2 + 2H_2O$	68.2
SO_3 (gas)	$SO_2 + H_2O$	-13.8

[a] These structures are most stable for specific pressure and temperature regions.

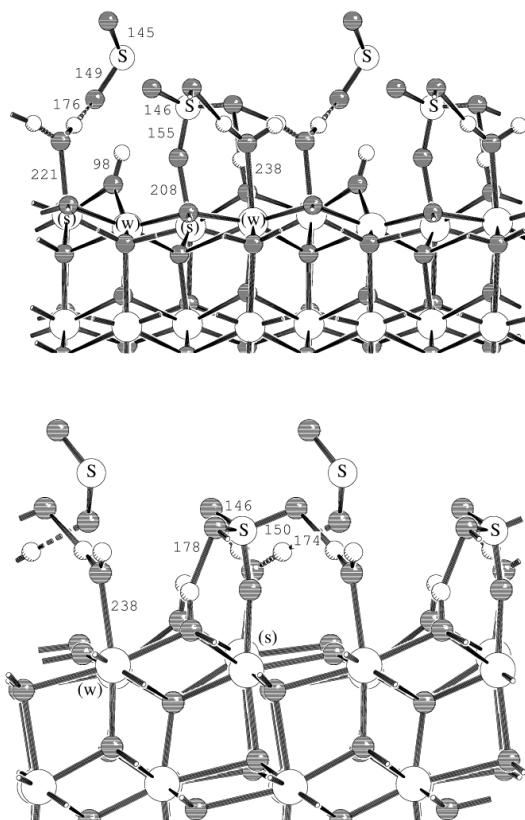**Figure 3.9** The structure of the reduced [$S_2O_7^{2-}$,$2H^+$,H_2O] accompanied by an additional water molecule [SO_4^{2-},SO_2,$2H^+$,$2H_2O$].

The oxidative initiation reaction is not catalytic but stoichiometric and the question arises, how long a catalyst may live, given that the concentration of sulfate on the surface of zirconia is finite. The current experiments show that the concentration of start molecules necessary to achieve an active catalyst is surprisingly small. For a period of 10h and a turnover of only 0.00088 mmol/g of sulfate/SO_3 were reduced. This corresponds to a ratio of approximately 500 butane molecules converted per SO_3 molecule reduced. A catalyst could, therefore, maintain its activity for 5000 h assuming similar operating conditions. It is important to note that such small concentrations are formed continuously through the bed, avoiding so high concentrations and the danger of higher rates of the inter-molecular reactions of condensation. This shows also why it is so difficult to add trace amounts of butenes to the catalyst and achieve a stable performance.

The important role of butene as initiating agent for n-butane isomerization on sulfated zirconia was clearly demonstrated by the far higher catalytic activity in the presence of only 26 ppm butene (0.033 μmol/g·s *vs.* 0.018 μmol/g·s). Supporting indirect evidence for the present findings is provided by liquid phase catalysis. The oxidation of alkane during isomerization in liquid acid, whose acid strength is not so high to protonate the alkanes, also

contributes to the initial step generating the active species. The formation of SO_2 [32] during n-butane isomerization in the presence of FSO_3H/HF acid and SbF_3 formation during activation of iso-butane in SbF_5 [33] are such examples. Similarly, the lack of reactivity of alkanes without tertiary hydrogen atoms in weaker superacids, such as CF_3SO_3H, can be overcome by adding alkenes.

The concentration of butenes in the reactant stream can also be influenced by the presence of hydrogen and oxygen. Hydrogen could play a double role, *i.e.*, it could lower the concentration of butenes in the reactor [34] and/or it could stop the reactions of the carbenium ions by acting as a hydride transfer agent [35]. It has also been suggested by Garin *et al.* [30] that iso-butene is rapidly hydrogenated on sulfated zirconia at low temperature in the presence of hydrogen. In this context it should be mentioned that the dissociation of molecular hydrogen on zirconia surface was reported to form surface Zr-H groups [36], which could be very active for hydrogenation. While the present data do not suffice to distinguish between these two possibilities, the linearly decrease of the catalytic activity with increasing of the hydrogen concentration in the feed suggests that the catalytic activity is directly related to the concentration of surface butene species.

It is noteworthy on the other hand that molecular oxygen works as promoter for the initial step of the reaction. Given the low reaction temperature of 100°C, we think that this is achieved by oxygen creating a small concentration of oxidation sites (labile SO_3 or labile pyrosulfates), which oxidize butane to butene. Alternatively, the direct observation of O_2^- species on the sulfated zirconia surface by ESR spectroscopy after adsorption of n-butane [37] or benzene [38] and a subsequent treatment with dry O_2 has also been reported. The formation of O_2^- species was attributed to the presence of Zr-H groups, which are formed on sulfated zirconia with reacting n-butane.

In the presence of oxygen clearly also the negative effect of a high concentration of olefins is seen. As the rate of butene molecules formed exceeds the rate of hydride transfer in a carbenium ion chain reaction, alternative pathways for the reaction of butenes are preferred, *i.e.* oligomerization leading to a rapid deactivation.

3.5. Conclusions

Butene species formed by oxidation of n-butane are shown to be the key intermediates during n-butane isomerization on sulfated zirconia. Butene is formed by a stoichiometric reaction between butane and a pyrosulfate type surface species. For the first time direct experimental evidence is given for all reaction products involved and the reaction intermediates have been modeled by theoretical chemistry. The initiating reaction occurs stoichiometrically, but the olefins formed induce a chain type reaction that converts 500 butane molecules per butene formed. This allows the sulfated zirconia catalysts to reach acceptable lifetimes and oxidative regeneration may lead to newly formed oxidation sites extending the lifetime further. Molecular hydrogen impedes the dehydrogenation reaction via pathways that basically are variants of hydride transfer. The presence of molecular oxygen induces reaction pathways to olefins, which rely on the generation of labile sulfate/SO_3 entities on the surface and/or the generation of O_2^- anions. Whatever the mechanism of formation, the present study also shows that the reaction rate and the catalyst stability depend on the concentration of olefins. At low concentrations of butenes the rate increases with the olefin concentration, at high concentration a high maximum activity is achieved, but the catalyst deactivates via formation of oligomers. The DFT calculations show clearly that the sulfur as well as the water content plays an important role in this initialization step by its influence on the energy of formation of the butene.

The evidence for the present pathway opens design strategies for new catalysts combining subtly redox chemistry with acid-base catalysis, opening so new generic pathways for activating and functionalizing alkanes.

Acknowledgments

References

[1]   X. Song, A. Sayari, Catal. Rev. Sci. Eng. 38 (1996) 329.

[2]   M. Hino, S. Kobayashi, K. Arata, J. Am. Chem. Soc. 101 (1979) 6439.

[3]   M. Hino, K. Arata, Chem. Commun. (1980) 851.

[4]   V. Adeeva, H. Liu, B. Xu, W.M.H. Sachtler, Top. Catal. 6 (1998) 61.

[5]   Y. Ono, Catal. Today 81 (2003) 3.

[6]   J. Sommer, R. Jost, M. Hachoumy, Catal. Today 38 (1997) 309.

[7]   T.K. Cheung, B.C. Gates, J. Chem. Soc., Chem. Commun. (1996) 1937.

[8]   T.K. Cheung, B.C. Gates, J. Catal. 168 (1997)522.

[9]   T.K Cheung, F.C. Lange, B.C. Gates, J. Catal. 159 (1996) 99.

[10]   S. Rezgui, A. Liang, T.K. Cheung, B.C. Gates, Catal. Lett. 53 (1998) 1.

[11]   B. Umansky, W.K. Hall, J. Catal. 124 (1990) 97.

[12]   F. Babou, G. Coudurier, J.C. Vedrine, J. Catal. 152 (1995) 341.

[13]   J. E. Tabora, R. J. Davis, J. Am. Chem. Soc. 118 (1996) 12240.

[14]   R. Srinivasan, R.A. Keogh, A. Ghenciu, D. Fărcaşiu, B.H. Davis, J. Catal. 158 (1996) 502.

[15]   D. Fărcaşiu, A. Ghenciu, Li Jing Qi, J. Catal. 158 (1996) 116.

[16]   V. Adeeva, J.W. de Haan, J. Janchen, G.D. Lei, V. Schunemann, L.J.M. van de Ven, W.M.H. Sachtler, R.A. van Santen, J. Catal. 151 (1995) 364.

[17]   K.T. Wan, C.B. Khouw, M. E. Davis, J. Catal. 158 (1996) 311.

[18]   http://webbook.nist.gov

[19]   J. P. Perdew, Phys. Rev. B 33 (1986) 8822.

[20]   Erratum ibid 34 (1986) 7406.

[21]   J. P. Perdew, Phys. Rev. B 34 (1986) 7406(E).

[22]   J. P. Perdew, Unified theory of exchange and correlation beyond the local density approximation. In Electronic Structure of Solids 1991.

[23]   P. Ziesche, H. Eschrig, (Eds.) Berlin, Akademie Verlag GmbH 1991.

[24]   P. E. Blöchl, Phys. Rev. B, 50 (1994) 17953.

[25]   G. Kresse, J. Joubert, Phys. Rev. B 59 (1999) 1758.

[26]   A. Hofmann, J. Sauer, J. Phys. Chem. B, submitted.

[27]   G. Kresse, J. Furthmüller, J. Hafner, Europhys. Lett., 32 (1995) 729.

[28]   G. Kresse, J. Furthmüller, J. Comput. Mat. Sci. 6 (1996) 15.

[29]   G. Kresse, J. Furthmüller, J. Phys. Rev. B 54 (1996) 11169.

[30]   Garin, F.; Andriamasinoro, D.; Abdulsamad, A.; Sommer, J. *J. Catal.* **1991**, *131*, 199 – 203.

[31]   X. Li, K. Nagaoka, J. A. Lercher, J. Cat. submitted.

[32]   G.A. Olah, O. Farooq, A.Husain, N. Ding, N.J. Trivedi, J.A. Olah, Catal. Lett. 10 (1991) 239.

[33]   J.C. Culmann, J. Sommer, J. Am. Chem. Soc. 112 (1990) 4057.

[34]   P. B. Weisz, E. W. Swegler, Science, 126 (1957) 31.

[35]   J. Meusinger, A. Corma, J. Catal. 152 (1995) 189.

[36]   J. Kondo, Y. Sakata, K. Domen, K. Maruya, T. Onishi, J. Chem. Soc. Faraday Trans. 86 (1990) 397.

[37]   D. Spielbauer, G.A.H. Mekhemer, E. Bosch, H. Knözinger, Catt. Lett. 36 (1996) 59.

[38]   F.R. Chen, G. Coudurier, J.F. Joly, J.C. Vedrine, J. Catal. 143 (1993) 616.

Chapter 4

Mechanism of chain propagation of butane skeletal isomerization on sulfated zirconia

Abstract

The isomerization of butane is initiated by an oxidative dehydrogenation and proceeds *via* a hydride transfer from n-butane to the iso-butyl carbenium ion. Transient experiments show conclusively that this process is fast compared to the isomerization step and, together with the physisorption of butane is concluded to be in quasi-equilibrium. The high selectivity to isomerization (~96 %) at low conversion implies that intra-molecular skeletal isomerization of butyl carbenium ions prevails. The reaction kinetics could be well described by Langmuir-Hinshelwood-Hougen-Watson rate equations over a wide range of partial pressures. At higher conversion the selectivity decreased. The by-products, *i.e.*, propane and pentanes, are formed *via* bimolecular routes as secondary and tertiary products. It is especially noteworthy that at higher conversion propane is formed almost exclusively indicating multiple alkylation and cracking steps to occur under such conditions.

4.1. Introduction

Sulfated zirconia and other sulfated metal oxides are of interest due to their unique activity for skeletal isomerization of short alkanes at low temperature [1, 2]. The kinetics of butane isomerization on sulfated zirconia has been studied [3, 4, 5, 6, 7] and the results have been reviewed in the recent years [8]. However, the differences of n-butane and iso-butane isomerization reactions indicate that the conclusions reached for a narrow set of conditions may not be generalized.

In general, an induction period can be observed, when butane is isomerized on sulfated zirconia at low temperature, which was assumed due to the formation of carbenium ion species on the catalytic surface [9, 10]. The presence of butene significantly shortened the induction period [11], which is rationalized with the easier formation of carbenium ions by protonation. The importance of carbenium ions during alkane skeletal isomerization on sulfated zirconia has also been evidenced by the negative effect of CO [9, 12] (formation of oxocarbenium ion), which can be directly observed by NMR spectroscopy. Quantum mechanical studies also contributed to understand the state of these carbenium ions and their conversion [13].

Two main mechanisms for butane isomerization on solid acid have been proposed: inter-molecular (bi-molecular) and intra-molecular (mono-molecular) routes [14, 15, 16, 17]. The intra-molecular skeletal isomerization of butyl carbenium ion requires the formation of a primary carbenium ion, which is a highly energetic demanding process. Therefore, the inter-molecular mechanism was speculated to be the preferred route, because it involves the less energetic demanding formation of a secondary carbenium ion, followed by cracking and a subsequent hydride transfer/desorption steps. Note that the kinetics of butane isomerization has been analyzed assuming the inter-molecular mechanism [7]. The high iso-butane selectivity (90-92 %) during n-butane isomerization was explained by the different stability and reactivity of the C_8 isomers, and the low reaction rate of iso-butane was ascribed to the steric hindrance of two iso-butyl groups forming the C_8 intermediate.

When n-butane isomerization was carried out in the presence of hydrogen, the reaction order for n-butane was higher than 1 [6]. Therefore, the inter-molecular mechanism was concluded to be dominate under these conditions. However, the opposite conclusion was reached using mono ^{13}C labeled n-butane under similar reaction conditions [15]. It should be noted that cracking products of branched octanes on sulfated zirconia at 373 K far different from those of butane reaction. Therefore, in another set of experiments it was concluded that branched octylcarbenium ions are not the main intermediates of butane isomerization [18].

In summary, the presently reported experiments do not allow to unequivocally conclude along which pathway n-butane skeletal isomerization proceeds. This is among other factors to be ascribed to the impure feeds, which induce different reactions including preferred oligomerization and deactivation. After having demonstrated in Chapter 3 that the initiation step consists of the oxidative dehydrogenation of n-butane [19], this Chapter addresses the propagation step of butane skeletal reaction on sulfated zirconia at 373 K *via* a kinetic analysis.

4.2. Experimental

4.2.1. Catalyst preparation

Sulfate-doped zirconium hydroxide was obtained from Magnesium Electron, Inc. (batch number XZO 1077/01). The as-received sample was heated to 873 K with an increment of 10 K/min and maintained at the final temperature for 3 h in static air to form sulfated zirconia with a concentration 0.05 mmol/g of Brønsted acid sites. The resulting catalyst was kept in a desiccator and was activated *in situ* as described below prior to the kinetic studies.

4.2.2. Adsorption isotherms and differential heats

The adsorption isotherms were measured in a SETARAM TG-DSC 111 instrument. Approximately 15 mg of pellets were charged into the quartz crucible used in the TG-DSC system. The sample was activated by heating to 673 K with an increment of 10 K/min and maintaining at 673 K for 2 h in vacuum ($p < 10^{-6}$ mbar). After activation, the temperature was stabilized at 373 K. n- and iso-Butane were introduced into the closed system in small doses and allowed to equilibrate with the sulfated zirconia until a further mass increase was not observed. The butane pulses were repeated until pressure reached 300 mbar. The differential heats of n-butane and iso-butane adsorption were determined at 308 K.

4.2.3. Butane isomerization

Isomerization of n-butane (99.5 %, Messer) and iso-Butane (99.95 %, Messer) were carried out in a quartz micro tube reactor (8mm i.d.) under atmospheric pressure. Sulfated zirconia pellets (355-710μm) (0.2 or 0.5 g for n-butane or iso-butane, respectively) were loaded into the reactor and activated *in situ* at 673 K for 2 h in He flow (10 ml/min). The catalyst was cooled to the 373 K and the reactant mixture (different n- or iso-butane partial pressures in He, total flow of 20 ml/min) was flown through the catalyst bed. Butane was

passed through an olefin trap containing activated zeolite H-Y (20g) before it was mixed with He. The butane concentration in the resulting gas was below the detection limit (1 ppm). The reaction products were analyzed using an on-line HP 5890 gas chromatography (GC) equipped with a capillary column (Plot Al_2O_3, 50m × 0.32 mm × 0.52mm) connected to a flame ionization detector (FID).

In order to investigate the catalytic activity and selectivity of sulfated zirconia for n-butane (5 % n-butane in He) at high conversion, 1.5 g of sulfated zirconia was loaded in the reactor and reactant flow rates of 2 and 0.5 ml/min were applied.

4.2.4. Transient kinetic analysis

A concentration transient study during n-butane isomerization at 373 K (0.2 g of sulfated zirconia, 20 ml/min of 5 % n-butane in He) on sulfated zirconia was performed after 5 h TOS (time on stream), when a stable activity was observed. The feed was steeply changed from 5 vol. % n-butane to 2 vol. % propane in He or pure He (20 ml/min). Samples of the effluent were collected using a VICI 32-port valve (16 loops) and analyzed by GC.

4.3. Results

4.3.1. Isotherms and differential heats of butane adsorption

The isotherms of butane adsorption at 373 K on activated sulfated zirconia are shown in Figure 4.1. Significant differences between n-butane and iso-butane adsorption were not observed. The isotherm could be described by a simple Langmuir model,

$$Q = \frac{Q_0 \cdot K_{ad} \cdot p}{1 + K_{ad} \cdot p}$$

in which Q denotes the concentration of butane adsorbed at a pressure p, Q_0 the maximum concentration of butane adsorbed and K_{ad} the adsorption constant. By linearly fitting the experimental data, the n-butane adsorption constant $K_{nad} = 28.2$ and the iso-butane adsorption constant, $K_{iad} = 23.5$ were obtained.

The differential heats of n-butane and iso-butane adsorption as a function of the butane coverage determined at 308 K are compared in Figure 4.2. For both butanes, the heats of adsorption showed a similar dependence on the coverage of butane, starting at approximately 60 kJ/mol (at low coverage) and modestly declined to about 40 kJ/mol at 40 μmol/g coverage. Thus, overall two isotherms (adsorption sites) seem to coexist, which may include chemisorbed butane molecules at low pressures.
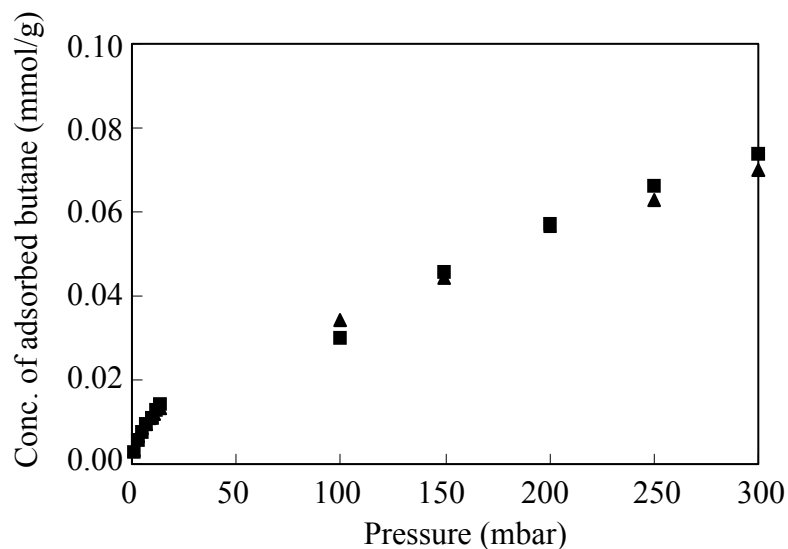
Figure 4.1 Isotherms of (▲) n-butane and (■) iso-butane adsorption at 373 K on sulfated zirconia (activated in vacuum at 673 K for 2 h).
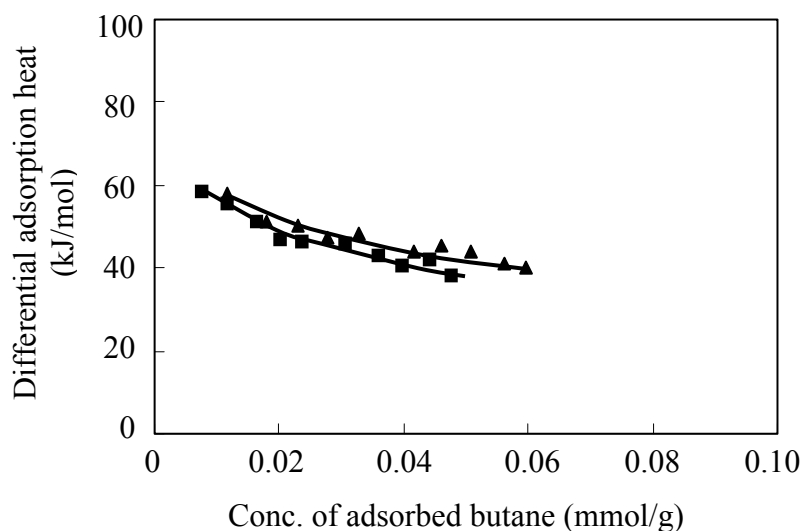

Figure 4.2 Differential adsorption heats of (▲) n-butane and (■) iso-butane adsorption at 308 K on sulfated zirconia (activated in vacuum at 673 K for 2 h).

4.3.2. n-Butane and iso-butane reactions at various partial pressures

The isomer formation rates versus time on stream (TOS) during butane skeletal isomerization on sulfated zirconia at 373 K at various partial pressures are shown in Figure 4.3 (A) and (B) for n-butane and iso-butane reaction, respectively. All the reactions showed an induction period depending upon the butane partial pressure. Higher partial pressure led to a shorter induction period, *i.e.,* the half time of induction period length ($t_{1/2}$) of the n-butane reaction at 50 mbar was 120 min, but only 28 min for the reaction at 170 mbar.

The half induction period lengths versus the partial pressure for n-butane and iso-butane isomerization reaction are shown in Figure 4.4 (A) and (B), respectively. Following the induction period, the catalyst showed a stable catalytic activity with only very slow deactivation.

Figure 4.3 (A): iso-Butane formation rates versus time on stream for n-butane skeletal isomerization on sulfated zirconia at 373 K for (□)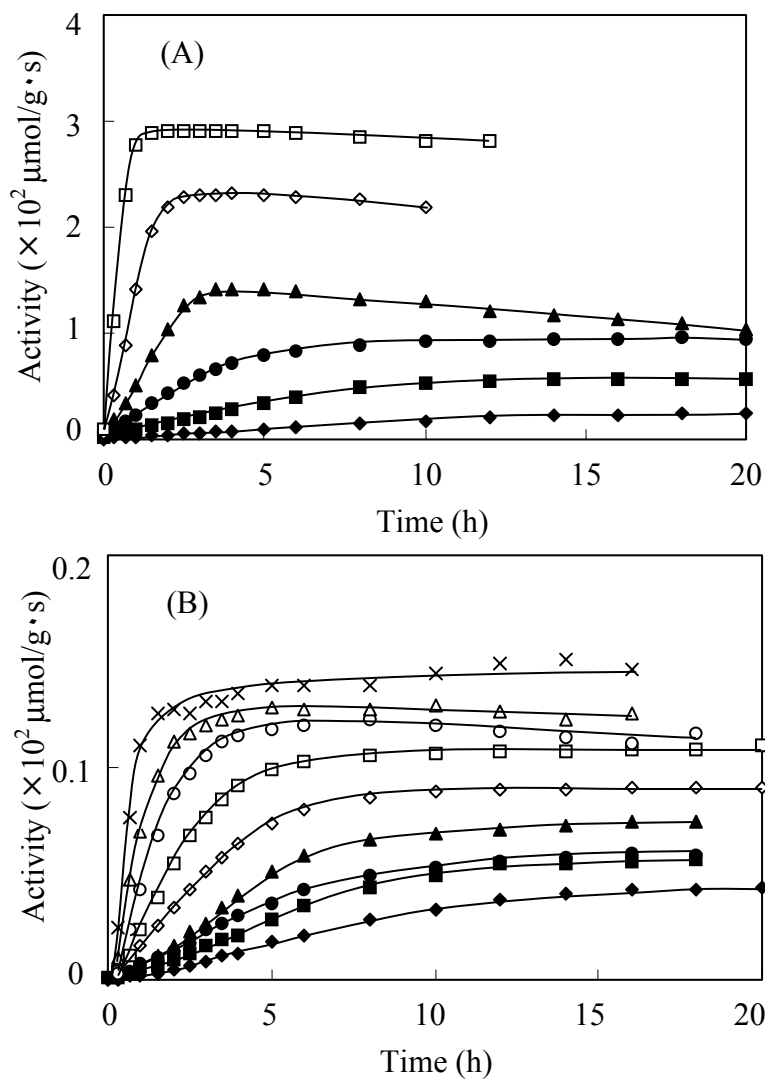 170, (◇) 100, (▲) 50, (●) 28, (■) 17 and (◆) 7 mbar n-butane in the feed; and (B): n-Butane formation rates versus time on stream for iso-butane skeletal isomerization on sulfated zirconia at 373 K for (×) 88, (△) 50, (○) 36, (□) 19, (◇) 13, (▲) 9, (●) 6, (■) 4.6 and (◆) 3.2 mbar iso-butane in the feed.
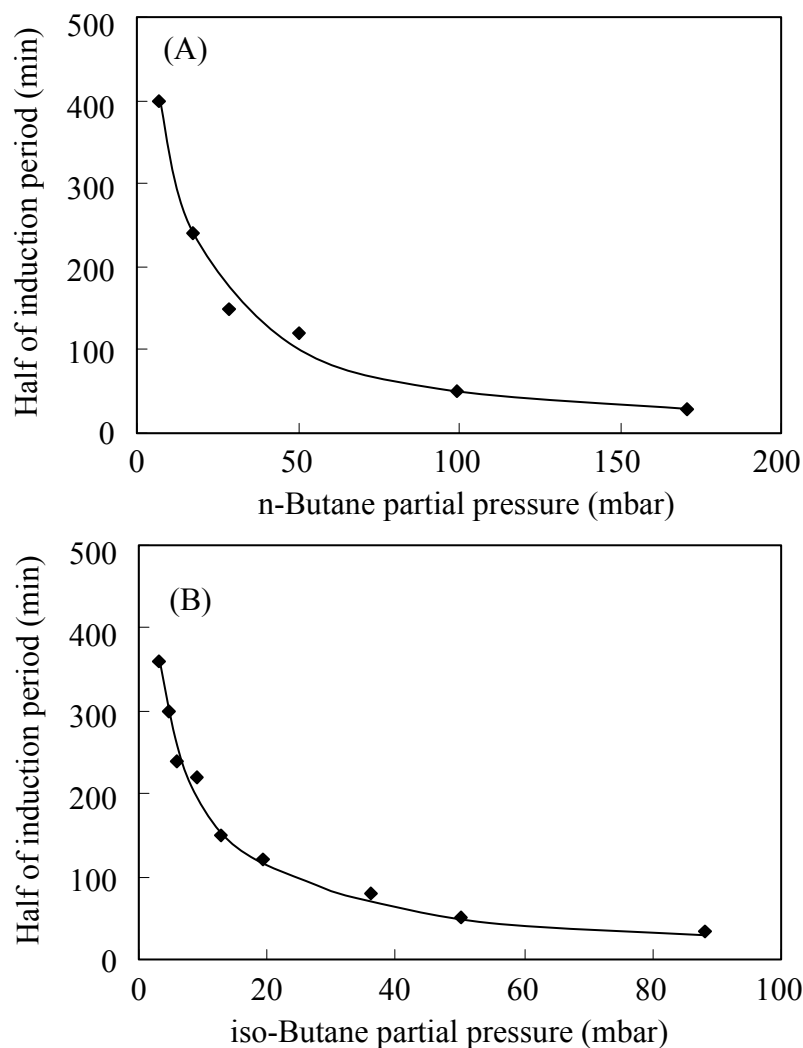
Figure 4.4 Half of the induction period versus partial pressure in the feed of n-butane (A) and of iso-butane (B).

Because the conversion of butane was lower than 1 %, the plug flow reactor is safely concluded to be operated in differential mode and the reaction rates can also be considered as the intrinsic forward reaction rates. The maximum rate of iso-butane formation increased with increasing n-butane partial pressure (see Figure 4.5 (A)). In addition, the selectivity to iso-butane was nearly constant (appr. 96 %) at all n-butane partial pressures. The main by-products were equimolar amounts of propane and pentanes (n- and iso-pentane with a ratio of 1:4). However, as shown in Figure 4.5 (B), the maximum rate of n-butane formation from iso-butane increased linearly only for iso-butane partial pressures lower than 19 mbar. For higher partial pressures, the formation rate increased more gradually indicating lower reaction order in a power rate law form. n-Butane formation rates were about 50 times lower than iso-

butane formation rates, and n-butane selectivity was approximately 80 % at all partial pressures.
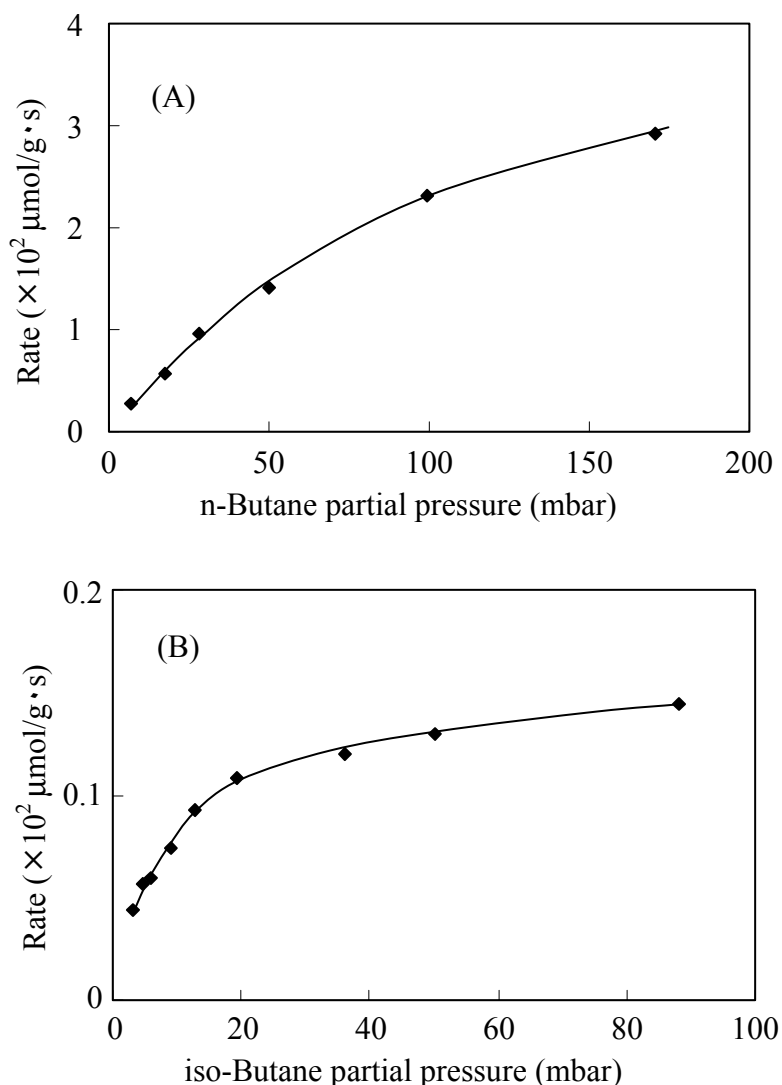
Figure 4.5 (A) iso-Butane formation rate versus n-butane partial pressure in the feed; and (B): n-Butane formation rate versus iso-butane partial pressure in the feed.

4.3.3. Transient kinetics

Figure 4.6 shows the normalized transients $F_{n,i,p}(t)$ following step change during transient experiment (where i is n-butane, iso-butane or propane and p is purge gas, He or 2 vol. % propane in He). During propane purge, the surface n-butyl carbenium ion will be desorbed by hydride transfer from propane and the absolute amount can be determined by integrating the difference of normalized transients during propane and He purge:

$$N_{n-C_4} = C_{n-C_4} \int \left[F_{n,\,n-C_4,\,C_3}(t) - F_{n,\,n-C_4,\,He}(t) \right] dt$$

where C_{n-C_4} is the concentration of n-butane in the product effluent. Also, the amount of iso-butane formation by hydride transfer from propane to iso-butyl carbenium ion can be obtained with the same method. The calculation results indicate that approximate $5*10^{-3}$ mmol/g of surface n-butyl carbenium ion and only around $3*10^{-5}$ mmol/g of iso-butyl carbenium ion on the catalyst surface at steady state of n-butane isomerization. Therefore, we conclude that the n-butyl carbenium ion is the dominant species during n-butane isomerization since its concentration is more than two orders of magnitude higher than that of the iso-butyl carbenium ion.
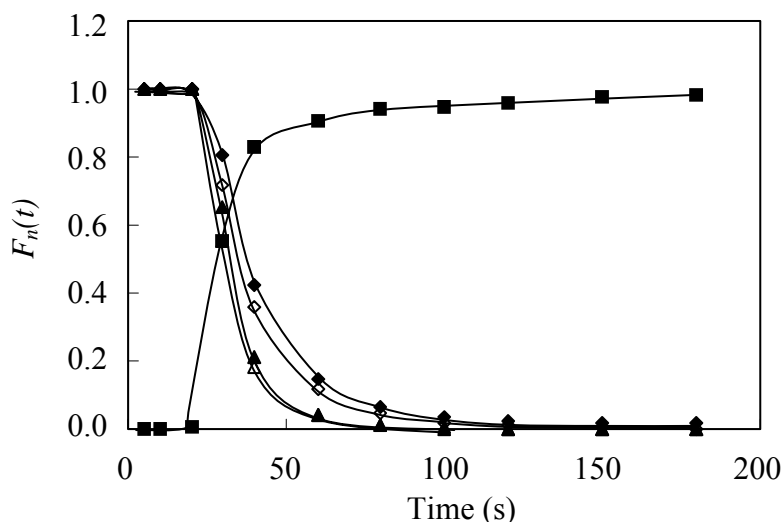
Figure 4.6 Normalized transients at 373 K (20 ml/min, 0.2 g cat.) (■) Propane, (◇) iso-butane, He, (◆) iso-butane, propane, (△) n-butane, He and (▲) n-butane, propane.

4.3.4. Product distribution at high conversion

iso-Butane selectivity during n-butane isomerization on sulfated zirconia at low conversion was approximately 96 %. However, as shown in Figure 4.7, it decreased with conversion. The slope of this decrease was low up to 60 % conversion, while above 60 % conversion the decline was by far more rapid. The selectivity varying with conversion can be expressed by an exponential equation:

$$S \% = 100 - 3.19 \times \exp\left(0.0328 \times Con \%\right)$$

where S is the iso-butane selectivity and Con is the n-butane conversion. The effect of n-butane conversion on the ratio between iso-butane and total butanes in the products is shown

in Figure 4.8. This ratio was almost linear with the conversion and reached the thermodynamic equilibrium value at 373 K, ~ 62 % [20] at high conversion (80 %). The iso-butane yield (Figure 4.9 (A)) increased linearly at conversions lower than 50 %. However, it decreased when the conversion was higher than 60 %. On the other hand, at low conversion, propane and pentane were formed in nearly equimolar amounts, while at high conversion propane was formed in larger amount compared to pentanes (see Figure 4.9 (B)).
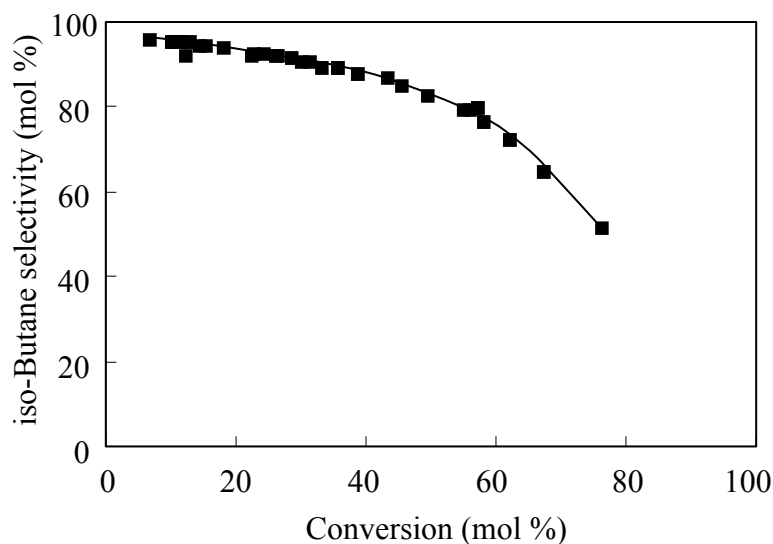

Figure 4.7 iso-Butane selectivity versus n-butane conversion during n-butane skeletal isomerization on sulfated zirconia at 373 K.
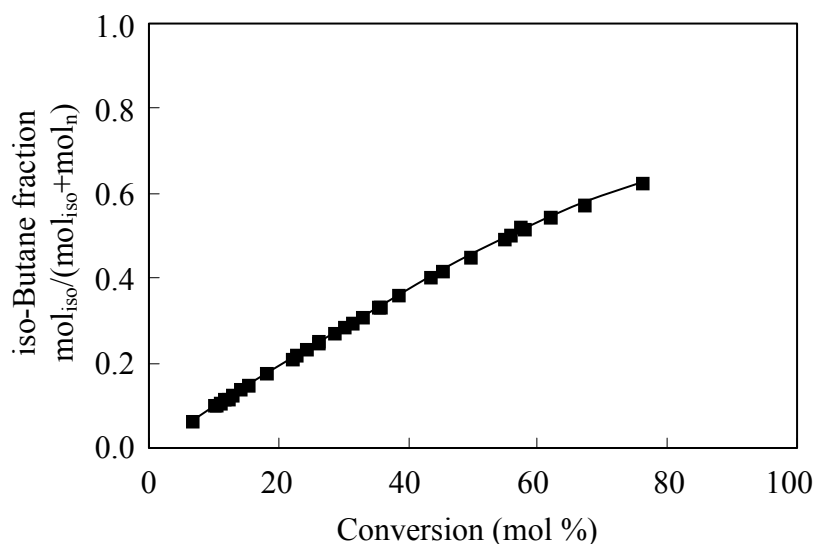
Figure 4.8 The iso-butane ratio to total butane in the products versus n-butane conversion during n-butane isomerization on sulfated zirconia at 373 K.
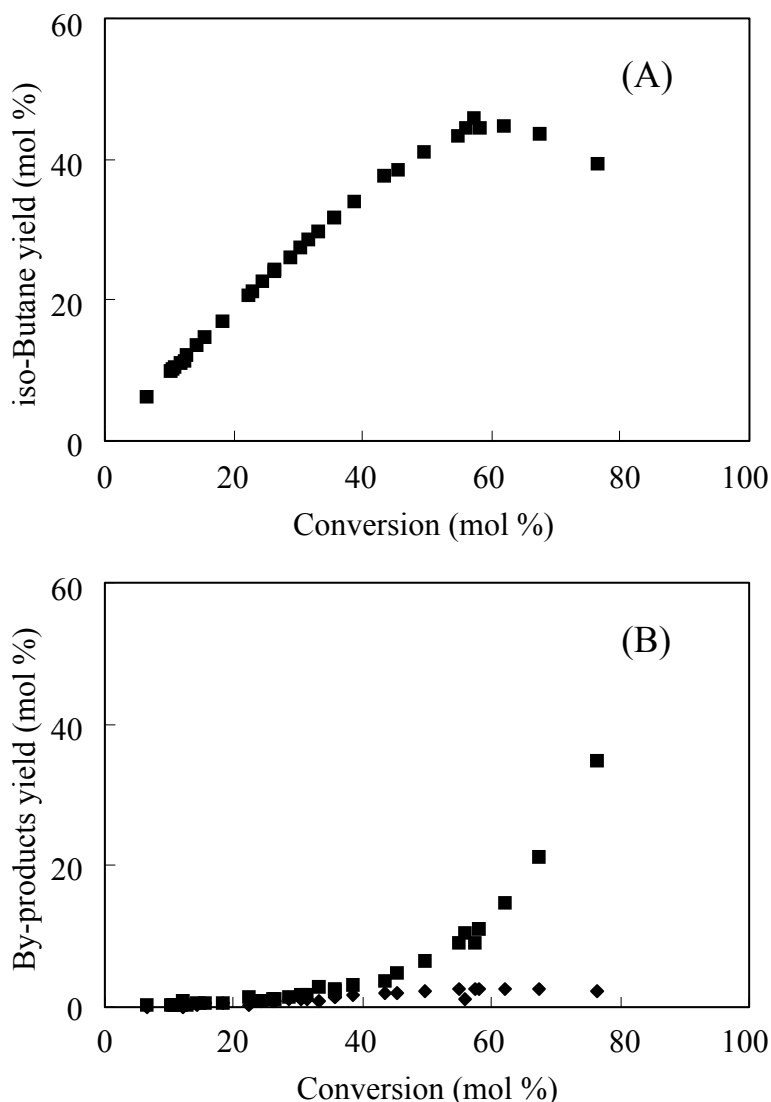
Figure 4.9 Yield of products (A) iso-butane, (B) (■) propane and (◆) pentanes versus n-butane conversion during n-butane isomerization on sulfated zirconia at 373 K.

4.4. Discussion

4.4.1. Butane skeletal isomerization and disproporationation

Without metal components, sulfated zirconia is on first sight only a selective isomerization catalyst at rather low conversions (conversions below 40 %). At higher conversion, the iso-butane selectivity decreased rapidly, especially when the iso-butane concentration in the product was close to the dynamic equilibrium concentration (62 %). This view varies when considering the yield conversion relations (see Figure 4.7). iso-Butane is clearly a primary product with high stability and a very high ultimate selectivity (close to 100 %) at low conversion, which shows clearly that propane and pentane are secondary products. The iso-butane selectivity decreased exponentially with conversion since the formation rate of propane following an exponential function with conversion. It is also obvious that a strong preference

to propane must be related to multiple further cracking and alkylation steps over these catalysts that occur in parallel to the isomerization reaction.

The high iso-butane selectivity at low conversion of n-butane strongly suggests that the intra-molecular route to be operative for n-butane skeletal isomerization. Considering the products from the cracking of potentially dimerized butenes (tri-methyl pentanes (TMP)) [21], the highest probability for the isomers suggests that the selectivity to iso-butane should not be higher than 80 %. For this model it was assumed that primarily TMPs are formed and are in thermodynamic equilibrium (2.2.4-tri-methyl pentane: 2.3.4-tri-methyl pentane: 2.3.3-tri-methyl pentane: 2.2.3-tri-methyl pentane = 63.5 : 9 : 10 : 17.5 [22]) and the cracking rates of different isomers are similar. In Scheme 4.1, the possible TMP isomer cracking reactions are compiled. Therefore, the iso-butane selectivity higher than 90 % in n-butane isomerization reaction cannot result solely from an inter-molecular dimerization route. In addition, the high n-butane selectivity during iso-butane reaction (80 %) cannot be rationalized with the dimer pathway, where the n-butane selectivity should not be higher than 32 %. On the other hand, theoretical calculations suggest that the activation energy from sec-butyl to primary butyl carbenium ions is only 76 kJ/mol, which indicates the intra-molecular skeletal isomerization of butyl carbenium ion is feasible [23].
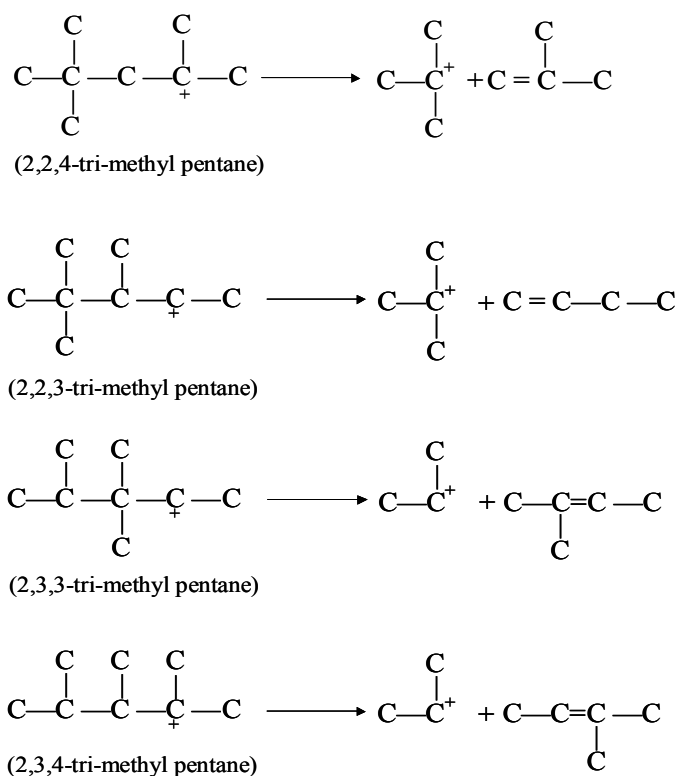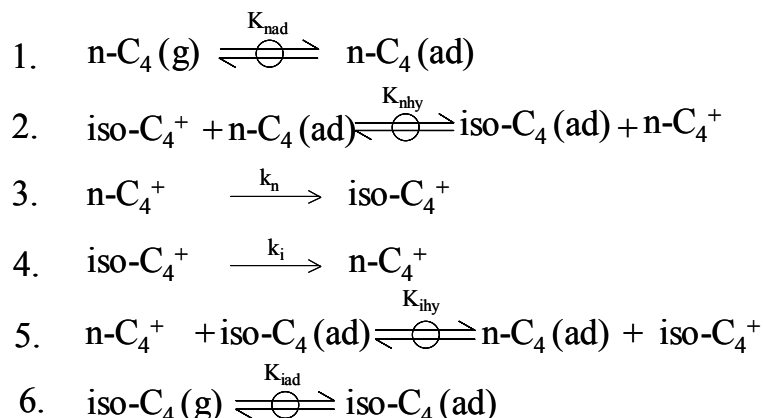

Scheme 4.1 Potential octane isomers cracking reaction.

73

Propane and (to a lesser degree) pentanes are the main by-products during butane isomerization on sulfated zirconia, once it proceeds *via* the inter-molecular dimerization pathway by forming C_8 species from two butyl species followed by rearrangement and cracking. The equal molar amounts of propane and pentanes in the product at low n-butane conversion in this study are in agreement with previous reports in the literature [7]. However, at high conversion, the yield of pentanes is much lower than that of propane, which suggests the formed pentanes or pentylcarbenium ions are consumed by further reactions.

Thus, the reversible isomerization and the irreversible disproportionation are responsible for the changing of selectivity with conversion. At low conversion, the isomerization rate is high and the – at least bimolecular – disproportionation proceeds slowly. At high conversion, the integral isomerization rate is lowered as a result of the reverse reaction of iso-butane. Especially, when the iso-butane concentration in the product is close to the thermodynamic equilibrium with n-butane, no apparent isomerization can be achieved. the isomerization product (iso-butane) will also contribute to the disproporationation reaction, thus, at n-butane conversion higher than 60 %, iso-butane yield decreases with the conversion.

4.4.2 Rate and equilibrium constants of butane skeletal isomerization reaction

Scheme 4.2 shows the possible mechanism of butane skeletal isomerization over sulfated zirconia at low temperature. Step 1 and 6 are quasi-equilibrated adsorption/desorption of gaseous n-butane and iso-butane on the surface with constant K_{nad} and K_{iad}, for n-butane and iso-butane, respectively. Step 2 and 5 are the steps of the hydride transfer from molecular butanes to butyl carbenium ions. The transient study indicates that the concentration of surface n-butyl carbenium ion is more than 100 times higher than that of iso-butyl carbenium ion, which indicates that the hydride transfer from propane to surface butyl species is faster than the surface butyl skeletal isomerization. Thus, we postulate here that hydride transfer steps during butane isomerization are also in quasi-equilibrium (at least for low conversion and, hence, high n-butane concentration) with the hydride transfer constants, K_{nhy} and K_{ihy}. A quantum chemical study of elementary steps of hydrocarbon transformation in acid zeolite catalysts also confirmed the fast hydride transfer step by comparing the relative activation energies, *i.e.*, 180-200 kJ/mol for hydride transfer and 257 kJ/mol for n-butene to iso-butene isomerization [24]. Equation 3 and 4 describe the skeletal isomerization reactions of the formed butyl carbenium ion with isomerization reaction rate constant, k_n and k_i, for n-butyl and iso-butyl, respectively.

1. $\text{n-C}_4\,(\text{g}) \; \underset{}{\overset{K_{nad}}{\rightleftharpoons}} \; \text{n-C}_4\,(\text{ad})$

2. $\text{iso-C}_4{}^+ + \text{n-C}_4\,(\text{ad}) \underset{}{\overset{K_{nhy}}{\rightleftharpoons}} \text{iso-C}_4\,(\text{ad}) + \text{n-C}_4{}^+$

3. $\text{n-C}_4{}^+ \; \xrightarrow{k_n} \; \text{iso-C}_4{}^+$

4. $\text{iso-C}_4{}^+ \; \xrightarrow{k_i} \; \text{n-C}_4{}^+$

5. $\text{n-C}_4{}^+ + \text{iso-C}_4\,(\text{ad}) \underset{}{\overset{K_{ihy}}{\rightleftharpoons}} \text{n-C}_4\,(\text{ad}) + \text{iso-C}_4{}^+$

6. $\text{iso-C}_4\,(\text{g}) \; \underset{}{\overset{K_{iad}}{\rightleftharpoons}} \; \text{iso-C}_4\,(\text{ad})$

Scheme 4.2 Proposed catalytic cycles for butane skeletal isomerization on sulfated zirconia.

Since the concentration of the products during butane reactions at low conversion was lower than 1 %, the reverse reaction was not considered for the fitting procedure. The observed isomerization rates of butane can then be well described by a Langmuir–Hinshelwood-Hougen-Watson type rate equation:

For n-butane reaction:

$$r_n = k_n{\cdot}K_n{\cdot}P_n/(1+K_n{\cdot}P_n) \qquad [1]$$

For iso-butane reaction

$$r_i = k_i{\cdot}K_i{\cdot}P_i/(1+K_i{\cdot}P_i) \qquad [2]$$

where $K_n = K_{nad} \cdot K_{nhy}$ and $K_i = K_{iad} \cdot K_{ihy}$ are equilibrium constants for n- and iso-butane reactions. The rates of isomer formation obtained from the butane reaction at various partial pressures are fitted with a linear method by Equation 1 for n-butane reaction and Equation 2 for iso-butane reaction. The values for the kinetic parameters are shown in Table 4.1.

Table 4.1. Kinetic parameters for butane skeletal isomerization on sulfated zirconia at 373 K.

	Rate constant (μmol/g·s)		$K_{ad} \cdot K_{hy}$
k_n	0.051	K_n	7.7
k_i	0.0015	K_i	127.1

The composed equilibrium constant K_i for iso-butane reaction, 127.1, is higher than that for n-butane reaction, 7.7. Thus, the iso-butane reaction rate reaches its maximum at lower

partial pressure. Since the isotherms of n-butane and iso-butane adsorption on sulfated zirconia at 373 K showed no significant difference, the higher equilibrium constant of the iso-butane isomerization should be related to its highly active tertiary hydrogen. After hydride transfer to n-butyl species, iso-butane forms the most stable iso-butyl carbenium ion.

Besides the equilibrium constant, the skeletal isomerization reaction rate constants, k_n and k_i, are also shown in Table 4.1, 0.051 μmol/g·s and 0.0015 μmol/g·s for n-butane and iso-butane reaction, respectively. More than one order of magnitude difference in the reaction rate constant was found for n-butane and iso-butane skeletal isomerization. The predicted isomer formation rates of butane skeletal isomerization versus butane partial pressure are shown in Figure 4.10 (A) and (B) for n-butane and iso-butane, respectively. The model fits the experimental results well.
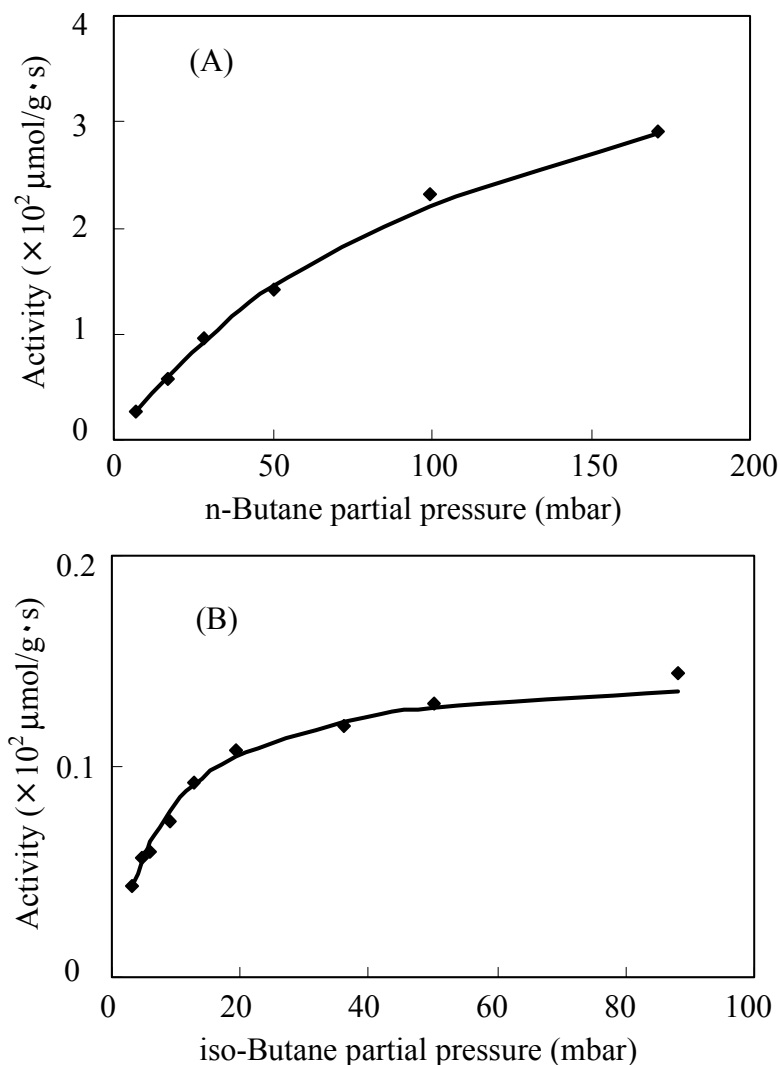

Figure 4.10 (A) Experimental (◆) and predicated (━) iso-butane formation rate versus n-butane partial pressure; and (B): Experimental (◆) and predicated (━) n-butane formation rate versus iso-butane partial pressure.

76

On the basis of surface Brønsted acid concentration, the kinetic data can be expressed in term of turnover frequencies (TOF) (see Table 4.2) of $1 * 10^{-3}$ s^{-1} and $3 * 10^{-5}$ s^{-1} for n-butane and iso-butane isomerization reaction, respectively. Furthermore, the Gibbs free energy of activation can be calculated from the transition state theory:

$$k = \frac{k_B T}{h} \exp\left(\frac{-\Delta G^{\#}}{RT}\right)$$

where k_B is Boltzmann constant, h Planck constant, and $\triangle G^{\#}$ Gibbs free energy of activation. The calculated Gibbs free energies of activation ($\triangle G^{\#}$) (see Table 4.2) were 113 kJ/mol and 124 kJ/mol for n-butane and iso-butane isomerization reaction, respectively. The activation enthalpy can be obtained by the equation: $\Delta H^{\#} = \Delta G^{\#} + T\Delta S^{\#}$, where $\triangle H^{\#}$ is the enthalpy of activation and $\triangle S^{\#}$ is entropy of activation. The standard entropy of transition state species was estimated by assuming that the transition state is similar to the carbenium ion [25]. Thus, $\triangle S^{\#} \approx 0$ and $\triangle H^{\#} = \triangle G^{\#}$. The true activation energies obtained by $Ea = \triangle H^{\#} + RT$, as shown in Table 4.2, are 117 and   128 kJ/mol for n-butane and iso-butane reaction, respectively.

The calculated activation energies based on our experimental results are much higher than the apparent activation energy reported previously, *i.e.*, 53 kJ/mol [9], 58 kJ/mol [3] and 44 kJ/mol [26] for n-butane and 80 kJ/mol [3] for iso-butane isomerization. However, since the apparent activation energies were measured at relatively low butane partial pressure ($K_n P \ll 1$) with exception of reference [3], the real activation energy should be obtained from following equation: $E_a = E_{a,app} + \triangle H_{ad}$. Since the enthalpy of butane adsorption on the sulfated zirconia is around 40-60 kJ/mol, the calculated true activation energies based on transition state theory are in good agreement with the expected true activation energies from experimental reports.

Table 4.2. Turnover frequencies (TOF) for butane skeletal isomerization on sulfated zirconia at 373 K and activation energy estimated *via* transition state theory.

Reaction	Rate (µmol/g·s)	TOF ($\times 10^4$ s^{-1})	$\triangle G^{\#}$ (kJ/mol)	Ea (kJ/mol)
n-butane	0.051	10.2	113	117
iso-butane	0.0015	0.3	124	128

The high relative activity of the active species formed from n-butane, *i.e.*, the n-butyl carbenium ion, should be related to differences between the ground state and the transition state [23]. Since the iso-butyl carbenium ion is the most stable species (that with the lowest

77

potential energy from the molecules and molecular species investigated), the activation energy from the tertiary carbenium ion to methyl cyclopropyl carbenium ion is higher than that from n-butyl carbenium ion [23]. However, the activation energy of iso-butane reaction is only 11 kJ/mol higher than that of n-butane reaction, contrary to the difference of the free carbenium ions, which would be around 67 kJ/mol [23]. This is explained by the fact that the carbenium ion resembles in the ground state more an alkoxy group than a free carbenium ion [13]. It is even demonstrated that the alkoxides formed in the zeolite frame with primary, secondary and tertiary carbenium ions have similar potential energies [27]. It is also suggested that with the assistance of the oxygen, the intra-molecular skeletal isomerization of butyl carbenium ion is facilitated providing by a lower energy demanding pathway compared to the reaction of free carbenium ions [16].

4.5 Conclusions

The isomerization is initiated by an oxidative dehydrogenation of n-butane and proceeds *via* hydride transfer from n-butane to the iso-butyl carbenium ion. Transient experiments show conclusively that this process is fast compared to the isomerization step and is concluded to be in quasi-equilibrium.

The change of iso-butane selectivity with n-butane conversion indicates isomers and by-products are not formed following the same mechanism. The high selectivity to isomerization for n- and iso-butane at low conversion (96 % and 80 %, respectively) indicates that the isomerization occurs *via* an intra-molecular mechanism. The true energies of activation (estimated by transition state theory using the thermodynamic and kinetic data measured in this study) suggests a true energy of activation of 117 to 128 kJ/mol in line with a somewhat energy demanding reaction pathway. Considering the heat of adsorption, this value agrees well with the reported values of apparent energies of activation in the literatures. The reactions can be modeled perfectly in the forward direction using a Langmuir-Hinshelwood-Hougen-Watson form with the physisorption of the alkanes and the hydride transfer steps being in quasi equilibrium.

The by-products, *i.e.,* propane and pentanes, are formed *via* bimolecular routes as secondary and tertiary products. It is especially noteworthy that at higher conversion propane is formed almost exclusively indicating multiple alkylation and cracking steps to occur under such conditions. Reversible isomerization and irreversible disproportionation are, thus, the cause of the reduced selectivity at high conversion.

It is interesting to note that the forward rate of iso-butane isomerization is significantly slower than the isomerization of n-butane. This lower activity is associated with a higher energy of activation for the isomerization of iso-butane. This is a consequence of the higher stability of the iso-butyl carbenium ion (iso-butyl alkoxy group) over the n-butyl carbenium ion. Therefore, the difference to methyl cyclopropyl carbenium ion and, hence, the true energy of activation will be higher. The strong covalent bonding of the carbenium ions in the ground state leads to a dampening of the large differences expected from free carbenium ion chemistry.

Acknowledgments

References
[1]   X. Song, A. Sayari, Catal. Rev. Sci. Eng. 38 (1996) 329.

[2]   G.D. Yadav, J. J. Nair, Micropor. Mesopor. Mater. 33 (1999) 1.

[3]   A.S. Zarkalis, C.Y. Hsu, B.C. Gates, Catal. Lett. 37 (1996) 1.

[4]   E.C. Sikabwe, R.L. White, Catal. Lett. 44 (1997) 177.

[5]   A.S. Zarkalis, C.Y. Hsu, B.C. Gates, Catal. Lett. 29 (1994) 235.

[6]   H. Liu, V. Adeeva, G.D. Lei, W.M.H. Sachtler, J. Mol. Catal. A 100 (1995) 35.

[7]   K.B. Fogash, R.B. Larson, M.R. Gonzalez, J.M. Kobe, J.A. Dumesic, J. Catal. 163 (1996) 138.

[8]   V. Adeeva, H. Liu, B. Xu, W.M.H. Sachtler, Top. Catal. 6 (1998) 61.

[9]   A. Sayari, Y. Yang, X. Song, J. Catal. 167 (1997) 346.

[10]   X. Li, K. Nagaoka, L. J. Simon, J. A. Lercher, A. Hofmann, J. Sauer, submitted for publication, 2004.

[11]   S. Hammache, J.G. Goodwin Jr, J. Catal. 211 (2002) 316.

[12]   M.V. Luzgin, A.G. Stepanov, V.P. Shmachkova, N.S. Kotsarenko, J. Catal. 203 (2001) 273.

[13]   V.B. Kazansky, Catal. Today 51 (1999) 419.

[14]   H. Matsuhashi, H. Shibata, H. Nakamura, K. Arata, Appl. Catal. A 187 (1999) 99.

[15]   V. Adeeva, G.D. Lei, W.M.H. Sachtler, Catal. Lett. 33 (1995) 135.

[16]   F. Garin, L. Seyfried, P. Girard, G. Maire, A. Abdulsamad, J. Sommer, J. Catal. 151 (1995) 26.

[17]   J. Sommer, R. Jost, M. Hachoumy, Catal. Today 38 (1997) 309.

[18]   A. Sassi, J. Sommer, Appl. Catal. A 188 (1999) 155.

[19]   X. Li, K. Nagaoka, L. J. Simon, J. A. Lercher, A. Hofmann, J. Sauer, submitted for publication, 2004.

[20]   M.J. Clveland, C.D. Gosling, J. Utley, J. Elstein, NPRA 1999 Annual Meeting.

[21]   A. Feller, A. Guzman, I. Zuazo, J. A. Lercher, J. Catal. 224 (2004) 80.

[22]   M. Guisnet, N.S. Gnep, Appl. Cat. A 146 (1996) 33.

[23]   M. Boronat, P. Viruela, A. Corma, J. Phys. Chem. 100 (1996) 633.

[24]   M.V. Frash, R.A. van Santen, Top. Catal. 9 (1999) 191.

[25]   G. Yaluris, J.E. Rekoske, L.M. Aparicio, R.J. Madon, J.A. Dumesic, J. Cat. 153 (1995) 54.

[26]   K.T. Wan, C.B. Khouw, M.E. Davis, J. Catal. 158 (1996) 311.

[27]   A.M. Rigby, G.J. Kramer, R.A. van Santen, J. Cat. 170 (1997) 1.

<div align="right">

Chapter 5

</div>

Preparation of active sulfated zirconia by sulfation with SO$_3$

Abstract

Highly active sulfated zirconia materials were prepared by sulfation of crystalline zirconia with gaseous SO$_3$. This direct method circumvents the use of liquid phase handling and separation procedures, as well as high temperature calcination step. Labile sulfate species introduced by the gas phase treatment are concluded to be one of the essential factors for the formation of active sites on sulfated zirconia. Detailed physicochemical characterization indicates that the surface bi-sulfate species cause the Brønsted acidity and that the Brønsted acid concentration is correlated to the sulfate content. The catalytic activity of SO$_3$ sulfated zirconia samples is correlated directly to the concentration of the tetragonal ZrO$_2$ phase with the monoclinic phase showing the lowest activity. For a given material the catalytic activity is also directly related to the concentration of highly covalent pyrosulfate species, which exhibit a characteristic S=O IR band at high frequency. *In situ* SO$_3$ sulfation of sulfated zirconia enhanced the initial activity for n-butane isomerization by 2 orders of magnitude, which further provides evidence for the key role of the labile sulfate species in activating light alkanes.

5.1. Introduction

Sulfated zirconia and other sulfated metal oxides have been studied for over two decades owing to their high catalytic activity for activation of short alkanes at low temperature. The influence of several preparation parameters on the catalytic activity have been thoroughly discussed, *i.e.,* the zirconia source precursor [1], sulfate source [2] and the calcination procedure [3, 4]. In summary, three statements are generally mentioned for the preparation of an active catalyst: (i) aqueous sulfation must be performed on amorphous zirconium hydroxide with sulfation of crystalline zirconia being ineffective [5], (ii) only the tetragonal ZrO_2 phase is active, while the monoclinic is inactive [6,7], (iii) calcination at high temperatures is a crucial step for the formation of active sites [8, 9, 10].

On the contrary, in a recent study, aqueous sulfation of zirconia stabilized in the tetragonal form by formation of a solid solution with Y_2O_3, has been reported to be a method for preparation of active sulfated zirconia [11]. However, the monoclinic zirconia, prepared from calcination of pure zirconium hydroxide cannot be effectively activated by sulfation. Therefore, it is concluded that the tetragonal phase is necessary to generate the active sites of sulfated zirconia.

It is noteworthy that synthesis of active monoclinic sulfated zirconia catalyst by one step method has been reported by Stichert *et al.* [12]. However, the produced material had only one-fourth of the catalytic activity of tetragonal materials with a similar amount and type of acid sites. The authors concluded that the isomerization of n-butane on tetragonal materials was favored by the arrangement of surface groups. Synthesis of active monoclinic SZ catalysts has also been reported in a few other articles [13,14,15]. In the first two [13,14] the catalysts had non-negligible amount of tetragonal zirconia and in every case the catalytic activity of the monoclinic catalysts was much lower than that of tetragonal sulfated zirconia.

In most of the literature, calcination of the resulting material is recognized to be the critical step for active sites formation. The high temperature treatment serves the formation of active sites by effective binding of sulfate to zirconia surface [8, 9]. At the same time, another function of the calcination step was also demonstrated to be the partial removal of sulfate species thus creating Lewis acid sites accessible to the alkane. The strength of these acid sites is said to be increased by electron withdrawing effect of the neighboring sulfate [10,11].

Preparation of sulfated zirconia also can be achieved by sulfation of crystalline metal oxides with SO_3. Yamaguchi *et al.* [16] reported that by sulfation with SO_3 at 573 K strong acid sites are generated on Fe_2O_3, the final catalyst being active for cyclopropane

isomerization. Recently, Haw *et al.* [17, 18] reported that formation of Brønsted acid sites on zirconia by SO$_3$ adsorption on the basis of NMR and theoretical studies.

In this study, *ex situ* sulfation with gaseous SO$_3$ of zirconia-based materials at low temperature (473 K) was carried out for preparation of sulfated zirconia without calcination at high temperature. This procedure allowed for the first time to vary independently solid-state parameters, such as phase composition and sulfate loading, which provides insight into more conventional sulfate based catalysts. In addition, *in situ* SO$_3$ sulfation at 373 K before starting the reaction was also performed to investigate the influence of very labile sulfate groups.

5.2. Experimental

5.2.1 Catalyst preparation

Sulfate-doped zirconium hydroxide was obtained from Magnesium Electron, Inc. (XZO 1077/01). The received material was heated up to 873 K with an increment of 10 K/min in static air and kept at 873 K for 3 h. This material is denoted as SZ in the following.

To wash this calcined material 20 g of SZ was suspended in 400 ml bi-distilled water for 20 min and then filtered. The washing procedure was repeated 3 times. Then, the filter cake was dried at room temperature. The resulting powder is denoted as SZ-WW.

NaOH solution (400 ml of 0.05 M) was used to extract the entire sulfate species of SZ. After filtration, the cake was washed carefully for several times with bi-distilled water to remove the residual NaOH. The resulting material is pure zirconia and denoted as SZ-BW.

Calcined zirconia (ZrO$_2$) used in this study was prepared by calcination of commercial zirconium hydroxide (Zr(OH)$_4$, Aldrich Com.) in air at 873 K with a ramp of 10 K/min for 3 h.

Sulfation by gaseous SO$_3$ was performed in a quartz tube, illustrated in Figure 5.1. In general, sulfated zirconia or zirconia (pellets, 355-710 μm, 0.5~2 g), were preheated in the quartz tube in the flow of nitrogen (50 ml/min) at 673 K for 2 h, and then cooled to 473 K before gaseous SO$_3$ was admitted. 50 ml N$_2$ was filled into SO$_3$ cylinder *via* needle valve 1, and then the SO$_3$ cylinder was connected to the flow system. When the valve 1 was opened, the SO$_3$ saturated nitrogen (50 ml) passed into quartz tube with the carrier gas. Samples of SZ, SZ-WW, SZ-BW and ZrO$_2$ were sulfated, hereafter referred to as SZ-SO$_3$, SZ-WW-SO$_3$, SZ-BW-SO$_3$ and ZrO$_2$-SO$_3$.
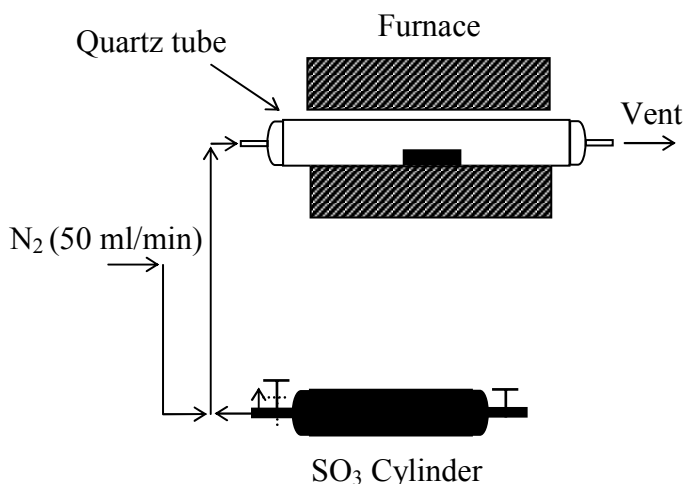
Figure 5.1 Scheme of sulfation with gaseous SO_3 on crystalline zirconia materials.

In situ SO_3 sulfation was also performed in order to investigate the influence of rehydration and activation of sulfated zirconia. 0.2 g of sulfated zirconia pellets (SZ) were treated at 673 K (heating rate: 10 K/min) for 2 h in helium (10 ml/min) followed by cooling to 373 K. Helium saturated with SO_3 (50 ml) at room temperature was subsequently flushed over the catalyst at 373 K and the catalyst was purged with helium (10 ml/min) for 0.5 h. Then, n-butane isomerization reaction was performed at this temperature.

5.2.2 Catalyst characterization

The sulfate contents of the catalysts were determined using ion chromatography (IC) as described in reference [19]. For this, 0.02 g of sulfated zirconia was suspended in a 0.01 N solution of NaOH for 20 min. Then, the solution was filtered through a 0.45 μm filter. The sulfur content in the liquid was determined by ion chromatography (Metrohm, 690 ion chromatograph equipped an IC anion column).

The BET surface area and the pore volume of the samples were determined by physisorption of nitrogen at 77.3 K using a PMI automated BET-sorptometer.

The XRD patterns were collected with a *Philips X'Pert-1* XRD powder diffractometer using Cu Kα radiation. The fraction of tetragonal phase of zirconia or sulfated zirconia was calculated using following equation:

$$X_t = I_t(111)/(I_m(111) + I_t(111) + I_m(11\bar{1})).$$

IR spectra of catalyst samples were collected using a Bruker IFS 88 (or alternatively a Perkin–Elmer 2000) spectrometer at 4 cm^{-1} resolution. Self-supporting wafers with a density of 5–10 mg/cm^2 were prepared by pressing the sample. The wafers were placed into in a stainless steel cell with CaF_2 windows, gradually heated up with 10 K/min to 673 K in a flow

of helium (10 ml/min), and held at that temperature for 2 hours. A spectrum was recorded after the temperature was stabilized at 373 K. For adsorption of pyridine the experiments were conducted in an evacuable cell. The sample wafer was gradually heated up with 10 K/min to 673 K and held at that temperature (base pressure of 10^{-6} mbar) for two hours. Subsequently, the samples were exposed to 0.1 mbar pyridine at 373 K followed by evacuation at that temperature.

5.2.3. n-Butane isomerization

n-Butane (99.5 % (Messer)) isomerization was carried out in a quartz micro tube reactor (8mm i.d.) under atmospheric pressure. 0.2 g of sulfated zirconia pellet (355~710μm) was loaded into the reactor and activated *in situ* at 673 K for 2 h in He flow (10 ml/min). The catalyst was cooled to 373 K and the reactant mixture (5 % n-butane in He, total flow of 20 ml/min) was fed through the catalyst bed. Butane reactant was passed through an olefin trap containing activated H-Y zeolite (20g), before it was mixed with He. After purification traces of butenes were not detected in the reactant mixture. The reaction products were analyzed using an on-line HP 5890 gas chromatography (GC) equipped with a capillary column (Plot Al$_2$O$_3$, 50m $\times$ 0.32 mm $\times$ 0.52mm) connected to a flame ionization detector (FID).

5.3. Results

5.3.1. Catalytic activity for n-butane skeletal isomerization

Figure 5.2 shows the catalytic activity *versus* time on stream for n-butane skeletal isomerization at 373 K on parent sample, SZ, water washed sample, SZ-WW, SO$_3$ sulfated samples, SZ-SO$_3$ and SZ-WW-SO$_3$. The calcined sulfated zirconia, SZ, showed moderate catalytic activity with a selectivity of 96 % to iso-butane. Washing SZ with water (SZ-WW) removes the labile sulfate fraction and resulted in an inactive sample [20]. Sulfation of SZ with gaseous SO$_3$ (SZ-SO$_3$) increased the catalytic activity for n-butane isomerization by a factor of 10. Also the catalytic activity of inactive SZ-WW was recovered and dramatically increased by sulfation with gaseous SO$_3$, reaching a catalytic activity which was comparable to that of SZ-SO$_3$.
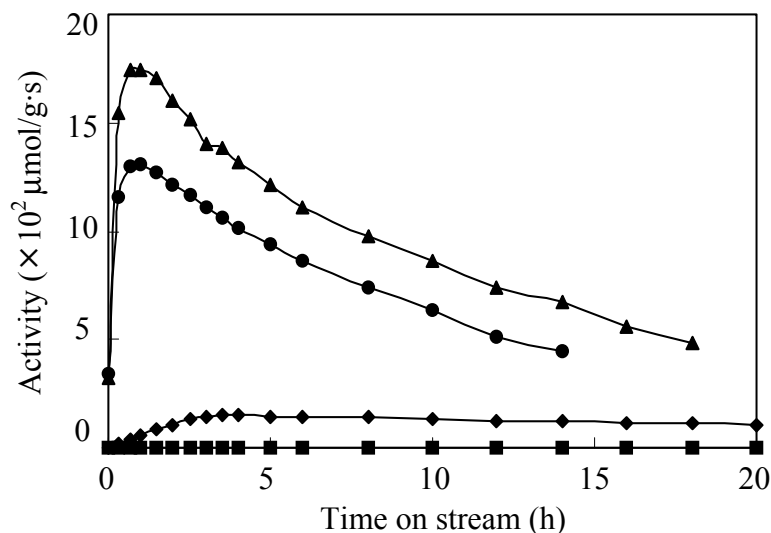
Figure 5.2 n-Butane reaction rate versus time on stream on sulfated zirconia at 373 K (■) SZ-WW, (◆) SZ, (●) SZ-WW-SO$_3$ and (▲) SZ-SO$_3$.

The SO$_3$ sulfation technique was also applied to the pure crystalline zirconias, ZrO$_2$ and SZ-BW. Figure 5.3 shows the catalytic activity for n-butane isomerization on ZrO$_2$-SO$_3$ and SZ-BW-SO$_3$ at 373 K. Contrary to the previous conclusion that crystalline zirconia is not capable for the generation of active sites for n-butane isomerization [5], ZrO$_2$-SO$_3$ and SZ-BW-SO$_3$, obtained by sulfation with gaseous SO$_3$ on the crystalline zirconia, exhibit catalytic activity at 373 K, which is higher than that of SZ.
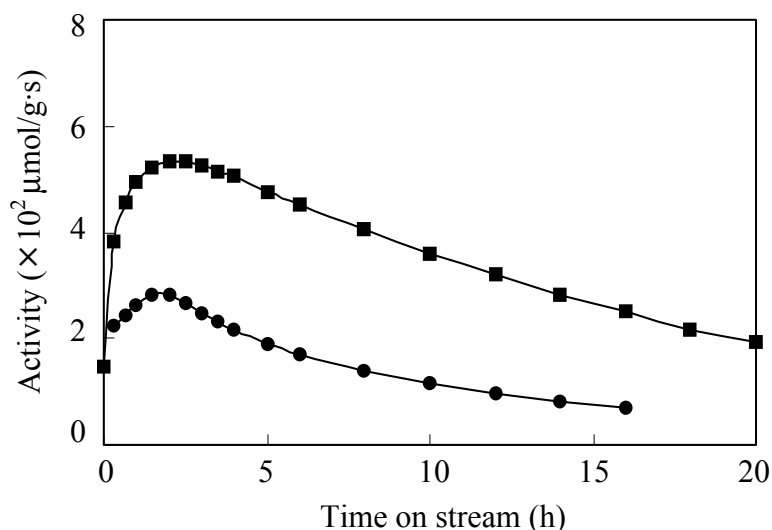

Figure 5.3 n-Butane reaction rate versus time on stream on sulfated zirconia at 373 K (●) SZ-BW-SO$_3$ and (■) ZrO$_2$-SO$_3$.

Although the *ex situ* SO$_3$ sulfated samples showed impressive catalytic activity, some of the very labile sulfate species could be lost during the heat treatment for activation of the

sample after exposure to moisture [21]. The reaction on *in situ* SO$_3$ sulfated sample was also performed to understand the function of the very labile sulfur species. In Figure 5.4, the *in situ* SO$_3$ sulfated SZ showed very high initial catalytic activity, which was around 2 orders of magnitude higher than the maximum activity of SZ. However, the so pretreated catalysts rapidly deactivated.
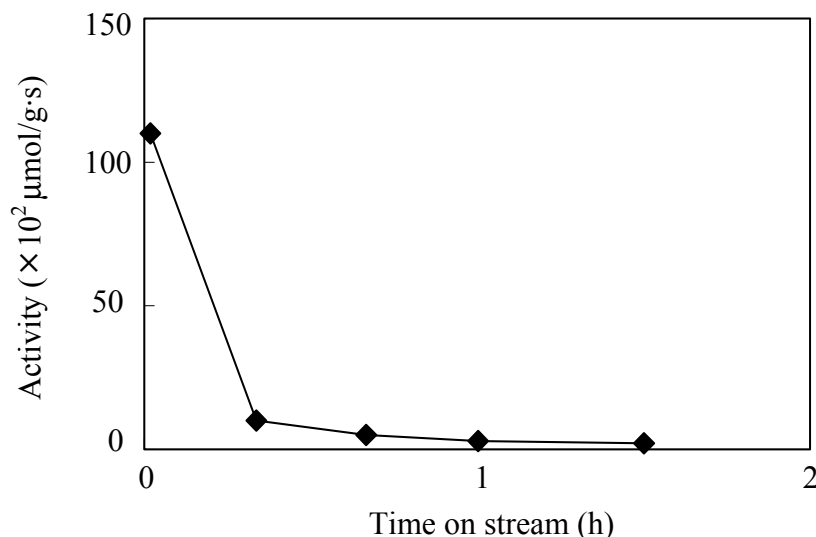

Figure 5.4 Rates versus time on stream for n-Butane isomerization at 373 K on *in situ* SO$_3$ sulfated SZ.

5.3.2. Physical properties

The BET area and sulfate content (SO$_4^{2-}$ mmol/g) of different samples are illustrated in Table 5.1. Both calcined commercial sulfated zirconia (SZ) and zirconia (ZrO$_2$) had specific surface areas higher than 100 m^2/g. Sulfation with gaseous SO$_3$ increased the sulfate contents of the sulfated zirconia samples, from 0.44 to 0.64 mmol/g for SZ and SZ-SO$_3$, respectively. According to the area the sulfate group occupies based on its kinetics diameter (0.31 nm^2 [22]) the sulfate concentrations of all SO$_3$ sulfated samples exceed the monolayer coverage (0.58 mmol/g for SZ-SO$_3$ and 0.66 mmol/g for ZrO$_2$-SO$_3$).

Table 5.1 Physical properties of zirconia and sulfated zirconia samples

Sample	BET area (m^2/g)	Sulfate content SO$_4^{2-}$ (mmol/g)
SZ	109	0.44
SZ-SO$_3$	n.d.	0.64
SZ-WW	n.d.	0.25
SZ-WW-SO$_3$	n.d.	0.91
SZ-BW-SO$_3$	n.d.	1.53
ZrO$_2$	123	n.d.
ZrO$_2$-SO$_3$	n.d.	1.15

n.d.: not determined

As shown in Figure 5.5, zirconia in the SZ sample had mainly a tetragonal structure. Water washing reduced the fraction of tetragonal phase and induced the formation of the monoclinic phase [20]. Moreover, after removal of all sulfate groups from sulfated zirconia using aqueous NaOH, the resulting material, SZ-BW, was almost exclusively monoclinic. The SO$_3$ sulfation treatment did not influence the XRD pattern of parent sample (SZ-BW). The XRD pattern of calcined zirconia, ZrO$_2$, contains both tetragonal and monoclinic phases.

The sulfate content of samples after SO$_3$ sulfation was directly related to the fraction of monoclinic phase, as shown in Figure 5.6. The higher fraction of monoclinic phase induced higher concentration of sulfate content. The difference between the concentrations of sulfate groups from pure tetragonal to pure monoclinic ZrO$_2$ was nearly a factor of two. This indicates that the monoclinic ZrO$_2$ phase forms a more stable sulfate than the tetragonal. It should be kept in mind, however, that the tetragonal materials contain sulfate groups and are, hence, more acidic on the surface, which in turn could reduce the strength of interaction with SO$_3$.
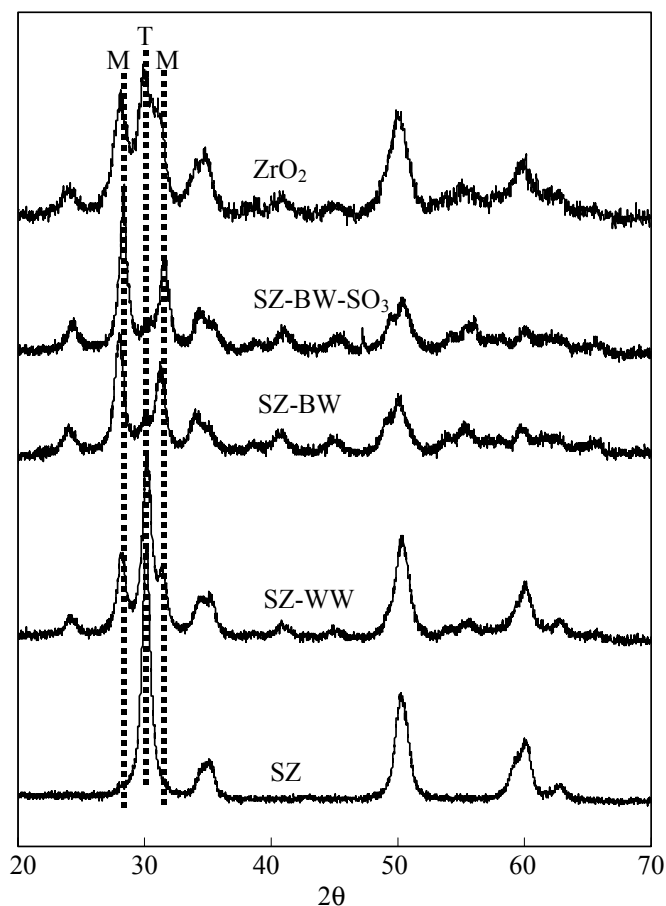
Figure 5.5 XRD profiles of sulfated zirconias and zirconias.
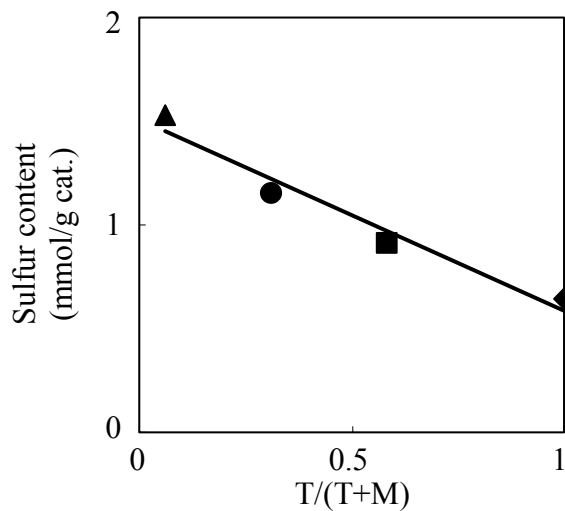T: tetragonal; M: monoclinic.

Figure 5.6 Correlation of fraction of tetragonal phase and sulfate content
($\blacklozenge$) SZ-SO₃; ($\blacksquare$) SZ-WW-SO₃; ($\bullet$) ZrO₂-SO₃ and
($\blacktriangle$) SZ-BW-SO₃.

5.3.3. IR spectroscopy

Surface hydroxyl groups

Figure 5.7 (A) compiles the IR spectra normalized by the wafer thickness in the region of the surface OH stretching bands after activation in He at 673 K for 2 h. The SZ sample showed a strong asymmetric band at 3634 cm^{-1} with a shoulder at 3660 cm^{-1} and very weak bands at 3740 and 3710 cm^{-1}. In addition, a weak band located at 3578 cm^{-1} was also observed in the IR spectrum of SZ. However, the water washed sample, SZ-WW, and pure zirconia, ZrO_2, with labile sulfate groups not being present on the surface, showed a very strong band at 3600 - 3700 cm^{-1}, which was assigned to a bridging OH group [23, 24]. Moreover, other OH bands between 3700 and 3800 cm^{-1} range were observed and assigned to terminal OH groups [23, 24]. SO_3 sulfation reduced the intensity of the OH bands above 3600 cm^{-1}, as shown in the spectra of SZ-SO_3, SZ-WW-SO_3, SZ-BW-SO_3 and ZrO_2-SO_3. Under the assumption that the molar extinction coefficient does not change dramatically, the decrease in the OH group concentration by SO_3 sulfation is attributed to the coverage by surface sulfates. Thus, SZ-BW-SO_3, whose sulfate content is the highest among the SO_3 sulfated samples, did not exhibit OH bands in that region of the IR spectrum. Instead, the samples containing labile sulfate species showed a band at 3570 cm^{-1}, previously assigned to the vibration mode of OH in adsorbed water [25].

Surface sulfate groups

The IR spectra of sulfate groups of the activated samples are shown in Figure 5.7 (B). All of the activated sulfated zirconia samples showed IR bands of the S=O group between 1300 and 1450 cm^{-1}. Such highly covalent sulfate groups on sulfated zirconia were usually previously ascribed to the presence of the very high acid strength on sulfated zirconia [26, 27]. SZ exhibited a maximum at 1404 cm^{-1}, while SO_3 sulfation slightly shifted it to 1405 cm^{-1} and induced the corresponding broad band (see spectrum (b). in Figure 5.7 (B) for SZ-SO_3). Water washing removed some of these highly covalent sulfate species and the maximum of the complex band appeared then at 1391 cm^{-1} [20]. With SZ-WW-SO_3, obtained by sulfation with SO_3 of SZ-WW, the high wavenumber IR band was observed indicating that the labile sulfate groups were restored. In the region of S-O vibration two bands located at 1011 cm^{-1} and 1043 cm^{-1} were clearly distinguished in the spectra of SZ, SZ-SO_3 and SZ-WW-SO_3. The strong bands in the 1100~1300 cm^{-1} range in the IR spectra of SO_3 sulfated samples, was

usually ascribed to the surface poly-sulfate groups, which are related to the sulfate content in the sample.

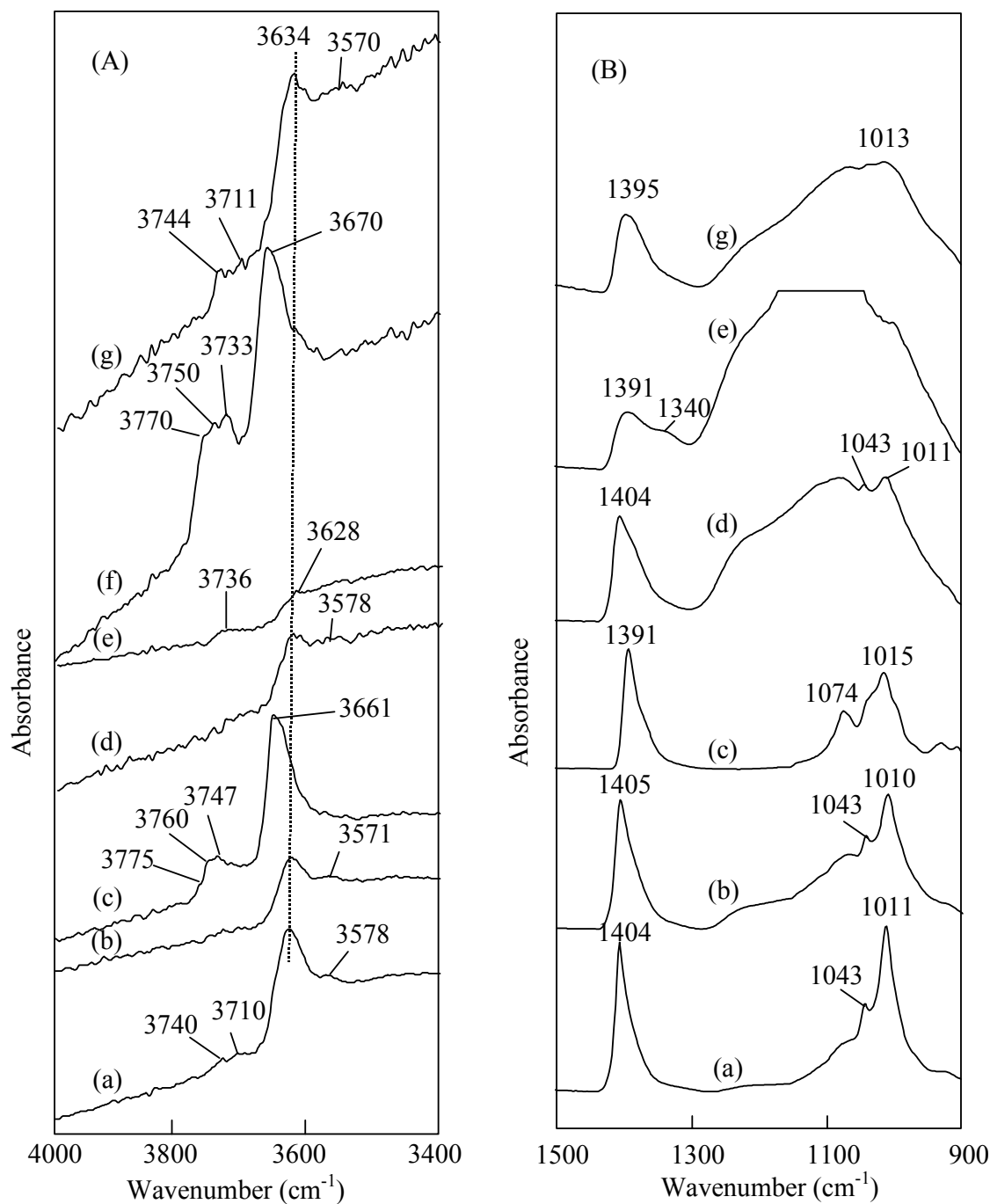**Figure 5.7** IR spectra in the regions of surface OH group (A) and surface sulfate group (B) of sulfated zirconias and zirconia (a) SZ; (b) SZ-SO₃; (c) SZ-WW; (d) SZ-WW-SO₃; (e) SZ-BW-SO₃; (f) ZrO₂; (g) ZrO₂-SO₃

Adsorption of pyridine

The IR spectra of adsorbed pyridine are widely used to identify the concentration and the nature of acid sites on solid acids [28]. The pyridinium ion shows a band at 1540 cm^{-1} and

provides a quantitative measure for the Brønsted acid sites. Pyridine coordinately bound to Lewis acid sites exhibits a band at 1440 cm^{-1}. The concentrations of Brønsted and Lewis acid sites on different samples, determined by the IR spectra of adsorbed pyridine, are shown in Table 5.2. Here, the molar absorption coefficients of the bands of adsorbed pyridine were set equal to those determined for zeolites [28]. Note that water washing treatment removed not only the water soluble sulfate groups of SZ, but also the Brønsted acid sites and led to an increase in Lewis acid site concentration [20]. Sulfation with SO$_3$ led to the re-formation of the Brønsted acid sites (see SZ-WW-SO$_3$) and the decrease in the concentration of Lewis acid sites. Comparing to the samples SZ, SZ-SO$_3$, SZ-WW and SZ-WW-SO$_3$, SO$_3$ sulfation increased the Brønsted acid site concentration by losing of Lewis acid sites, which indicates some of the labile sulfate is coordinately bound to the Lewis acid sites. In addition, SO$_3$ sulfation also induced Brønsted acidity on pure ZrO$_2$, which showed only Lewis acid bound pyridine otherwise. With the exception of SZ-WW (having no Brønsted acid sites) the concentration of Brønsted acid sites of sulfated ZrO$_2$ are directly related to the sulfate concentration (see Figure 5.8).

Table 5.2 Concentration of Brønsted and Lewis acid sites on zirconia and sulfated zirconia samples determined by IR spectra of adsorbed pyridine.

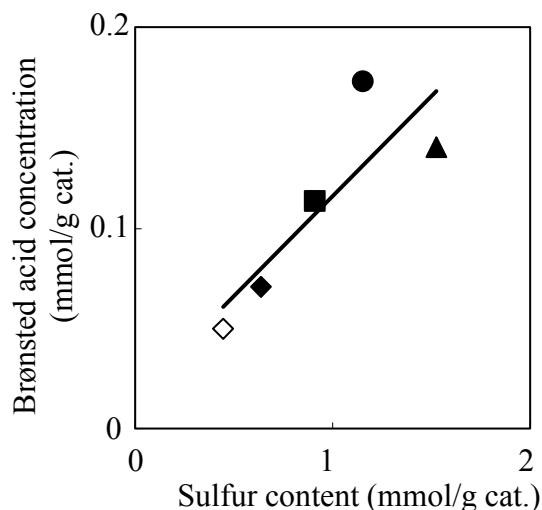| Sample	Acid sites (mmol/g)	
	Brønsted	Lewis
SZ	0.050	0.106
SZ-SO$_3$	0.071	0.073
SZ-WW	0	0.163
SZ-WW-SO$_3$	0.113	0.054
SZ-BW-SO$_3$	0.135	0.037
ZrO$_2$	0	0.206
ZrO$_2$-SO$_3$	0.173	0.089

Figure 5.8 Relation between sulfate content and concentration of Brønsted acid sites (◇) SZ; (◆) SZ-SO₃; (■) SZ-WW-SO₃; (●) ZrO₂-SO₃ and (▲) SZ-BW-SO₃.

5.4 Discussion

The calcined sulfated zirconia (SZ) was active for n-butane skeletal isomerization at 373 K. However, removal of the water soluble sulfate by water washing rendered the catalyst inactive [20]. On the other hand, SO₃ sulfation induced a very high catalytic activity in the parent sample SZ indicating that the SO₃ deposition on the properly activated sulfated zirconia generates more active sites. In addition, SO₃ sulfation on the inactive water washed sample (SZ-WW), induced an activity comparable to that of the sample SZ-SO₃. The pronounced promoting effect of SO₃ sulfation on the catalytic activity of sulfated zirconia gives strong evidence that the labile sulfate species, generated by the adsorption of SO₃, are essential for the formation of active sites. Crystalline zirconia samples, ZrO₂ and SZ-BW, can also be used for the preparation of active sulfated zirconia by SO₃ sulfation, even though it is generally reported that the sulfation on crystalline zirconia with liquid sulfation agents is not effective in generating active sites.

The important role of the labile active sulfate species is further evidenced by the *in situ* SO₃ sulfation experiment. The extremely high initial activity of sulfated zirconia after *in situ* SO₃ sulfation indicates that the concentration of the very active sulfate species induced by adsorbed SO₃ is dramatically increased. It should be noted that these labile sulfates are very sensitive towards thermal treatment, especially after rehydration under ambient conditions.

Even though labile sulfates are very important for the active sites a linear relationship between the sulfate content and the catalytic activity does not exist. Here, we speculate that only a fraction of labile sulfate is responsible for the generation the active sites, others acting

93

as spectators. As shown in the IR spectra of SO$_3$ sulfated samples, the extra sulfate species exhibited a broad band between 1100 and 1300 cm^{-1}, which is a feature of sulfates with low covalent character, comparable to that of symmetric inorganic sulfate groups.

The IR spectra in the S=O vibration region of the SO$_3$ sulfated samples are shown in Figure 5.9. It is clearly shown that the sample with the most intense band in this region, was the most active one, for instance, the activity for n-butane isomerization at 373 K was 0.175 μmol/g·s on SZ-SO$_3$, while SZ-BW-SO$_3$ was the least active sample (0.028 μmol/g·s), although its sulfate content was the highest among all the SO$_3$ sulfated samples.
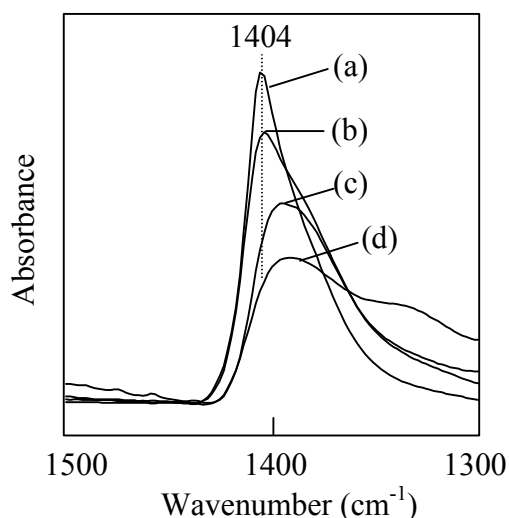

Figure 5.9 IR spectra in the region of S=O stretching vibration of sulfated zirconias: (a) SZ-SO$_3$; (b) SZ-WW-SO$_3$; (c) ZrO$_2$-SO$_3$ and (d) SZ-BW-SO$_3$.

Although the claim that monoclinic zirconia is not suitable for preparation of active sulfated zirconia was criticized, the catalytic activity of the monoclinic sulfated zirconia was always much lower than that of the tetragonal one. In this study, SZ-BW-SO$_3$, an almost pure monoclinic sulfated zirconia, showed a much lower catalytic activity than that of pure tetragonal sulfated zirconia, SZ-SO$_3$. The catalytic activity versus the fraction of tetragonal phase of the SO$_3$ sulfated samples is shown in Figure 5.10. The linear relationship between activity and tetragonal phase fraction implies that the tetragonal phase is more favorable for generating, after SO$_3$ sulfation, active sites for n-butane isomerization. The importance of tetragonal phase could be related to its surface morphology. As suggested by Benaïssa *et al*. [29], the presence of sulfate groups near or on the zirconia crystallites containing high-Miller-index surfaces could give rise to the highly acidic sites of sulfated zirconia. However, the number of such catalytic sites would be very small. We observed a remarkable correlation

between tetragonal phase fraction, intensity of the IR band in the S=O region in the samples prepared by SO_3 sulfation and catalytic activity.
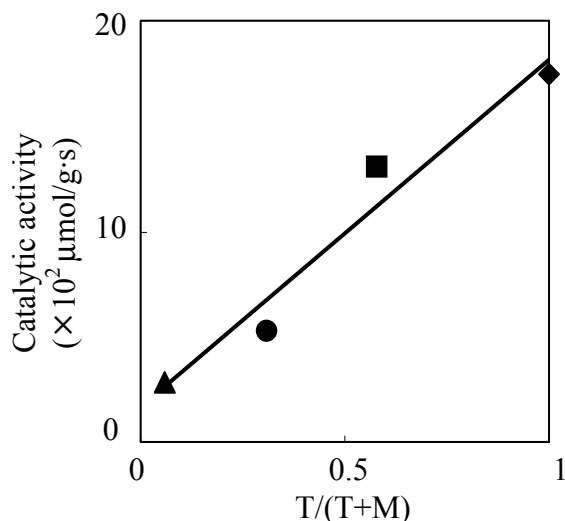

Figure 5.10 Correlation of catalytic activity of SO_3 sulfated samples and the fraction of tetragonal phase (◆) SZ-SO_3; (■) SZ-WW-SO_3; (●) ZrO_2-SO_3 and (▲) SZ-BW-SO_3.

Pure zirconia and water washed sulfated zirconia are materials with only Lewis acidity. The presence of labile sulfate groups leads to the formation of Brønsted acid sites. The Brønsted acid site concentration increased in parallel to the concentration of sulfate species, especially for the samples prepared from the same zirconia support, *i.e.*, SZ, SZ-SO_3, SZ-WW-SO_3 and SZ-BW-SO_3. At the same time the SO_3 sulfation dramatically decreased the intensity of the bands corresponding to the hydroxyl groups.

Two different models have been suggested with respect to the formation of Brønsted acid site on sulfated zirconia. Ward and Ko [30] proposed that the strong Brønsted acid sites of sulfated zirconia are the Zr-OH surface hydroxyl groups whose proton donating ability is strengthened by electron withdrawing inductive effect of the S=O groups. On the other hand, Kustov *et al.* [31] and Adeeva *et al.* [32] proposed that surface bi-sulfate species instead of the zirconia surface OH groups are responsible for the Brønsted acidity of sulfated zirconia. Since in our study the higher concentration of Brønsted acid sites is present on the material whose IR spectrum presents OH bands of lowest intensity, we conclude that the Brønsted acid sites mainly result from bi-sulfate species or hydrated pyrosulfate species. Water could interact with adsorbed SO_3 (pyrosulfates) and could generate S-OH groups causing the Brønsted acidity.

It is interesting to note that the increase in the concentration of labile sulfates by SO_3 sulfation induced a decrease of the Lewis acid sites. This suggests that a fraction of labile

sulfate species is coordinatively bound to Lewis acid sites. The Lewis acid sites of metal oxides are coordinatively unsaturated metal cations that are prone strongly interact with other molecules, *i.e.,* H_2O, CO_2 or CO. It is interesting to note that the adsorption of SO_3 on zirconia based catalysts has been also used for titrating the anion vacancies [33].

It has been claimed that the calcination at high temperature of sulfated zirconia precursors, obtained by aqueous sulfation of an amorphous zirconium hydroxide or of crystalline zirconia, is a crucial step for generating active sites. The function of the calcination is to convert the amorphous zirconium hydroxide to the tetragonal zirconia and to cause the sulfate groups to bind with the zirconia surface thus forming form the active sites [8,9,34]. However, the calcination is claimed to have another important function, *i.e.*, the elimination of the excess sulfate groups from Lewis acid sites (coordinatively unsaturated Zr^{4+}) becoming so accessible to the reactants. It has also reported that the electron withdrawing effect of sulfate groups increases the strength of the Lewis acid [10, 11].

However, in this study, SO_3 sulfation at 473 K on the zirconia materials, pre-heated at 673 K, induced the formation of active sites without high temperature calcination, which suggests that the active sites are generated solely by the effective interaction between SO_3 and zirconia surface. This is further evidenced by the extremely high initial catalytic activity of the *in situ* SO_3 sulfated sample, where SO_3 sulfation was performed at 373 K without further activation at high temperature. As the labile sulfate groups are involved mainly in the generation of butene by oxidative dehydrogenation, the present results suggest that it is mainly the concentration of the sites generating olefins for the isomerization and hydride transfer cycle is the reason for the variations in the catalytic activity. It is subject to further investigations, how the concentration of Brønsted acid sites and the depositions of oligomers from the olefins formed in higher concentration contributes to the steady state activity of these samples.

5.5 Conclusions

Sulfation with gaseous SO_3 was shown to be an effective technique for preparation of active sulfated zirconia for n-butane isomerization at low temperature, which avoids complex preparation procedures and allows tailoring the activity of catalysts. The results show that labile sulfate species are essential for the formation of active sites, which can be removed by water washing treatment and recovered by SO_3 sulfation on zirconia materials pre-heated at 673 K. The decrease in the Lewis acidity after SO_3 sulfation indicates that at least some of the labile sulfates are coordinatively bound to the Lewis acid sites. The labile sulfate groups induce the Brønsted acidity on zirconia surface. The increase in Brønsted acid sites and the

significant decrease in zirconia surface OH groups by SO_3 sulfation indicate that Brønsted acid sites are affiliated with bi-sulfate species. The fraction of the tetragonal phase of zirconia supports is a determining factor for the catalytic acidity of samples after SO_3 sulfation; higher fraction of tetragonal phase induces higher the catalytic activity and more highly covalent sulfate species. This suggests that the surface morphology of tetragonal zirconia favors weak interaction with the sulfate groups and facilitates the formation of active sites by condensation of sulfate groups (pyrosulfates) and/or the chemisorption of SO_3 on existing sulfate groups.

Acknowledgments

References

[1]   T. Yamaguchi, K. Tanabe, Y.C. Kung, Mater. Chem. Phys. 16 (1986) 67.

[2]   J.R. Sohn, H.W. Kim, J. Mol. Catal. 52 (1989) 361.

[3]   D. Fărcaşiu, J.Q. Li, Appl. Catal. A 175 (1998) 1.

[4]   M.T. Tran, N.S. Gnep, G. Szabo, M. Guisnet, Appl. Catal. A 171 (1998) 207.

[5]   M. Hino, S. Kobayashi, K. Arata, J. Am. Chem. Soc. 101 (1979) 6439.

[6]   R.A. Comelli, C.R. Vera, J.M. Parera, J. Catal. 151 (1995) 96.

[7]   C. Morterra, G. Cerrato, F. Pinna, M. Signoretto, J. Catal. 157 (1995) 109.

[8]   D. Fărcaşiu, J.Q. Li, Appl. Catal. A 128 (1995) 97.

[9]   F. Lonyi, J. Valyon, J. Engelhardt, F. Mizukami, J. Catal. 160 (1996) 279.

[10]   C. Morterra, G. Cerrato, M. Signoretto, Catal. Lett. 41 (1996) 101.

[11]   C. Morterra, G. Cerrato, G. Meligrana, M. Signoretto, F. Pinna, G. Strukul, Catal. Lett. 73 (2001) 113.

[12]   W. Stichert, F. Schüth, J. Catal. 174 (1998) 242.

[13]   C.R. Vera, J.M. Parera, J. Catal. 165 (1997) 254.

[14]   C. Morterra, G. Cerrato, C. Emanuel, V. Bolis, J. Catal. 142 (1993) 349.

[15]   A.F. Bedilo, A.S. Ivanova, N.A. Pakhomov, A.M. Volodin, J. Mol. Catal. A 158 (2000) 409.

[16]   T. Yamaguchi, T. Jin, K. Tanabe, J. Phys. Chem. 90 (1986) 3148.

[17]   J.F. Haw, J. Zhang, K. Shimizu, T. N. Venkatraman, D.P. Luigi, W. Song, D.H. Barich, J.B. Nicholas, J. Am. Chem. Soc. 122 (2000) 12561

[18]   J. Zhang, J.B. Nicholas, J.F. Haw, Angew. Chem. Int. Ed. 39 (2000) 3302.

[19]   P. Canton, R. Olindo, F. Pinna, G. Strukul, P. Riello, M. Meneghetti, G. Cerrato, C. Morterra, A. Benedetti, Chem. Mater. 13 (2001) 1634.

[20]   X.Li, K. Nagaoka, J.A.Lercher, submitted for publication (2004).

[21]   X.Li, K. Nagaoka, L.J. Simon, J.A.Lercher, A. Hofmann, J. Sauer, submitted for publication. (2004)

[22]   N. Katada, J. Endo, K. Notsu, N. Yasunobu, N. Naito, M. Niwa, J. Phys. Chem. B 104 (2000) 10321.

[23]   W. Hertl, Langmuir 5 (1988) 96.

[24]   A.A. Tsyganenko, V.N. Filimonov, J. Mol. Struct. 19 (1973) 579.

[25]   T. Merle-Méjean, P. Barberis, S. Ben Othmane, F. Nardou, P.E. Quintard, J. Eur. Ceram. Soc. 18 (1998) 1579.

[26]   T. Yamaguchi, T. Jin, K. Tanabe, J. Phys. Chem. 90 (1986) 3148.

[27]   M. Waqif, J. Bachelier, O. Saur, J.C. Lavalley, J. Mol. Catal. 72 (1992) 127.

[28]   C.A. Emeis, J. Catal. 141 (1993) 347.

[29]   M. Benaïssa, J.G. Santiesteban, G. Diaz, C.D. Chang and M. Jose-Yacaman, J. Catal. 161 (1996) 694.

[30]   D. A. Ward and E. I. Ko, J. Catal. 157 (1995) 321.

[31]   L.M. Kustov, V.B. Kazansky, F. Figueras, D. Tichit, J. Catal. 150 (1994) 143.

[32]   V. Adeeva, J.W. de Haan, J. Janchen, G.D. Lei, V. Schunemann, L.J.M. van de Ven, W.M.H. Sachtler, R.A. van Santen, J. Catal. 151 (1995) 364.

[33]   R.G. Silver, C.J. Hou, J.G. Ekerdt, J. Catal. 118 (1989) 400.

[34]   T. Yamaguchi, K. Tanabe, Mater. Chem. Phys. 16 (1986) 67.

Chapter 6

Summary

The isomerization of n-butane to iso-butane is a very important process in petrochemical industry. However, the disadvantages of the present process (Butamer process), using platinum chloride on alumina as catalyst, are need of continuous introduction of chloride to maintain the catalyst activity, corrosiveness and high costs for disposing of the catalyst. Sulfated zirconia and promoted sulfated zirconia are believed to be the promising alternative catalysts due to their highly catalytic activity at low temperature. A thorough understanding of the surface chemistry of n-butane activation as well as isomerization on sulfated zirconia and a detailed insight into the active sites are helpful for the development of an effective catalyst.

In this thesis, n-butane isomerization reaction on calcined commercial sulfated zirconia catalyst (MEL 1077/01) was investigated with various techniques, *i.e.* n-butane TPD, *in situ* IR as well as kinetic studies in order to elucidate the reaction mechanism. Water washing of the active sulfated zirconia and SO_3 sulfation on the crystalline zirconia were employed for understanding the structure of the active sites.

In **Chapter 2**, the influence of water washing of active sulfated zirconia was discussed and it was concluded that labile sulfate species are essential for the generation of active sites. It was found that at least two types of sulfate groups exist on the surface of active sulfated zirconia. One of those types of sulfate groups can be removed by washing with water at ambient temperature. Approximately 40 % of the sulfur in the sulfated zirconia can be removed in this way. A fraction of the sulfate removed *via* this way is located on top of a Lewis acid site (coordinatively unsaturated Zr^{4+}), which has a more covalent S=O bond than all species remaining on the surface after washing. It can be clearly identified by a narrow S=O band at 1404 cm^{-1}. The hydroxyl groups affiliated with these labile sites and the sites of the catalytically active Brønsted acid sites is characterized by a broad IR band characteristic of hydrogen bonded OH groups. It is shown, however, that the OH groups of ZrO_2 are not involved in the catalysis and in the generation of strong Brønsted acid sites able to protonate pyridine.

The catalytic isomerization of n-butane requires the labile sulfate. In the absence of the labile sulfate the material is completely inactive for n-butane isomerization at 373 K. Because the washing procedure increases the concentration of Lewis acid sites without decreasing their strength, we can unequivocally conclude that Lewis acid sites of sulfated zirconia are insufficient to catalyze n-butane isomerization. We conclude in consequence that Brønsted acid sites affiliated with the labile sulfate groups are indispensable for this reaction

The activation of n-butane isomerization on sulfated zirconia at 373 K was discussed in ***Chapter 3***. Butene species formed by oxidation of n-butane are shown to be the key intermediates during n-butane isomerization on sulfated zirconia. Butene is formed by a stoichiometric reaction between butane and a pyrosulfate type surface species. For the first time direct experimental evidence is given for all reaction products involved and the reaction intermediates have been modeled by theoretical chemistry. The initiating reaction occurs stoichiometrically, but the olefins formed induce a chain type reaction that converts 500 butane molecules per butene formed. This allows the sulfated zirconia catalysts to reach acceptable lifetimes and oxidative regeneration may lead to newly formed oxidation sites extending the lifetime further. Molecular hydrogen impedes the dehydrogenation reaction via pathways that basically are variants of hydride transfer. The presence of molecular oxygen induces reaction pathways to olefins, which rely on the generation of labile sulfate/SO_3 entities on the surface and/or the generation of O_2^- anions. Whatever the mechanism of butane formation, the present study also shows that the reaction rate and the catalyst stability depend on the concentration of olefins. At low concentrations of butenes the rate increases with the olefin concentration. At high concentration a high maximum activity is achieved, but the catalyst deactivates *via* formation of oligomers. The DFT calculations show clearly that the sulfur as well as the water content plays an important role in this initialization step by its influence on the energy of formation of the butene.

The mechanism of propagation step of n-butane isomerization on sulfated zirconia at low temperature was discussed in ***Chapter 4***. The change of iso-butane selectivity with n-butane conversion indicates isomers and by-products are not formed following the same mechanism. The high selectivity to isomerization for n- and iso-butane at low conversion (96 % and 80 %, respectively) indicates that the isomerization occurs *via* an intra-molecular mechanism. Scheme 6.1 demonstrates the overall n-butane isomerization mechanism on sulfated zirconia at low temperature. The initial step of n-butane isomerization on sulfated zirconia is the *in situ* generation of butene by oxidative dehydrogenation of n-butane and isomerization takes place as monomolecular skeletal isomerization of the n-butyl carbenium ion to the iso-butyl carbenium ion. The chain reaction is propagated by a hydride transfer from n-butane to the iso-butyl carbenium ion.

+ SO$_3$ ⟶ + SO$_2$ + H$_2$O

H$^+$ ⟶ +

Skeletal isomerization

Hydride transfer
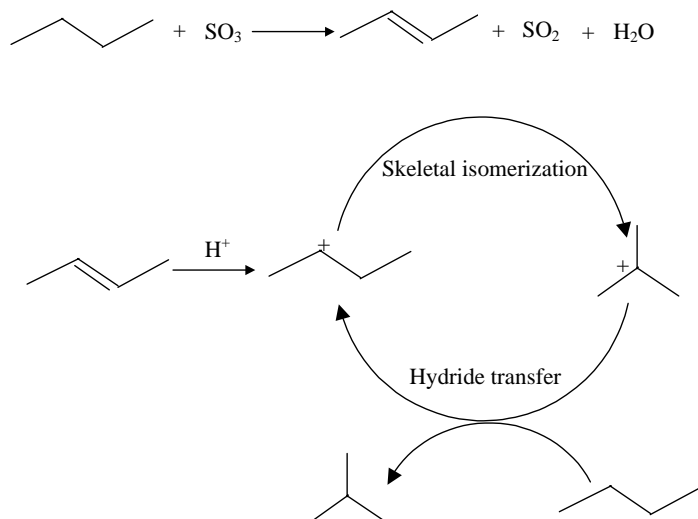
Scheme 6.1 Proposed n-butane isomerization mechanism on sulfated zirconia at low temperature.

The true energies of activation (estimated by transition state theory using the thermodynamic and kinetic data measured in this study) suggests a true energy of activation of 117 to 128 kJ/mol in line with a somewhat energy demanding reaction pathway. Considering the heat of adsorption, this value agrees well with the reported values of apparent energies of activation in the literatures. Transient experiments show conclusively that the hydride transfer step fast compared to the isomerization step and is concluded to be in quasi-equilibrium. The reactions can be modeled perfectly in the forward direction using a Langmuir-Hinshelwood-Hougen-Watson form with the physisorption of the alkanes and the hydride transfer steps being in quasi equilibrium.

The by-products, *i.e.*, propane and pentanes, are formed *via* bimolecular routes as secondary and tertiary products. It is especially noteworthy that at higher conversion propane is formed almost exclusively indicating multiple alkylation and cracking steps to occur under such conditions. Reversible isomerization and irreversible disproporationation are, thus, the cause of the reduced selectivity at high conversion.

It is interesting to note that the forward rate of iso-butane isomerization is significantly slower than the isomerization of n-butane. This lower activity is associated with a higher energy of activation for the isomerization of iso-butane. This is a consequence of the higher stability of the iso-butyl carbenium ion (iso-butyl alkoxy group) over the n-butyl carbenium ion. Therefore, the difference to methyl cyclopropyl carbenium ion and, hence, the true energy of activation will be higher. The strong covalent bonding of the carbenium ions in the ground state leads to a dampening of the large differences expected from free carbenium ion

chemistry. The energy profile of isomerization/hydride transfer steps of n-butane skeletal isomerization on sulfated zirconia is shown in Figure 6.1.
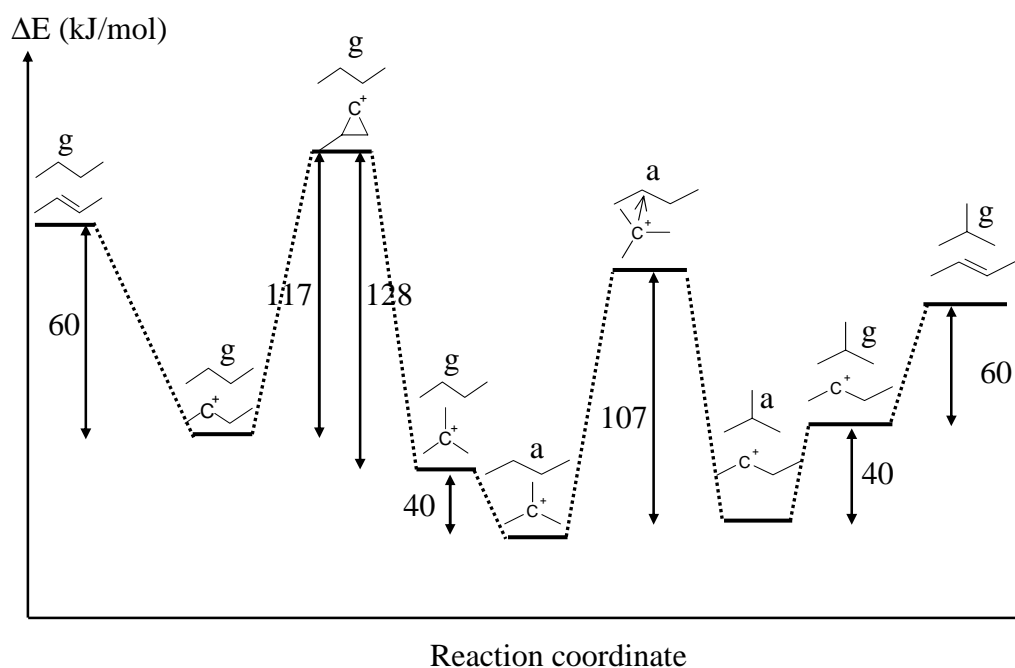

Figure 6.1 Energy profile of isomerization/hydride transfer steps corresponding to isomerization of n-butane to iso-butane.

Gaseous SO_3 sulfation was confirmed to be an effective technique for preparation of active sulfated zirconia for n-butane isomerization at low temperature, which circumvents the high temperature calcination, the crucial step for generation of active sites in the conventional preparation method. ***Chapter 5*** focused on the active sites formation during gaseous SO_3 sulfation on crystalline zirconia at 473 K. The catalytic activity of calcined sulfated zirconia (SZ) was promoted dramatically by SO_3 sulfation. The results show that labile sulfate species are essential for the formation of active sites, which can be removed by water washing treatment and recovered by SO_3 sulfation on zirconia materials pre-heated at 673 K. The decrease in the Lewis acidity after SO_3 sulfation indicates that at least some of the labile sulfates are coordinately bound to the Lewis acid sites. The labile sulfate groups induce the Brønsted acidity on zirconia surface. The increase in Brønsted acid sites and the significant decrease in zirconia surface OH groups by SO_3 sulfation indicate that Brønsted acid sites are affiliated with bi-sulfate species. The fraction of the tetragonal phase of zirconia supports is a determining factor for the catalytic acidity of samples after SO_3 sulfation; higher fraction of tetragonal phase induces higher the catalytic activity and more highly covalent sulfate species. This suggests that the surface morphology of tetragonal zirconia favors weak interaction with

103

the sulfate groups and facilitates the formation of active sites by condensation of sulfate groups (pyrosulfates) and/or the chemisorption of SO_3 on existing sulfate groups.

Curriculum vitae

Xuebing Li was born on March 10, 1972 in Tianjin, P. R. China. After finishing high school in 1990, he started his study in Department of Chemistry, Tsinghua University, P. R. China and received his bachelor degree in 1995. He went on to study physical chemistry in Department of Chemistry, Tsinghua University under the supervision of Professor Qiming Zhu. In 1998, he finished his thesis, entitled *catalytic cracking of coal tar at high temperature*, and obtained his master degree. He was employed as research assistant in the Department of Chemistry at Tsinghua University in 1998. He joined TCII catalysis and reaction engineering group of Professor J. A. Lercher at Technical University of Munich, Germany and started a research on butane skeletal isomerization on sulfated zirconia at low temperature in 2000. The results are described in this thesis.

List of publications

Structural and Active site Characterization of Sulfated Zirconia Catalysts for Light Alkane Isomerization
M. Standke, C. Breitkopf, H. Papp, S. Wrabetz, B. Klose, X. Yang, R. E. Jentoft, X. Li, L. J. Simon, J. A. Lercher, Proc. DGMK-Conference Berlin, October 9–11, 2002 ISBN 3-931850-98-6, pp. 23-30.

Characterization and catalytic property for n-butane skeletal isomerization of two sulfated zirconias
X. Li, K. Nagaoka, L. J. Simon, J. A. Lercher, C. Breitkopf, S. Matysik, H. Papp, S. Wrabetz, F. C. Jentoft, in preparation.

Labile sulfates as key components in active sulfated zirconia for n-butane isomerization at low temperature
X. Li, K. Nagaoka, J. A. Lercher, J. Cat. 2004, accepted.

Activation of n-butane isomerization on sulfated zirconia: oxidation of n-butane by surface groups
X. Li, K. Nagaoka, L. J. Simon, J. A. Lercher, A. Hofmann, J. Sauer, submitted for publication, 2004.

Mechanism of chain propagation of butane skeletal isomerization on sulfated zirconia
X. Li, K. Nagaoka, L. J. Simon, J. A. Lercher, in preparation.

SO$_3$ sulfation - preparation of active sulfated zirconia for n-butane skeletal isomerization at low temperature
X. Li, K. Nagaoka, J. A. Lercher, in preparation.

Influence of calcination procedure on the catalytic property of sulfated zirconia
X. Li, K. Nagaoka, L. J. Simon, J. A. Lercher, in preparation.